The Journal of Gemmology

Volume 29 No. 4
October 2004

The Gemmological Association and Gem Testing Laboratory of Great Britain

Gemmological Association and Gem Testing Laboratory of Great Britain

27 Greville Street, London EC1N 8TN
Tel: +44 (0)20 7404 3334 • **Fax:** +44 (0)20 7404 8843
e-mail: information@gem-a.info • **Website:** www.gem-a.info

President: E A Jobbins

Vice-Presidents: N W Deeks, R A Howie, D G Kent, R K Mitchell

Honorary Fellows: Chen Zhonghui, R A Howie, K Nassau

Honorary Life Members: H Bank, D J Callaghan, E J Gübelin, E A Jobbins, J I Koivula, I Thomson, H Tillander

Council: S Burgoyne, A T Collins, T M J Davidson, S A Everitt, R R Harding, L Hudson, E A Jobbins, I Mercer, J Monnickendam, M J O'Donoghue, E Stern, P J Wates, V P Watson

Members' Audit Committee: A J Allnutt, P Dwyer-Hickey, J Greatwood, B Jackson, L Music, J B Nelson, C H Winter

Branch Chairmen: Midlands – G M Green, **North East** – N R Rose, **North West** – D M Brady, **Scottish** – B Jackson, **South East** – C H Winter, **South West** – R M Slater

Examiners: A J Allnutt MSc PhD FGA, L Bartlett BSc MPhil FGA DGA, Chen Meihua BSc PhD FGA DGA, S Coelho BSc FGA DGA, Prof A T Collins BSc PhD, A G Good FGA DGA, D Gravier FGA, J Greatwood FGA, S Greatwood FGA DGA, G M Green FGA DGA, He Ok Chang FGA DGA, G M Howe FGA DGA, B Jackson FGA DGA, B Jensen BSc (Geol), T A Johne FGA, H Kitawaki FGA CGJ, Li Li Ping FGA DGA, M A Medniuk FGA DGA, T Miyata MSc PhD FGA, M Newton BSc DPhil, C J E Oldershaw BSc (Hons) FGA DGA, H L Plumb BSc FGA DGA, N R Rose FGA DGA, R D Ross BSc FGA DGA, J-C Rufli FGA, E Stern FGA DGA, S M Stocklmayer BSc (Hons) FGA, Prof I Sunagawa DSc, M Tilley GG FGA, R K Vartiainen FGA, P Vuillet à Ciles FGA, C M Woodward BSc FGA DGA, Yang Ming Xing FGA DGA

The Journal of Gemmology

Editor: Dr R R Harding

Assistant Editors: M J O'Donoghue, P G Read

Associate Editors: Dr C E S Arps (Leiden), G Bosshart (Horgen), Prof A T Collins (London), J Finlayson (Stoke-on-Trent), Dr J W Harris (Glasgow), Prof R A Howie (Derbyshire), Dr J M Ogden (London), Prof A H Rankin (Kingston upon Thames), Dr J E Shigley (Carlsbad), Prof D C Smith (Paris), E Stern (London), Prof I Sunagawa (Tokyo), Dr M Superchi (Milan)

Production Editor: M A Burland

Vol 29, No.4, October 2004 ISSN: 1355–4565

Pearls from the lion's paw scallop

Kenneth Scarratt[1] and Henry A. Hänni[2]

1. AGTA Gemological Testing Center, New York, NY10017, USA
e-mail: info@agta-gtc.org
2. SSEF Swiss Gemmological Institute, Basel, Switzerland
e-mail: gemlab@ssef.ch

In memory of Alexander E. Farn, former Director of the London Chamber of Commerce DPPS Laboratory, Vice President of the Gemmological Association and Gem Testing Laboratory of Great Britain, author and gentleman.

Abstract: *Pearls from the Lion's Paw scallops* Nodipecten (Lyropecten) nodosus *L. 1758 and* Nodipecten (Lyropecten) subnodosus *Sowerby 1835 are rare and have only recently come to the notice of the gemmological community. They are non-nacreous but differ in surface appearance and composition to other non-nacreous pearls such as the Conch and Melo varieties. The surface appearance is comprised of a patchwork of cells with each cell being formed from three sub-cells. The orientation of these sub-cells and the low magnification fibrous appearance of structures within them give the scallop pearl a peculiar surface sheen. SG and Raman data indicate that the perfectly round 5.91 ct scallop pearl described is composed in the main of calcite rather that being dominated by aragonite as is the case for the Melo and Conch pearls. In addition the chemistry, infrared, and UV/visible spectra for the 5.91 ct scallop pearl are described. These data are compared with similar data from lion's paw shells and detailed submicroscopic structures are described for the shells.*

Keywords: *lion's paw scallop,* Nodipecten magnificus, Nodipecten nodosus, Nodipecten subnodosus, *USA*

Introduction

Not frequently seen but relatively well known to gemmologists are those often quite valuable (Shigley *et al.*, 2000) natural pearls, formed within molluscs that do not produce nacre (Gutmannsbauer and Hänni, 1994; Hänni, 1999). Examples of these non-nacreous pearls are the Conch pearl from *Strombus gigas* (Farn, 1977; Fritsch and Misiorowski, 1987; Moses, 2001), the clam pearl from *Tridacna gigas* (Anderson, 1971), the horse-Conch pearl from *Pleuroploca gigantean* and the Melo pearl from any of the various Melo volutes (Brown and Kelly, 1990; Scarratt, 1992, 1996; Traub, 1999). The most

ISSN: 1355-4565

Figure 1: *A* Nodipecten subnodosus *shell.*

common of these rare non-nacreous pearls is the spectacular variety produced by *Strombus gigas* or the Queen Conch, and the rarest being the spectacular Melo pearls. Of late another non-nacreous pearl variety, the scallop pearl has become known and thus far a very limited number recorded. The following briefly describes *Nodipecten (Lyropecten) nodosus* L. 1758 (Atlantic Lion's Paw) and *Nodipecten (Lyropecten) subnodosus* Sowerby 1835 (Pacific Lion's Paw) and one particular pearl that was produced by one of these colourful scallops. Another scallop pearl produced by the Atlantic Sea Scallop (Placopecten magellanicus) has also been recently described (Wight, 2004).

The lion's paw scallop: its description, distribution and habitats

The scallops or pectens are bivalves that have been a part of man's existence from the earliest of times, both as a source of food and adornment. The shapes of the shells and wide variety of colours and patterns have caused them to be a significant collector's item, to be the focus of scientific study, to serve as industrial symbols such as that of the oil company Shell, and to feature as the centre piece of art forms. A particularly impressive art form where the focal point is the lion's paw shell (*Figure 1*) (so called as the shell resembles a lion's paw (Anonymous, 2003)) may be seen in a brooch created by Cartier (Paris) *ca.* 1958 (*Figure 2*). The shell is accompanied by turquoise and sapphires and set in gold (Anonymous, 2004), the brooch being valued in the region of $28,000 (Fitzpatrick, 2002).

Of the many scallops there are three bearing the common name Lion's Paw. One of these is the exceedingly rare *Nodipecten magnificus* (Sowerby, 1835) which is largely restricted to the Galapagos Islands (although one was recently dredged off the coast of

Colombia (Hill and Carmihael, 2004)) and given this rarity is not a focus of this paper. The other two are *Nodipecten (Lyropecten) nodosus* L. 1758 (Atlantic Lion's Paw) and *Nodipecten (Lyropecten) subnodosus* Sowerby 1835 (Pacific Lion's Paw), the largest pectinid in tropical waters and the one described as the probable source of the scallop pearl portrayed herein. *N. nodosus* is found in the seas off the south-eastern USA to Brazil and *N. subnodosus* in the seas off western Central America at depths between 25 and 150 m. Together the shell colours are exceptional both in their variety and depth (Hill and Carmihael, 2004). The outer surface of the shell may be several shades of brown, sometimes described as chocolate brown (Norris, 2003) and yellow to orange while the interior varies from pearly white to shades of purple and brown (*Figure 1*). The outer surface of the *N. nodosus* shell most commonly displays several rows of rounded nodular protuberances located on about eight rounded ribs (although many from the southern Caribbean are smooth (Hill and Carmihael, 2004)) potentially differentiating it from shells of *N. subnodosus* which typically have no such protuberances. Both the Atlantic and Pacific Lion's Paws have fan-shaped (typical of scallops in general) equal valves with unequal ears (Wye, 1991).

Scanning electron microscope studies give some insight into the architecture of the lion's paw shell. Classical nacre consists of fine tabular aragonite which provides the typical nacreous lustre.

Non-nacreous shell material from *Strombus gigas* consists of aragonite fibres lying in bunches in crossed arrays (Kamat *et al.*, 2000). The scallop shell displays a different structure. A surface image shows fibres lying in bunches in different directions almost parallel to the surface (*Figure 3*).

The thickness of the fibres is around 0.5 μm. An image of a broken section shows that under the surface the bunches of fibres still have a crossed orientation (*Figure 4*). At higher magnifications the fibres can be seen as geometrically not very well defined rods with the width and depth almost equal (*Figure 5*). At a magnification of 10,000× there is no trace of organic material in or between the fibres.

From the SEM images of the shell (*Figures 3, 4* and *5*) it becomes clear that depending on the direction of light the fibres will be in either a 'conducting' (ends of the fibres towards the light) position and appear dark, or 'reflecting' (other directions towards the light) position and appear light. This phenomenon is also responsible for the shimmering silk-like appearance seen in other shells that have a similar construction, e.g. *Strombus gigas* and the Melo volutes. In these shells too, bunches of fibres are in crossed orientation (Kamat *et al.*, 2000) and either reflect or conduct incoming light but in this case producing the ubiquitous flame-like pattern (Farn, 1977) well known for these materials.

Barrios-Ruiz reports (Barrios-Ruiz *et al.*, 2003) that *N. subnodosus* was cultured in La Paz Bay (1995-1996) and noted that the culture is feasible. However, high water temperatures in La Paz Bay in summer reduced growth and survival rates.

Figure 2: *A brooch consisting of turquoise, sapphires and gold set on a lion's paw shell, created by Cartier (Paris) ca. 1958; courtesy of Primavera Gallery, New York, photo Noel Allum.*

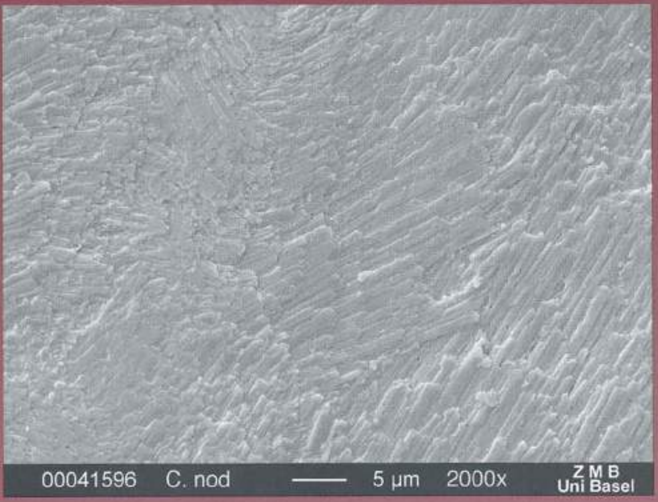

Figure 3: Fibres lying in bunches in different directions almost parallel to the surface of the scallop shell.

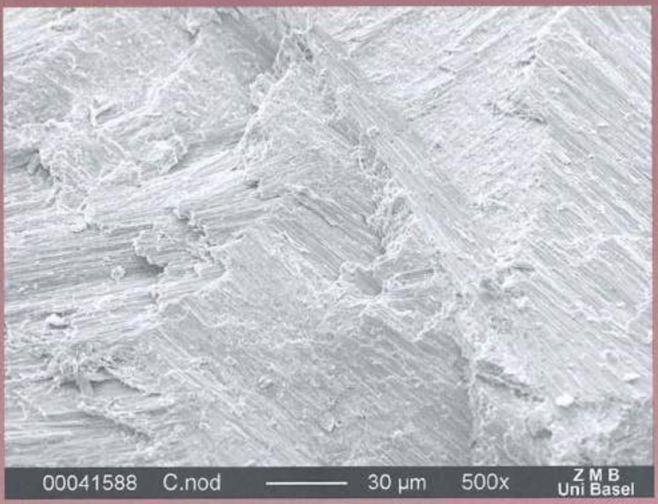

Figure 4: A broken section of a scallop shell shows that under the surface the bunches of fibres still have crossed orientations.

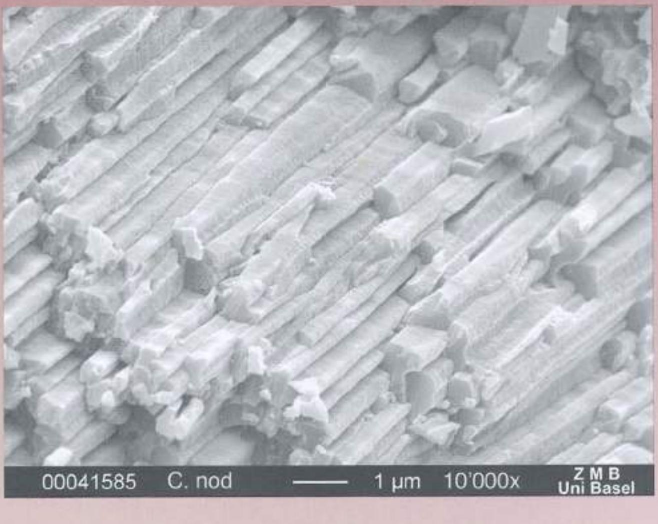

Figure 5: At higher magnifications the fibres in the scallop shell can be seen as rods with width and depth almost equal, but neither round nor square, and not geometrically well defined in cross section.

A natural pearl from the lion's paw scallop

Materials and methods

While the authors have been given the opportunity to view and perform limited examinations on several, they have had the opportunity to complete a detailed examination on only one scallop pearl which is said to be derived from *Nodipecten (Lyropecten) subnodosus*. The data included in this paper are gathered from that one pearl which is perfectly round and weighs 5.91 ct (*Figures 6* and *7*). Several shells of both the Atlantic and Pacific lion's paw types have also been examined and these data are compared with the pearl.

Analytical techniques employed by the authors include microscopy using gemmological microscopes at magnifications ranging from 15 to 60× and the Leica DMLM connected to a Raman microscope at magnifications of up to 1000×. Scanning electron microscopy of shell sections was performed at the University of Basel (ZMB SEM Laboratory) with a Philips ESEM XL 30 FEG with magnifications up to 10,000×; specific gravity (SG) determinations were determined hydrostatically using an appropriately fitted Mettler electronic balance with water at room temperature; UV/visible spectra were recorded in reflectance mode using a Zeiss MCS 500/501 spectrometer recording data for these purposes between 250 and 800 nm; infrared data were obtained using a Thermo-Nicolet Avatar 360 FTIR spectrophotometer utilizing a diffuse reflectance accessory (pearl) and a Thermo-Nicolet Magna 560 using a 4× beam condenser (shell), both at a resolution of 4 cm^{-1}; Raman data were recorded from a Renishaw Raman system 1000 spectrometer incorporating a 512 nm argon ion laser; and qualitative chemical compositions were measured using an Energy Dispersive X-ray Fluorescence Spectrometer (EDXRF) manufactured by EDAX (DX95) operating in vacuum at 35 kV and 450 µA. X-radiographs were produced using a Faxitron X-ray unit at 90 kV and 3 ma.

The LA ICPMS instrument used is a prototype excimer ArF laser (193 nm). Sample material is ablated (craters of 5 - 80 μm in diameter) and then flushed into an Elan 6000 quadrupole ICP mass spectrometer for 'simultaneous' multi-element analysis. The laser optics were developed in collaboration with Microlas (Göttingen). With this prototype instrument we can quantify as little as 0.01 ppm of trace elements in minerals, gemstones or archaeological samples from single spot ablations.

Figure 6: The 5.91 ct scallop pearl on a scallop shell which shows the two colour zones at the rim and centre.

Results

Appearance

Natural pearls from the lion's paw scallop, *N. subnodosus*, occur in a variety of shapes and colours and have been described as resembling high-fired pottery (Norris, 2003). They may be drop-shaped, oval, button, round, off-round or baroque, while the colour range has been variously described as white to deep royal purple with varying shades of oranges, pinks and plum (Hurwit, 1998; Anonymous, 2003). The surface of the pearls displays a shimmering sheen effect particularly when viewed under a bright light. The first short gemmological reports appeared on these rare pearls in 1998 and 1999 (Hurwit, 1998, 1999). A further general description appeared in 2004 (Federman, 2004).

The inside of the lion's paw shell shows two colour zones indicating different materials; a wide ruffle-like margin at the edge with a distinctive sheen which is an orange to purple colour (*Figures 6* and *8*) and a white interior. The external mantle tissue

Figure 7a: A close-up of the 5.91 ct scallop pearl from the collection of Mr. Olivier Galibert and described in the text.

Figure 7a: A group of four scallop pearls of various qualities and shapes (from the collection of K.C. Bell)

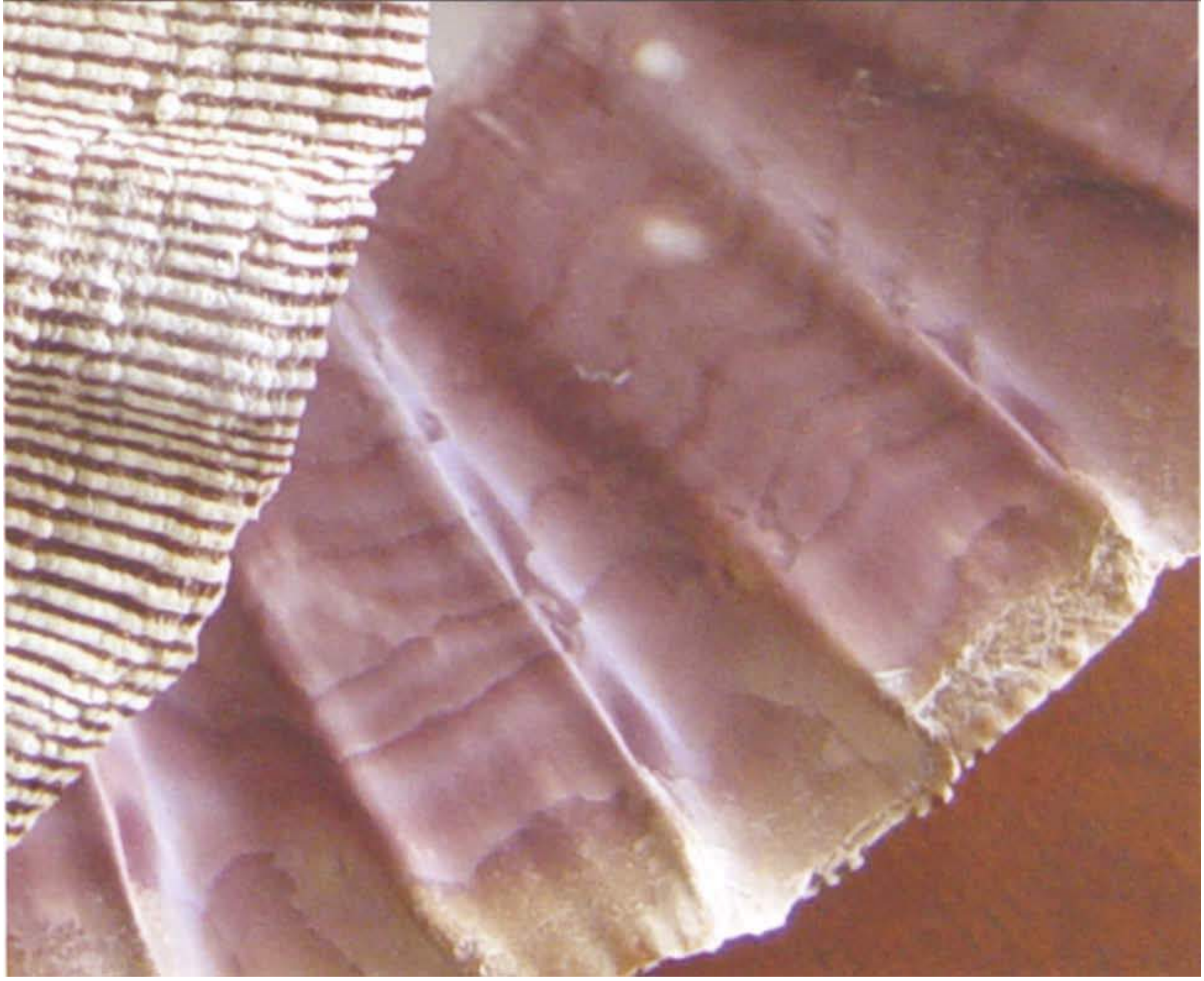

Figure 8: A wide ruffle-like margin with a distinctive sheen at the edge of a scallop shell.

produces two materials as a function of age (Gutmannsbauer and Hänni, 1994); the younger mantle tissue produces the pigmented purple material and at a genetically programmed moment in the life of the mantle tissue cell, this production changes and the cell precipitates the white material, with no pigment.

It thus depends upon the moment of a pearls harvest, whether it is purple (produced by the mantle tissue in the juvenile period) or white (produced by the epithelium that has shifted to the second stage) or a combination of the two. The purple margin on the shell is relatively wide when compared with the *Pinctada* or *Pteria* shells where the columnar growth produces smaller rims. We can thus expect a large number of lion's paw pearls to be of a plum colour with only the older pearls having a white coating.

Chemical composition

As is common with pearls of all varieties, scallop pearls are composed principally of calcium carbonate (Hurwit, 1998). An examination of the chemistry of the 5.91 ct scallop pearl using EDXRF confirmed Ca as being dominant with Sr also showing a significant presence. An examination of the lion's paw shells revealed similar data. In both the pearl and the shells examined, various trace elements were also recorded, but since some are possibly the result of contamination picked up since recovery, they are not reported here.

A few shell samples (see *Table I*) were analysed by LA ICPMS to compare their trace element composition with that of a Pacific lion's paw shell. LA ICPMS is a method that is increasingly used in gemmology for the detection of low concentrations and for light elements (Heinrich *et al.*, 2003). In *Table I* concentrations of some elements are shown, the figures (in microgram per gram – ppm) are mean values from three point analyses. The sample shell of the Pacific Lion's Paw shows the highest magnesium concentration compared to all other shells. With its low manganese content

Table I: *Trace element contents in (ppm) of some shell materials identified by LA ICPMS.*

	Lion's Paw (Pacific)	P. maxima (Australia)	P. margaritifera (Tahiti)	Hyriopsis schlegeli (China)	Unio (China)	A. plicata (China)
Na	2119	6674	8019	2092	1857	2369
Mg	813	185	508	20	31	20
B	18	20	22	4	4	4
P	311	34	35	188	113	137
K	54	62	113	12	65	13
Mn	0.6	3	0.7	760	658	733
Sr	924	1077	926	666	2588	384
Ba	0.4	0.4	0.1	253	509	137

it is in line with other saltwater shell material.

Structure

The structure at the surface of pearls produced by the lion's paw scallop is unique and upon sight is sufficient to identify the origin of such a pearl. The structure at the surface may be described as a segmented patchwork of cells, each cell comprising three differently oriented sub-segments. Within each sub-segment there is what appears to be at low magnifications a 'fibrous structure' (*Figures 9* and *10*) that is differently oriented for each sub-segment. Light reflecting from these 'fibrous structures' produces a shimmering effect similar to that produced by tiger's-eye and this is a unique feature of this type of pearl. Although the light shimmering effect is also seen in the shells of both *N. nodosus* and *N. subnodosus* (*Figure 8*) it is not in the segmented form as observed on the pearl.

SG and X-radiography

The SG of the 5.91 ct scallop pearl was determined to be 2.65 which is rather low for non-nacreous pearls. SGs determined for the Melo pearls have been found to be fairly consistent and are generally 2.84 to 2.85 (Traub *et al.*, 1999), although a few lower values down to 2.78 have been recorded. However, these lower values can be attributed to a greater amount of organic/less X-ray absorbent material contained within these pearls. For Conch pearls Webster (Webster, 1994) gave an SG range of 2.81 to 2.87. From this it has been suggested (Fritsch and Misiorowski, 1987) that a composition for Conch pearls of 40% calcite and 60% aragonite was likely, the individual specific gravities for calcite and aragonite being 2.71 and 2.93 to 2.95 respectively. The 2.65 SG recorded for the 5.91 ct scallop pearl suggests a higher content of calcite than aragonite. This conclusion is strengthened by the Raman data.

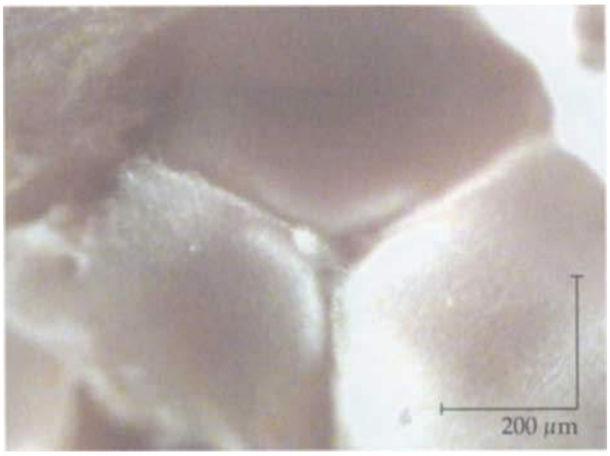

Figure 9: *The structure at the surface of the scallop pearl may be described as a segmented patchwork of cells, each cell comprising three differently oriented sub-segments.*

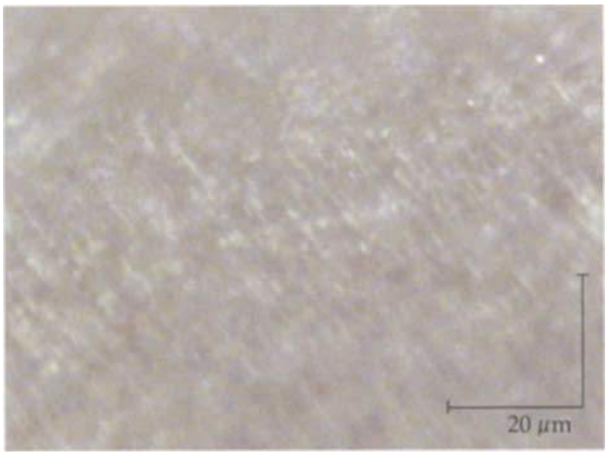

Figure 10: *Within each sub-segment (see Figure 9) there is what appears to be at low magnifications a 'fibrous structure'.*

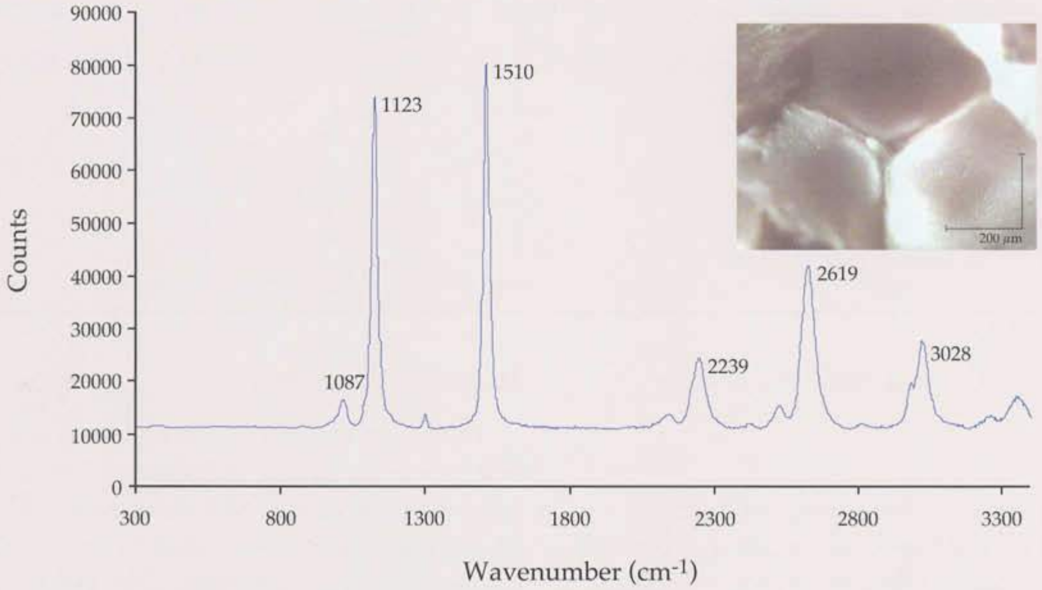

Figure 11: The Raman spectrum of the 5.91 ct scallop pearl.

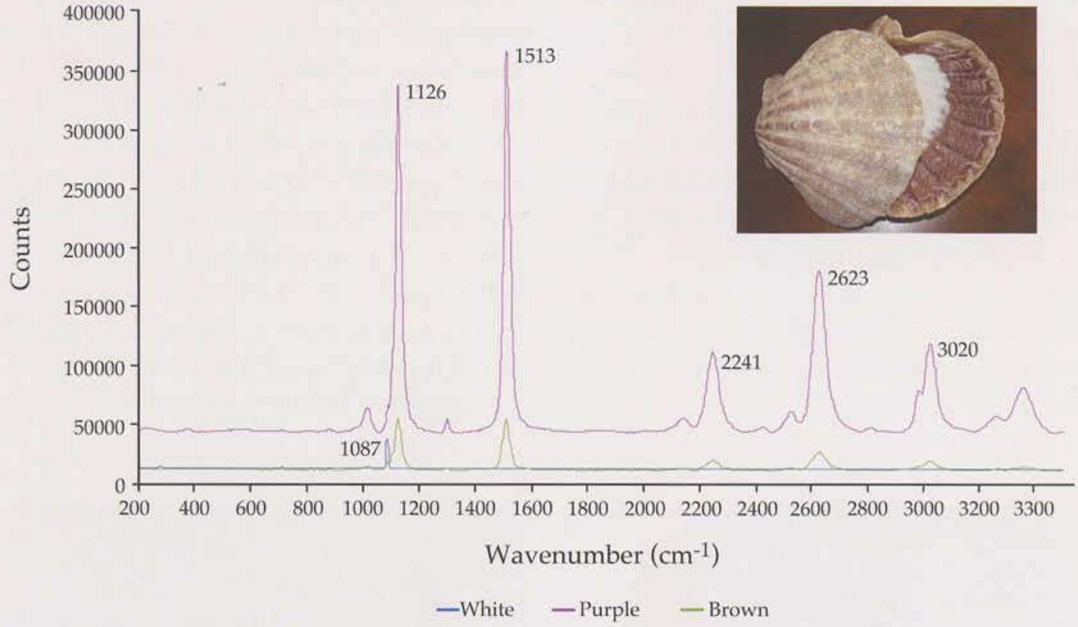

Figure 12: Raman spectra of the purple, brown and white areas of the interior of a N. subnodosus *shell.*

While being the most powerful technique in the arsenal of the gemmologist when distinguishing natural from cultured pearls, X-radiography relies upon the differences in X-ray absorbance between the alternating crystalline and organic layers that are generally present within a nacreous pearl (natural or cultured) (Kennedy, 1998; Akamatsu *et al.*, 2001) but these differences are not necessarily obvious in non-nacreous pearls. Non-nacreous pearls tend to have a structure that consists of dense closely packed crystal arrays without large amounts of organic material being present. Therefore,

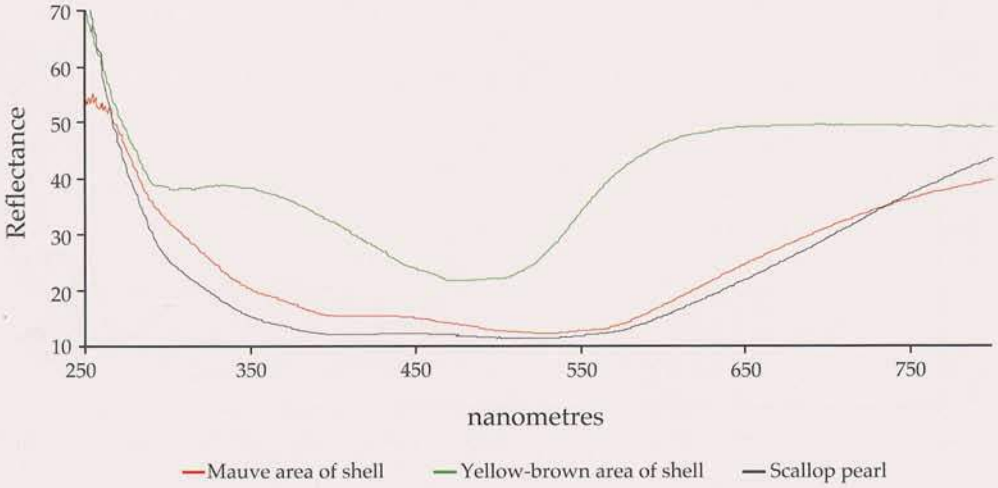

Figure 13: The UV/visible spectra recorded for the 5.91 ct scallop pearl and the yellow-brown and purple areas of the scallop shell.

in general non-nacreous pearls are opaque to X-rays and only occasionally show the presence of organic material by X-radiography. As was to be expected, radiographs taken of the 5.91 ct scallop pearl revealed only a small centrally placed dark arc partially surrounding a dark but extremely small central core, and a few very faint arcs towards the periphery of the pearl. While these structures were sufficient to confirm that it was a cyst-type pearl and of natural origin the apparent small amount of organic material present could not explain the low SG (Traub *et al.*, 1999) but rather supported the conclusion that calcite rather that aragonite is the main component of this scallop pearl.

Raman, UV/visible and infrared spectra

Raman spectra (Kiefert *et al.*, 2001) for the 5.91 ct pearl were collected from several different areas and compared. All areas examined produced the same spectrum with primary peaks located at 1123, 1510, 2239, 2619 and 3028 cm^{-1} (*Figure 11*). These peaks are due to the carotenoids (Fritsch and Misiorowski, 1987; Moses, 2001; Huang *et al.*, 2003; Withnall, *et al.*, 2003) present in the pearl. A peak of comparatively very weak intensity located at 1087 cm^{-1} and which we can attribute to calcite (Li and Chen., 2001; Huang *et al.*, 2003; Kiefert *et al.*, 2004) was also noted. The spectrum for this pearl differs from those recorded for other non-nacreous pearls such as those produced by *Strombus gigas* (the Conch pearl) and the Melo volutes (the Melo pearl). Both the Conch and Melo pearls show peaks normal for aragonite (rather than calcite) at 1085 cm^{-1} and 703 and these are also dominant over the carotenoid peaks. The Raman spectrum for the scallop pearl is similar to that shown by natural red coral.

The Raman spectrum of the 5.91 ct scallop pearl was compared with the spectra produced from the white, purple and brown areas on the interior of one *N. subnodosus* shell (*Figure 12*). The white area produced the complete Raman spectrum typical of calcite with peaks at 281, 713, 1087 and 1433 cm^{-1} and none indicating the presence of any carotenoids; the brown area showed relatively low intensity carotenoid peaks at

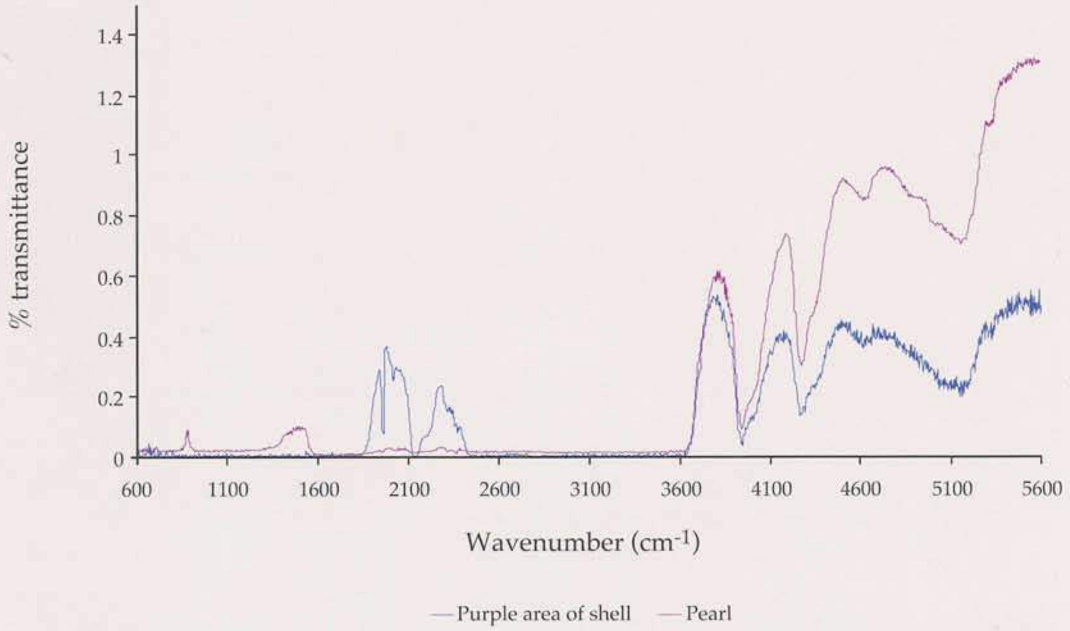

Figure 14: The infrared spectra recorded for the scallop pearl and the purple area of a scallop shell.

1126, 1513, 2241, 2623 and 3020 cm^{-1} that allowed the main calcite peak at 1087 cm^{-1} to be clearly recorded. In contrast, the spectra from the purple area showed carotenoid peaks of such intensity (about six times the count rate) as to completely obscure the strongest calcite peak.

UV/visible spectra were recorded in reflectance mode for the 5.91 ct pearl, and for white, purple and brown areas on the interior of one *N. subnodosus* shell (*Figure 13*). The spectra recorded for purple areas of the shell's interior and that for the pearl showed similar features. Broad but shallow absorption features were noted centred at 540 and 410 nm. For the yellow-brown areas on the shell two merging features were noted at approximately 510 and 460 nm; and for the white areas, as to be expected, only a flat line with no features was recorded.

The infrared spectra were obtained from both the 5.91 ct pearl and the purple area of a lion's paw shell *(N. nodosus) (Figure 14).* Above 1550 cm^{-1} both spectra were similar with features at 1960, 2018, 2140, 3932, 4264, 4593 and 5133 cm^{-1}. Below 1550 cm^{-1} the scallop pearl had additional features at 1508 and 1457 cm^{-1}.

Discussion

The shell of the lion's paw scallop is one of the most beautiful of all seashells (Hill and Carmihael, 2004) and it is therefore not surprising that any pearls produced by this mollusc should also be beautiful. However, it is surprising that given the beauty of the shells and their desirability to collectors, that knowledge of the scallop pearl has not reached gemmologists until recently.

Pearls from the lion's paw scallop are distinctive in so much as their surface structure is dissimilar to that of any other non-nacreous pearl. They are probably composed predominantly of calcite rather than aragonite and the strength of the carotenoid Raman peaks (in relation to the calcite peaks) is very distinctive. The combination of colour, structure and optical effects is unique among pearls and without doubt as a gem material they are exceedingly rare.

Acknowledgements

The authors gratefully acknowledge the cooperation and assistance of their colleagues in the AGTA and SSEF Laboratories; Olivier Galibert is thanked for allowing the full examination of the 5.91 ct scallop pearl described; Jeremy Norris for sight of several scallop pearl samples of all shapes, sizes and colours plus stimulating discussions on the subject as well as donation of a *N. subnodosus* shell; K.C. Bell for the loan of several samples (see Figure 7b) some of which will eventually be used for destructive analysis; and the authors are indebted to Wes Rankin for the gift of a *N. nodosus* shell. The Primavera Gallery of Madison Avenue, New York, is thanked for allowing, as owners of the item, the reproduction of Figure 2. We thank Dr T. Pettke, SFIT, Institute of Isotope Geochemistry, Zürich, Switzerland, for the LA ICPMS data.

References

Akamatsu, S., Li T.Z., Moses, T.E., and Scarratt, K., 2001. The current status of Chinese freshwater cultured pearls. *Gems & Gemology*, 37(2), 96-113

Anon., 2003. Scallop pearls. *http://www.allnaturalpearls.com/scallop.htm* 2003, December

Anon., 2004. Cartier, Paris shell pin. *http://www.primaveragallery.com/jewel.asp* 2004, May

Anderson, B. W., 1971. More notes from the Laboratory: Pearls from the Giant Clam. *The Journal of Gemmology*, 12(6), 206-8

Barrios-Ruiz, D., Chávez-Villalba, J., and Cáceres-Martínez, C., 2003. Growth of *Nodipecten subnodosus* (Bivalvia: Pectinidae) in La Paz Bay, Mexico. *Aquaculture Research*, 34(8), 633

Brown, G., and Kelly, S.M.B., 1990. A rare baler shell pearl. *Australian Gemmologist*, 17(8), 307-8

Farn, A.E., 1977. Notes from the Laboratory: Pink Conch pearl. *The Journal of Gemmology*, 15(7), 361-2

Federman, D., 2004. Gem profile: scallop pearl: Baja Beauty. *Modern Jeweler*, April, 38

Fitzpatrick, K., 2002. Splash! Marine-inspired jewelry. *http://www.departures.com/wg/wg_0702_seajewels.html* accessed May 2004

Fritsch, E., and Misiorowski, E., 1987. The history and gemology of Queen Conch pearls. *Gems & Gemology*, 23(4), 208-21

Gutmannsbauer, W., and Hänni, H.A., 1994. Structural and chemical investigations on shells and pearls of nacre forming salt-and fresh-water bivalve molluscs. *The Journal of Gemmology*, 24(4), 241-52

Hänni, H.A., 1999. Sur la formation de nacre et de perles. *Revue de Gemmologie A.F.G.*, 137, 30-6

Heinrich, C.A., Pettke, T., Halter, W.E., Aigner, M., Audedat, A., Günther, D., Hattendorf, B., Guillong, M., and Horn, I., 2003. Quantitative multi-element analysis of minerals, fluid and melt inclusions by Laser-Ablation Inductively-Coupled Mass-Spectrometry. *Geochim. Cosmochim. Acta.*, 67, 3473-97

Hill, L., and Carmihael, P., 2004. *The World's Most Beautiful Seashells*, 7th edn. World Publications, Tampa, FL

Huang, F., Yun, X., Yang, M., and Chen, Z., 2003. Pearl cultivation in Donggou, Ezhou, Hubei, and cathodoluminescence of cultured pearls. *The Journal of Gemmology*, 28(8), 449-62

Hurwit, K., 1998. Gem Trade Lab Notes: Non-nacreous 'pearls'. *Gems & Gemology*, 34(4), 288

Hurwit, K., 1999. Gem Trade Lab Notes: Update on non-nacreous pearls. *Gems & Gemology*, 35(2), 140

Kamat, S., Su, X., Ballarini, R., and Heuer, A.H., 2000. Structural basis for the fracture toughness of the shell of the Conch *Strombus gigas*. *Nature*, 405, 1036-40

Kennedy, S., 1998. Pearl identification. *The Australian Gemmologist*, 20(2), 2-19

Kiefert, L., Hänni, H., and Ostertag, T., 2001. Raman Spectroscopic Applications to Gemmology. In: *Handbook of Raman Spectroscopy, from the Research Laboratory to the Process Line*, Lewis, H.G.M.E.I.R. (Ed.). Marcel Dekker, New York/Basel

Kiefert, L., Moreno, D. McL., Arizmendi, E., Hänni, H., and Elen, S., 2004. Cultured Pearls from the Gulf of California, Mexico. *Gems & Gemology*, 40(1), 26-38

Li L., and Chen Z., 2001. Cultured pearls and colour-changed cultured pearls: Raman spectra. *Journal of Gemmology*, 27(8), 449-55

Moses, T., 2001. Gem Trade Lab notes: Conch 'pearl', highly unusual necklace layout. *Gems & Gemology*, 37(3), 213

Norris, J., 2003. Scallop pearls. *http://www.oasispearl.com/scallop.html* 2003, December

Scarratt, K., 1992. Notes from the Laboratory: Orange Conch pearls. *The Journal of Gemmology*, 23(3), 137-8

Scarratt, K., 1996. *Pearls and corals from Asia.* Gemmologia Europa VI, CISGEM, Milan, 12-27

Shigley, J.E., Dirlam, D.M., Laurs, B.M., Boehm, E.W., Bosshart, G., and Larson, W.F., 2000. Gem localities of the 1990s - calcareous concretions. *Gems & Gemology*, 36(4), 309-10

Traub, J., Zucker, B., Content, D., and Scarratt, K., 1999. *Pearl and the Dragon: A Study of Vietnamese Pearls and a History of the Oriental Pearl Trade*, Content, Derek J., Rare Books Incorporated, Houlton, Maine, USA

Webster, R., 1994. *Gems: Their Sources, Descriptions and Identification.*, 5th edn. Butterworth-Heinemann, Oxford

Wight, W., 2004. Scallop pearls from Digby, Nova Scotia, Canada. *Canadian Gemmologist*, 25(1), 18-29

Withnall, R., Chowdhry, B.Z., Silver, J., Edwards, H.G.M., and de Oliveira, L.F.C., 2003. Raman spectra of carotenoids in natural products. *http://www.cephbase.utmb.edu/refdb/pdf/7824.pdf* Accessed August 2004

Wye, K. R., 1991.*The Encyclopedia of Shells*. Quato Publishing plc, London.

A treatment study of Brazilian garnets

Sigrid G. Eeckhout[1], Antonio C.S. Sabioni[1] and Ana Cláudia M. Ferreira[2]

1. *Department of Physics/ICEB, Federal University of Ouro Preto, Minas Gerais, Brazil*
2. *Department of Mining and Geology, Federal University of Paraíba, Brazil*

Abstract: *Over the past decade, there has been noticeable growth in interest in coloured stones worldwide, which has led to an increase in gem exploration, production and marketing. Since garnet displays a very large variety of colours, it deserves further attention. Although reports on enhanced gemstones are widespread in the gemmological literature, very few studies have been performed on the enhancement of garnets. We report the first systematic, scientific treatment study on Brazilian garnets from known geological localities, including thermal and diffusion treatment. Iron-containing species become opaque and produce a 'silvery skin'. Light yellow grossular turns to orange similar to that of Imperial-topaz. Other garnet varieties have stable colours, confirming the absence of colour centres. A preliminary diffusion treatment of some rough grossular has produced attractive green and orange stones. Since orange gemstones are becoming increasingly popular and since the diffusion-treated green grossulars resemble some emeralds in colour, they may be of economic importance in the future if quantities are confirmed to justify commercial mining.*

Introduction

Colour is one of the most important aspects of the beauty of a gemstone and it is a significant contributor to a gemstone's value. Members of the garnet family have been used as gems since prehistoric times, and they are found in a wide range of colours. Red pyrope and almandine are probably the most common and most widely used gem varieties. In recent years, purplish-red rhodolite garnet has become increasingly popular. Andradite is the most lustrous of all garnets and has three gem varieties, viz. green demantoid, yellow topazolite, and opaque, black or dark red melanite. New finds of spessartine in Namibia, Nigeria (Shigley *et al.*, 2000) and Brazil (Ferreira, 1997) have sparked renewed interest in the rare orange variety. Grossular garnet is found in various colours, with the varieties hessonite (cognac) and tsavorite (green) being the most popular. Uvarovite, the rarest of the familiar garnets, is seldom used as a gem. It is the only garnet variety that does not occur in Brazil (Delaney, 1996). Colour-change garnets found in Madagascar change from blue-green in daylight to purple in incandescent light (Schmetzer and Bernhardt, 1999).

Many Brazilian museums have garnet specimens but their locations are usually

ISSN: 1355–4565

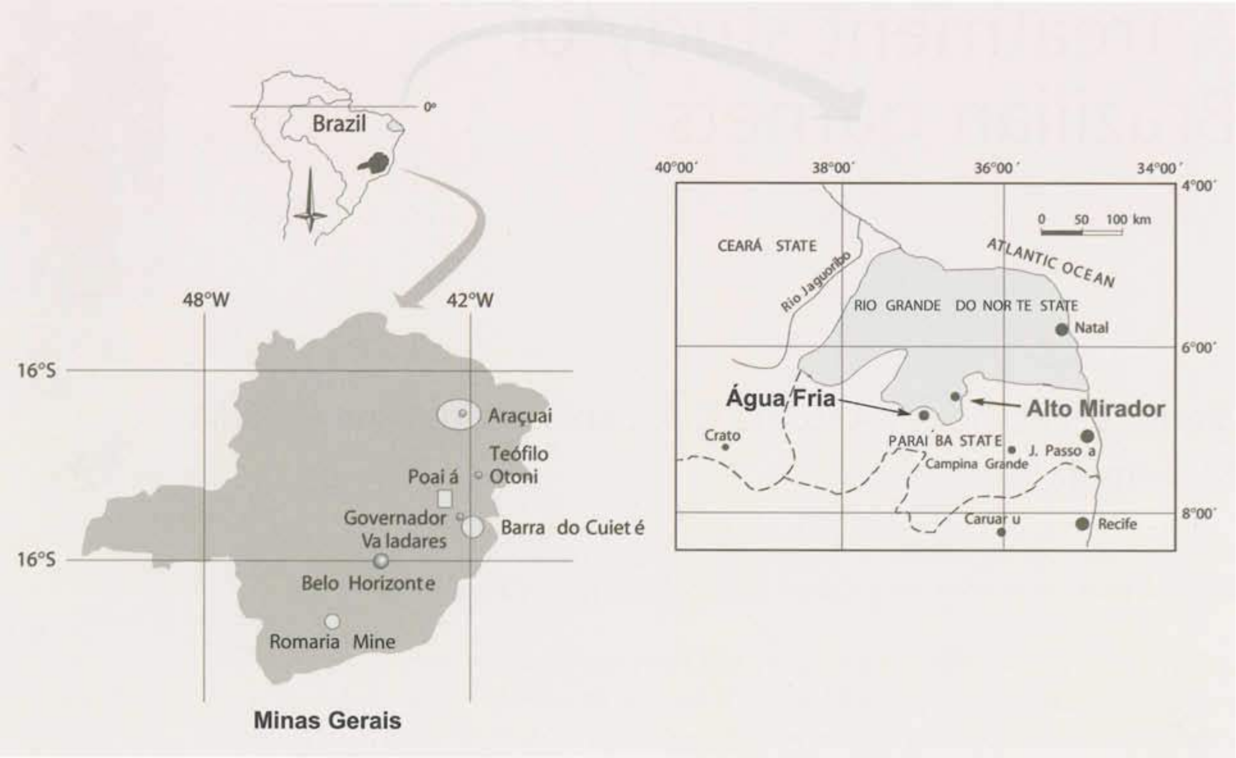

Figure 1: Maps of parts of Brazil indicating localities of the studied garnets.

poorly described. Furthermore, details of the geological environment or the mineralogical affinities of Brazilian garnet occurrences reported in the literature are very scarce. As a consequence, the range of Brazilian garnets, including pyrope, almandine-pyrope, almandine-spessartine, spessartine, spessartine-almandine, grossular and the gem-varieties rhodolite and hessonite, will be outlined before describing our experimental work.

Since gem treatment is a field of high potential wherein less attractive gemstones are transformed to more desirable stones by various methods such as chemical treatment, heating and irradiation, a range of garnet varieties was assembled for study. Although reports on enhanced gemstones are widespread in the gemmological literature (e.g. Nassau, 1994; McClure and Smith, 2000, and references therein), very few studies have been performed on the enhancement of garnets. During the first stage of our experimental work on gem garnets from Brazil, heat treatments were performed on representative samples, since thermal enhancement is the most common and easiest type of treatment for gems. Furthermore, the results of heat-treatment on most stones are stable and permanent under normal conditions of wear. In the following stage some selected grossular garnets were diffusion treated and preliminary results were obtained.

Materials and methods

Occurrence and geology of garnet samples

Garnets occur in many geological environments in Brazil. These include metamorphic rocks, igneous rocks, pegmatites, kimberlites and in sediments as detrital grains (Deer *et al.*, 1982). However, gem-quality garnets have been found in only two of these environments, namely pegmatites and alluvial deposits, and recovered as a byproduct of some other gemstone mining objective (Delaney, 1996). Localities of the studied garnets are shown in *Figure 1*.

Pyrope

Pyrope is one of the main locator minerals in diamond prospecting. Pyrope garnets have been recovered from the Romaria mine (originally called Água Suja) which is now defunct, on the Marrecos Ranch, SW of Monte Carmelo, Minas Gerais state. The geology of the Romaria mine has been described by Svisero *et al.* (1981).

Almandine-pyrope

The almandine-pyrope garnets are from the Fazenda Balisto, Município Peixe, WSW of São Valério da Natividade, Tocantins state. They possess an unusual, attractive, purplish-red colour and are therefore called rhodolite in the jewellery trade (Wegner *et al.*, 1998). They are found in alluvial gravels and their source is not yet known.

Almandine-spessartine

The almandine-spessartine garnets are from the Serra dos Marimbondos granitic pegmatite, Carnaúba dos Dantas, Seridó district, Rio Grande do Norte state (Ferreira, 2001, pers. comm). The garnets are concentrated in ore-shoots with feldspar, quartz and muscovite.

Spessartine

Gem-quality spessartine samples have been recovered from the Alto Mirador granitic pegmatite, Seridó district, NE of Carnaúba dos Dantas, Ermo village, Rio Grande do Norte state (Ferreira, 1984, 1997; Ferreira *et al.*, 2000). The highly fractured, complex and internally zoned Alto Mirador pegmatite belongs to the lithium-rich Borborema sub-province of the northeastern gemmological province (Pinto and Pedrosa-Soares, 2001). The garnets occur in fracture fillings and in open cavities or pockets and the colours range from reddish orange and yellowish orange to orange. *(Figure 2)*.

Spessartine-almandine

Spessartine-almandine varieties were collected from the substitution bodies of the Poaiá pegmatite. Sao José da Safira district, Minas Gerais state. The Poaiá pegmatite is one of the most important garnet-bearing pegmatites of the Sao José da Safira district and the gemstones possess orange-red, reddish-orange or cognac colours (*Figure* 2) (Cassedanne and Cassedanne, 1977).

Figure 2: *Samples of rough spessartine with diameters up to 2.5 cm and spessartine-almandine garnets with colours varying from reddish orange and orange to yellowish orange.*

The pegmatite is situated in the Eastern gemmological province (Pinto and Pedrosa-Soares, 2001).

Grossular

Grossular samples were collected from (1) the Barra do Cuieté pegmatite, Governador Valadares district, Minas Gerais state and (2) the Água Fria skarn, Santa Luzia, Paraíba state (Tavares *et al.*, 2000). The Barra do Cuieté pegmatite belongs to the Eastern gemmological province, whereas the Água Fria skarn belongs to the lithium-rich Borborema sub-province of the northeastern gemmological province (Pinto and Pedrosa-Soares, 2001). Transparent cognac-red grossular (hessonite) samples were found in the tailings of an old mine in Água Fria.

Characterization of samples

For the garnets listed in *Table I*, refractive indices were measured with an Eickhorst Gem Led refractometer on faceted stones (12 for the spessartine samples and 3 for the other compositions) and specific gravities were obtained from rough stones (10 for the spessartine samples and 4 for the other varieties) by hydrostatic weighing.

Three selected crystals of each garnet type mentioned in *Table I* were characterized

*Table I: **Chemical composition and physical properties of Brazilian garnets.***

Variety	Pyrope	Almandine-pyrope	Almandine spessartine	Spessartine			Spessartine almandine			Grossular
Locality	Romaria mine	Fazenda Balisto	Serra dos Marimbondos pegmatite	Alto Mirador pegmatite			Poaiá pegmatite			Barra do Cuieté pegmatite
Colour	red	purplish red	red	reddish orange	orange	yellowish orange	reddish orange	reddish orange	cognac colour	light yellow
n	Not measured	>1.79	>1.79	>1.79	>1.79	>1.79	1.755-1.760	1.755-1.760	1.755-1760	1.740
SG	4.17	4.08-4.11	4.17	4.11-4.22	4.11-4.22	4.11-4.22	4.16-4.18	4.16-4.18	4.16-4.18	3.86
Wt.%	Chemical composition									
SiO_2	40.03	37.88	36.97	36.74	36.82	36.71	35.21	35.17	35.16	37.55
TiO_2	0.29	0.03	0.02	0.15	0.20	0.06	0.01	0.02	0.00	0.04
Al_2O_3	21.13	21.79	21.35	21.12	21.19	21.14	20.80	20.68	20.75	21.01
FeO	9.12	36.49	28.37	2.69	2.72	1.23	11.94	17.44	14.54	1.47
Fe_2O_3	0.00	0.00	0.00	0.30	0.30	0.13	0.00	0.00	0.00	0.00
MnO	0.43	0.04	11.98	38.06	38.28	40.41	30.90	25.85	28.47	0.03
MgO	21.33	4.54	1.55	0.85	0.86	0.50	0.00	0.00	0.00	0.05
CaO	4.24	0.06	0.42	0.22	0.20	0.39	0.15	0.21	00.19	37.35
Cr_2O_3	2.32	0.00	0.00	0.00	0.00	0.00	0.00	0.00	0.00	0.00
Total	98.89	100.83	100.66	100.13	100.57	100.57	99.01	99.37	99.11	97.50
Mol%										
Pyrope	71.7	18.3	6.3	3.3	3.3	2.0	0.0	0.0	0.0	0.3
Almandine	17.0	81.7	64.7	6.7	6.7	3.0	27.3	40.4	33.3	3.0
Grossular	10.3	0.0	1.3	0.7	0.7	1.0	0.3	0.3	0.3	96.7
Spessartine	1.0	0.0	27.7	89.3	89.3	94.0	72.4	59.7	66.4	0.0

Note: FeO obtained by microprobe was calculated as FeO + Fe_2O_3 based on the results of a Mössbauer study, and this for all samples.

by powder X-ray diffraction with a Rigaku Geigerflex diffractometer using CuKα radiation and graphite monochromator. Additional diffraction patterns were recorded on powders, which were scraped from the surface of heat-treated pyrope, almandine-spessartine and spessartine-almandine garnets.

Chemical analyses were performed on thin sections of one selected, rough sample of each type mentioned in *Table I* using a JEOL JXA-8900RL electron microprobe (15 kV and 20 nA). The standards used were albite for Si, olivine for Fe and Mg, rhodonite for Mn, anorthite for Al and Ca, rutile for Ti and Cr_2O_3 for Cr, and raw data were corrected using the ZAF program. Several line scans across each sample were made to look for any chemical zoning. Data were collected from five points on spessartine samples and from ten points on other samples. The elements determined were Si, Fe, Mg, Mn, Ca, Al, Cr and Ti, and to ensure that no other elements with an abundance above the microprobe detection limit were present preliminary, qualitative runs in wavelength-dispersive mode were performed on three spots of each sample in the complete spectral area. The structural formulae were calculated on the basis of 12 oxygen atoms. To do this, total iron obtained by microprobe was converted to FeO and Fe_2O_3 based on the results of a Mössbauer study on similar samples of all garnet types. Mössbauer spectra (MS) were collected at room temperature (RT) using a conventional, constant acceleration spectrometer in conjunction with a 1024 multi-channel analyzer. Mössbauer experiments were additionally performed at room temperature on hessonite samples which previously had been subjected to heat treatments in air at 800°C for four hours and at 600°C for seven days.

For the UV-Vis spectroscopic measurements, platelets 1mm thick were cut from representative rough samples of each garnet mentioned in *Table I*. The platelets were cut from the samples used for the chemical analyses. The platelets were polished on both sides to obtain a thickness ranging from 0.25 to 0.35 mm. To facilitate handling, small crystals were embedded in epoxy, which was later removed by dissolution in acetone. All platelets were checked optically for the absence of both liquid and solid inclusions. UV-Vis spectra were measured, before and after treatment, using a Hitachi U-3501 spectrophotometer in the spectral region 300 to 1100 nm.

In order to identify the diffusion-treated, rough, non-transparent grossular stones, the Rutherford back-scattering technique was used. This is a non-destructive, analytical tool that uses elastic scattering of 1-3 MeV charged particles to analyse the surface and the outer few micrometres of solids.

Treatments

Heating experiments were performed in oxidising, inert and reducing atmospheres and at various temperatures up to 1000°C. For the heating experiments, a batch of 9 to 10 representative, rough stones from each of the following types was assembled: pyrope, almandine-spessartine, reddish-orange and yellowish-orange spessartine, cognac coloured spessartine-almandine, grossular and hessonite. Only the pyrope and grossular samples were not of gem quality.

One representative sample of each variety and colour was not treated, and was retained as a comparator for the heat-treated garnets. The heating experiments were conducted under the following conditions:

1. in air at 800°C for four hours
2. in air at 900°C for four hours
3. in air at 1000°C for four hours
4. in air at 900°C for 24 hours
5. in an oxygen saturated atmosphere ($P_{O_2} = 1$ atm) at 800°C for four hours
6. in an oxygen saturated atmosphere ($P_{O_2} = 1$ atm) at 900°C for four hours
7. in an argon saturated atmosphere ($P_{Ar} = 1$ atm) at 900°C for four hours and
8. in a reducing atmosphere ($P_{H_2} = 1$ atm) at 900°C for four hours.

The hessonite sample was further heated in air for seven days at 600°C, and rough rhodolite was heated in air at 600°C for 24 hours and at 800°C for four hours. After cooling down in air, each heat-treated garnet was compared with the non-treated, reference sample.

In subsequent experiments, four representative light yellow grossular rough samples were subjected to diffusion treatments. The diffusion-treatment process usually involves embedding rough or fashioned stones in a powder consisting of a colouring agent such as iron oxide, within a corundum crucible. The crucible is then subjected to heating in a furnace at relatively high temperatures (900°C). Before the diffusion experiments on the four stones one was kept as a comparator for the diffusion-treated garnets, one was put in iron oxide, one in chromium oxide and one in cobalt oxide; only a very small amount of material was used in each crucible, and they were then placed in a furnace at 900°C for 44 hours.

Results

Characterization of the natural garnet samples

Chemical composition

X-ray diffraction confirmed that all the samples studied belong to the garnet family, and the compositions determined and summarized in *Table I* confirm this.

Physical properties

The refractive index, n, and the specific gravity, SG, of most of the garnets studied are summarized in *Table I*. The pyrope samples studied are small and well rounded. The almandine-pyrope garnets show distinctly weathered surfaces, but the dodecahedral

Figure 3: Rough garnet species before (upper row) and after (lower row) heat treatment at 800°C for four hours in an oxygen saturated atmosphere (P_{O_2} = 1 atm). The following stones are depicted from left to right: reddish-orange and yellowish-orange spessartine, hessonite, almandine-spessartine, grossular, cognac colour spessartine-almandine and pyrope. The average size of the stones is 0.5 cm in diameter.

habit remains visible. The almandine-spessartine garnets occur as anhedral or intergrown crystals with diameters of up to 10 cm. The majority of the spessartine garnets are euhedral with well-developed crystal faces, commonly dodecahedral {011} or trapezohedral {112}; they show lively and brilliant colours varying between reddish orange, orange and yellowish orange *(Figure 2)*. The spessartine-almandine garnets occur as dispersed crystals within the primary minerals (quartz, microcline, muscovite, biotite and K-feldspar) or as gem-quality aggregates, up to several decimetres, within the substitution bodies which are composed of quartz, K-feldspar, albite, muscovite and lepidolite. The spessartine and spessartine-almandine samples are transparent, have vitreous lustre and possess few or no inclusions. No colour-change phenomena were observed when viewed in natural and incandescent light.

Spectral features

UV-Vis spectroscopy was used to determine the causes of colour differences both within and between the garnet varieties. Characteristic absorption peaks for the various types of garnets studied are listed in *Table II*. All pyrope, almandine-pyrope, and almandine-spessartine spectra are characterized by a broad band at ~570 nm, a band at 526 nm, and a broad band at 505 nm. A sharp absorption band at 410 nm and shoulders at

Table II: Characteristic absorption peaks in spectra of the Brazilian garnets studied.

	Pyrope	Almandine-pyrope	Almandine spessartine	Spessartine	Spessartine-almandine	Hessonite	Assignment
Absorption maxima (nm)							
370						•	Fe^{3+}
<390				•	•		ultraviolet charge transfer
410				•	•		Mn^{2+}
421				•	•		Mn^{2+}
429				•	•		Mn^{2+}
459				•	•		Mn^{2+} + Fe^{2+}
482				•	•		Mn^{2+}
505	•	•	•				Fe^{2+}
526	•	•	•				Fe^{2+}
529				•	•		Mn^{2+} + Fe^{2+}
~570	•	•	•				Fe^{2+}

Table III: ***Results of garnet heat treatment.***

	Pyrope	Almandine-pyrope	Reddish-Orange spessartine	Yellowish-Orange Spessartine	Cognac colour Spessartine-almandine	Grossular	Hessonite
In air at 800°C for 4 hours	silvery lustre	silvery lustre	no changes	no changes	silvery lustre	Imperial-topaz colour	no changes
In air at 900°C for 4 hours							
In air at 1000°C for 4 hours		opaque with burned appearance			opaque with burned appearance		
In air at 900°C for 24 hours							
$P_{O_2} = 1$ atm at 800°C for 4 hours		silvery lustre			silvery lustre		
$P_{O_2} = 1$ atm at 900°C for 4 hours							
$P_{Ar} = 1$ atm at 900°C for 4 hours							
$P_{H_2} = 1$ atm at 800°C for 4 hours	no changes	no changes			no changes	no changes	

421, 429, 459, 482 and 529 nm characterize the spectra of the spessartine and spessartine-almandine garnets. Furthermore, a broad absorption below 390 nm extends into the visible region. The strong band at 370 nm is the main characteristic of the absorption spectrum of hessonite.

Garnet treatment

Heat treatments

After heat treatments (*Table III*), both in oxidizing (in air or in an oxygen saturated atmosphere of $P_{O_2} = 1$ atm) and inert atmospheres ($P_{Ar} = 1$ atm), on Brazilian pyrope, almandine-spessartine and spessartine-almandine garnets, a silvery lustre was observed over the whole surface of each heat-treated stone. This silvery lustre is caused by formation of a hematite coating, which was confirmed by powder X-ray diffraction. The silvery lustre is more spectacular on heat-treated almandine-spessartine and spessartine-almandine than on pyrope (*Figure 3*). In a reducing atmosphere, however, no changes were observed and the colours of the treated stones remained unchanged; UV-Vis spectra also remained unchanged. After heat treatment in air at 1000°C for four hours and at 900°C for 24 hours, these iron-rich varieties become opaque and have a completely burned, charcoal-like appearance, which remains even after recutting or repolishing. The powder X-ray diffraction spectrum of such a 'burned' stone indicates that no crystal structure changes occurred and that no hematite was formed.

Following a report that some rhodolite garnets change from purple to a hessonite-type brown on heating at about 600°C (Nassau, 1994), we additionally conducted heating experiments in air on rhodolite. After heating at 600°C for 24 hours, no differences were detected and the absorption spectrum before and after heat-treatments remains the same.

It is apparent from *Table III*, columns 4, 5 and 8, that the heating experiments performed on spessartine and hessonite caused no change of colour (see also *Figure 3*), and there were no changes in their UV-Vis spectra. On the basis of the Mössbauer results, the small amount of total iron in the non-treated hessonite contains 48% Fe^{3+}, that in the hessonite heated at 800°C for four hours contains 51% Fe^{3+} and in the hessonite heated at 600°C for seven days the iron is 55% ferric. So, although no changes in colour were detected after the treatments, there was slight oxidation of the iron.

In all treatments except that in a reducing atmosphere, light yellow grossular turns to orange, showing the Imperial-topaz colour (see *Table III*, column 7 and *Figure* 3). The stone remains light yellow after treatment in a strongly reducing atmosphere (P_{H_2} = 1 atm).

Figure 4: *Light yellow, orange and green grossular. The orange and green colours were obtained after diffusion treatment of the light yellow material with Fe and Co, respectively. The stones have a diameter of about 8 mm.*

Diffusion treatments

The preliminary diffusion treatments produced an orange diffusion layer on the pale yellow grossulars in the presence of either Fe or Cr oxide and a green diffusion layer in the presence of Co oxide. The diffusion-treated pale yellow grossular stones in oxides of iron or chromium show an Imperial-topaz colour, comparable to that of the heat-treated grossulars.

Discussion

The structural formula of garnet is generally represented as $X_3Y_2Si_3O_{12}$, where X and Y refer respectively to eight- and six-fold coordinated cationic sites. The X sites are occupied by rather large, divalent cations, generally Ca^{2+}, Mn^{2+}, Fe^{2+} or Mg^{2+}, whereas the Y sites are occupied by smaller trivalent cations, such as Al^{3+}, Fe^{3+}, V^{3+} or Cr^{3+}. When each site is occupied by only one type of ion, the result is identified as an end member of the garnet mineral group.

Physical properties

The measured refractive index, n, and specific gravity, SG, of the garnets studied, as listed in *Table I*, correspond well with published data (Deer *et al.*, 1982; Ferreira, 1997; Tavares *et al.*, 2000; Wegner *et al.*, 1998). All values fall within the ranges mentioned by Stockton and Manson (1985).

Spectral features

The UV-Vis absorption spectra of pyrope, almandine-pyrope and almandine-spessartine are characterized by common iron bands (Schmetzer *et al.*, 2001). These are a broad band at ~570 nm, a band at 526 nm and a broad band at 505 nm and according to Frentrup and Langer (1982), the Fe^{2+} ions in the eight-coordinated site produce the near-red colour.

The spectra of all spessartine and spessartine-almandine garnets in our study are characterized by iron and manganese bands (Schmetzer *et al.*, 2001). They show a sharp absorption band at 410 nm [Mn], and broad or weak maxima at 421 [Mn], 429 [Mn], 459 [Mn + Fe], 482 [Mn] and 529 [Mn + Fe] nm. The broad absorption below 390 nm, extending into the visible region, is due to ultra-violet charge transfer, caused by electron transfer from O^{2-} ligands to a central Fe^{3+} metal ion (Rossman 1988). Frentrup and Langer (1982) further suggested that a broad band at 370 nm, present in synthetic spessartine, might additionally point to the presence of ferric iron in octahedral coordination. The overall shapes of the absorption spectra correspond very well with the one of synthetic spessartine (Frentrup and Langer, 1982). Comparison between the three spectra reveals, however, that the small differences in colour within the spessartines cannot be explained fully from the spectra. A qualitative correlation between the presence of chromophore atoms (iron and manganese in the present case), microprobe analyses, and the colour of these spessartines might be that the reddish hue is due to the presence of somewhat larger amounts of iron *(Table I)*. The absorption band at 370 nm of hessonite is due to the presence of Fe^{3+} at the dodecahedral sites and causes the cognac colour (Frentrup and Langer, 1982).

Heat treatments

A silvery lustre was observed on pyrope, almandine-spessartine and spessartine-almandine after heat treatment in air, in an oxygen-saturated atmosphere (P_{O_2} = 1 atm) and in an inert atmosphere (P_{Ar} = 1 atm) *(Table III)*. Friedman (1988) was the first to report that on heating almandine in air, the surface acquired a silvery lustre. This author attributed the silvery lustre to the formation of specular hematite, but did not confirm it. In the present study all powders scratched from the surfaces of heat-treated pyropes and almandines were confirmed as hematite. This means that garnet decomposes at the surface to form hematite. The fact that the silvery lustre is more spectacular on heat-treated almandine-spessartine and spessartine-almandine than on pyrope *(Figure 3)* can be related to the somewhat lower iron content of the pyrope *(Table I)*. In a reducing atmosphere, however, no transitions were observed and the colour of the treated stones remained unchanged.

Although Mössbauer experiments performed at room temperature on hessonites pointed to slight oxidation of Fe^{2+} to Fe^{3+} in the garnet lattice after heat treatment, this had no effect on the already distinct colour of the stones.

The Imperial-topaz colour caused by heating pale yellow grossular *(Table III)* may well be caused by a change in the valence state of iron, but due to its very low concentration this could not be confirmed by Mössbauer spectroscopy. The grossular remains light yellow after treatment in a strongly reducing atmosphere.

Diffusion treatments

The diffusion treatments produced an orange diffusion layer on the rough grossular stones in the presence of Fe and Cr and a green diffusion layer in the presence of Co. Oxides of cobalt are typically used to produce a blue diffusion layer which, when applied to an orange stone, produces the green colour. Pollack (1999) recently reported that diffusion treatment on light yellow garnet in the presence of Co produces stones which are green to blue-green. Rutherford Back Scattering reveals that the coloration occurs as a layer near the surface, hence recutting or repolishing of the surface may seriously affect the stone's appearance. It is important to keep in mind that the properties described are based on a very small amount of sample material. Furthermore, experimentation is continuing with the goal of confirming the results and of increasing the depth of penetration of the diffused layer. Generally speaking, the higher the temperature maintained and the longer the period used for the heating, the greater will be the depth of colour. However, at excessively high temperatures, the surface may be damaged.

Conclusions

Orange stones are an increasingly popular choice in jewellery, and the imperial-topaz colour derived from light yellow grossular offers potential for economic interest. However, the amounts of this mineral in gem-quality likely to be available from Brazil are relatively small and would not justify commercial mining on this basis alone. Consequently, enhancements of most garnets are unlikely to really threaten the gem trade.

The heat-treated, iron-containing garnet varieties are easily detected, even by the unaided eye, since they become opaque and produce a 'silvery skin'. For the other varieties, it is more difficult to make a decision between the treated and natural stones as they are most likely due to small internal modifications. For the rough, non-transparent, diffusion-treated grossulars, Rutherford Back Scattering reveals that the coloration occurs in a surface layer.

References

Cassedanne, J.P., and Cassedanne, J.O., 1977. Les garnets de Poaiá – Brésil. *Revue de Gemmologie* **52**, 2-4

Deer, W.A., Howie, R.A., and Zussman, J., 1982. *Rock-forming minerals, Vol. 1A: Orthosilicates.* Longman, London, 919 pp

Delaney, P.J.V., 1996. Gemstones of Brazil: Geology and occurrences. *Rem Revista Escola de Minas*, Ouro Preto, 123 pp

Ferreira, A.C.M., Ferreira, J.A de M., and Tavares, J.F., 2000. O pegmatito Alto Mirador: descricao e mineralogia, *XVIII Simpósio de Geologia do Nordeste, Recife*, **16**, 157 pp

Ferreira, J.A. de M., 1984. *Caracterização gemológica e estudos geoeconômicos de espécies raras de minerais gemas do Alto Mirador, Rio Grande do Norte.* Monographia do curso de pós-graduação lato-sense em Gemologia, Universidade Federal de Minas Gerais/Conselho National de Pesquisa

Ferreira, J.A. de M., 1997. Gemas raras do Seridó: espessartitas e gahnitas do Alto Mirador. *Jornal das Pedras*, **10**, 18-21

Frentrup, K.-R. and Langer, K., 1982. Microscope absorption spectrometry of silicate microcrystals in the range 40,000-5,000 cm^{-1} and its application to garnet end members synthesized at high pressures. In: Schreyer W. (Ed). *High-pressure researches in geoscience.* E. Schweizerbartsche Verlagsbuchhandlung, Stuttgart, pp 247-58

Friedman, D., 1988 Specular heat-treatment garnet. *Australian Gemmologist*, **16**, 477

McClure, S.F. and Smith, C.P., 2000. Gemstone enhancement and detection in the 1990s. *Gems and Gemology*, **36**(4), 336-59

Nassau, K., 1994. *Gemstone enhancement: history, science and state of the art. 2nd ed.* Butterworth-Heinemann Ltd. Oxford.

Pinto, C.P., and Pedrosa-Soares, A.C., 2001. Brazilian gem provinces. *Australian Gemmologist*, **21**, 12-6

Pollack, R., 1999. Pat. US 5 888 918, March 30, 1999

Rossman, G.R., 1988. Vibrational spectroscopy of hydrous components. In: *Mineralogical Society of America Reviews in Mineralogy*, **18**, 193-206

Schmetzer, K. and Bernhardt, H.-J., 1999. Garnets from Madagascar with a colour change of blue-green to purple. *Gems and Gemology*, **35**(4), 196-201

Schmetzer, K., Hainschwang, T., Kiefert, L. and Bernhardt, H.-J., 2001. Pink to pinkish orange Malaya garnet from Bekily, Madagascar. *Gems and Gemology*, **37**(4), 296-308

Shigley, J.E., Dirlam, D.M., Laurs, B.M., and Boehm, E.W., 2000. Gem localities of the 1990s. *Gems and Gemology*, **36**(4), 292-335

Stockton, C.M., and Manson, D.V., 1985. A proposed new classification for gem-quality garnets. *Gems and Gemology*, **21**(4), 205-18

Svisero, D.P., Felitti, W., and Almeida, J.S., 1981. Geologia da mina de diamantes de Romaria, município de Romaria. *M.G. Mineração e Metalurgia*, **44**, 425, 4-14

Tavares, J.F., Ferreira, A.C.M., and Ferreira, A. de M., 2000. Uma grande grossulária gema em tactito. *I Simpósio Brasileiro de Tratmento e Caracterização de Gemas*, Ouro Preto, 67 pp

Wegner, R., Ramos de Brito, A., Karfunkel, J., Henn, U., and Lind, Th., 1998. Granate aus der Umgebung von São Valério, Tocantins, Brasilien. *Zeitschrift der Deutschen Gemmologischen Gesellschaft*, **47**(3), 147-52

The nature of channel constituents in hydrothermal synthetic emerald

Rudolf I. Mashkovtsev* and Sergey Z. Smirnov

Institute of Mineralogy and Petrography, SB RAS, 630090, Novosibirsk, Russia
** Corresponding author, e-mail: rim@uiggm.nsc.ru*

Abstract: *Hydrothermal synthetic emeralds manufactured by Biron, Regency and Tairus have been distinguished from natural and synthetic emeralds using chemical analysis and infrared (IR) spectroscopy. Polarized IR spectra have been obtained from plates. Hydrothermal synthetic emeralds possess infrared absorption features not present in natural emeralds, and these features have been investigated. We infer that the system of five narrow bands in the 3000-2600 cm*$^{-1}$ *region is related to the dimer formation of HCl molecules, which have been incorporated in the channels parallel to the* c-*axis during growth of Biron and Regency emeralds. In Regency emeralds, a double band with maximum at 3295 and shoulder near 3232 cm*$^{-1}$ *and a broad band between 3000 and 2500 cm*$^{-1}$ *are attributed to hydrogen-bonded* NH_4^+ *ions. In Russian hydrothermal synthetic emeralds the strong infrared spectral features related to molecular water are generally similar to those of some natural emeralds but there are also broad bands due to* Ni^{2+} *and* Cu^{2+} *ions in the near-infrared regions which enable one to distinguish Russian hydrothermal synthetic from natural emeralds. Other bands unrelated to water in hydrothermal synthetic emeralds are also discussed.*

Keywords: *ammonium ion, emerald, HCl molecule, IR spectroscopy*

Introduction

The hydrothermal syntheses of emeralds have much in common with the growth of natural emerald. As a consequence of improving techniques, identification of synthetic stones has become increasingly difficult. As the gemmological properties of hydrothermal synthetic emerald overlap those of natural emerald, the most conclusive results are obtained by the microscopic examination of their inclusions. However, even this technique becomes ineffective when the emerald is clean or does not have diagnostic inclusions. Therefore, advanced testing by such techniques as absorption and infrared (IR) spectroscopy and/or energy-dispersive X-ray fluorescence (EDXRF) analysis should be used for conclusive diagnosis of synthetic gems (Koivula *et al.*, 1996; Schmetzer, 1996). The application of these tools is based on the distinction of the minor impurity contents of natural and synthetic emeralds. In synthetic emeralds there are impurities which have not been detected in any natural emeralds. For example, chlorine is present as a structural constituent in the Biron and Linde or Regency hydrothermal synthetic emeralds, as well as in recent Chinese synthetic emeralds (Hänni, 1982; Stockton, 1984; Kane and Liddicoat, 1985; Schmetzer *et al.*, 1997). In some Colombian emeralds, chlorine has been found but only as a brine component and, probably, in NaCl crystals in three-phase inclusions (Bosshart, 1991). Recently, using a micro-proton-induced X-ray emission (micro-PIXE) technique for bulk analysis of an inclusion-free region in some Colombian, Zambian and Brazilian emeralds, chlorine was found as a structural component but in lower amounts than in Biron hydrothermal synthetic emeralds (Yu *et al.*, 2000). Measurable amounts of nickel and copper were found in Lechleitner fully synthetic and Russian hydrothermal synthetic emeralds (Hänni, 1982; Schmetzer, 1988; 1990).

Spectroscopy in the visible and IR regions is a powerful method for gem identification and research (Fritsch and Stockton, 1987; Fritsch and Rossman, 1987, 1988). To date, papers concerning the spectroscopic distinction of natural from synthetic emeralds include Wood and Nassau, 1968; Leung *et al.*, 1986; Stockton, 1987; Schmetzer and Kiefert, 1990; Diaz *et al.*, 1994; and Zecchini and Maitrallet, 1998. The method is promising because the technique is non-destructive, extremely rapid, and comparatively inexpensive.

The main features in the IR spectra of natural emeralds are the presence or absence of absorption features from two types of water molecules (type I is observed in alkali-free emerald and type II is bound to alkalis) incorporated in channels parallel to the *c*-axis (*c*-channels) of the beryl structure (Wood and Nassau, 1967, 1968; Flanigen *et al.*, 1967; Nassau, 1976; Schmetzer and Kiefert, 1990). Flux-grown emeralds have no spectral features in the range of water absorption, as has been revealed by previous authors. Linde and Biron hydrothermally-grown synthetic emeralds have absorption bands associated with only type I water molecules, whereas the natural emeralds have absorption bands of both type I and II water molecules (Wood and Nassau, 1967, 1968; Schmetzer and Kiefert, 1990). But the absorption of water molecules is a poor criterion to use in distinguishing natural from synthetic emeralds, as practical problems in the examination of large faceted gems arise from low transparencies in the mid-infrared range (4000 – 3400 cm^{-1}) where the absorption peaks of the water molecules are located. There are also difficulties in taking oriented spectra in the near-infrared range (8000 – 5000 cm^{-1}). Two polarized spectra corresponding to the two principal optical directions in the crystal are needed if one is to clearly distinguish the two types of water molecules (Wood and Nassau, 1967, 1968; Schmetzer *et al.*, 1997). Furthermore, in some emeralds from Colombia the absorption due to type II water is weaker than in most natural emeralds (Zecchini and Maitrallet, 1998). Also, Lechleitner and Russian hydrothermally-grown synthetic emeralds show the absorption bands associated with both type I and type II water molecules (Schmetzer and Kiefert, 1990). Fortunately however, additional measurements in other spectral ranges enable one to solve these problems. A very sharp absorption at 2357 cm^{-1} is characteristic of natural emeralds (Zecchini and Maitrallet, 1998), an absorption which is due to carbon dioxide within the natural crystal (Wood and Nassau, 1967, 1968). Lechleitner and Russian hydrothermal synthetic emeralds can be identified by either visible-range absorption spectroscopy (Schmetzer, 1988, 1990) or by the weak absorption features in mid- and near-infrared ranges (Stockton, 1987; Koivula *et al.*, 1996). There are distinct absorption features in the range from 3400 to 2600 cm^{-1} of Biron and Linde hydrothermal emeralds (Leung *et al.*, 1986; Stockton, 1987; Zecchini and Maitrallet, 1998) and in Chinese hydrothermal emeralds (Schmetzer *et al.*, 1997).

We have tentatively assigned a doublet at 3295 and 3232 cm^{-1} to ammonia, and a system of five strong bands in the 3000 – 2600 cm^{-1} range to various forms of HCl molecules which are incorporated in the *c*-channels of Biron and Regency hydrothermal synthetic emeralds (Mashkovtsev, 1996; Mashkovtsev and Solntsev, 2002). Also Schmetzer *et al.* (1997) associated an identical system of absorption bands with the chlorine-bearing hydrothermal synthetic emeralds (Biron, Chinese, and Linde or Regency). In the present paper we wish to gain an insight into the cause of the IR spectroscopic features of hydrothermally-grown emeralds in the range between 10000 and 2000 cm^{-1}, in the main, using data obtained from polished plates of emerald.

Materials and methods

Samples of the major commercially-produced hydrothermal synthetic emeralds and of natural emerald from the Ural Mountains, Russia, have been tested to obtain their IR absorption spectra. Detailed investigations were performed on 11 rough and 10 faceted stones. Biron synthetic emerald was represented by four halves of gem-quality rough crystals, sawn parallel to seed, of 17.20 to 107.40 ct and five faceted stones of between 1.370 and 1.750 ct. Two slices from different rough crystals and one 1.46 ct emerald-cut samples of Regency (Linde) hydrothermal synthetic emerald were examined. Tairus hydrothermal synthetic emeralds from Novosibirsk, Russia were represented by 4 oval mixed cuts weighing between 0.2 and 0.5 ct and by many rough crystals. As there is no difference in chemistry of the growth processes for crystals of types 1 and 2 according to the Tairus Research scientists (see also Koivula *et al.*, 1996), we used only type 1 emeralds as representative for recent commercial Tairus production. Natural emeralds from the Urals (Malyshev mine) were represented by three rough crystals and one 1.161 ct rectangular faceted stone. Polarized spectra were obtained from 0.6 to 3.3 mm thick plates cut from rough crystals.

Mid-infrared absorption spectra were obtained using a Brucker IFS 113v Fourier transform infrared (FTIR) spectrometer in the range 4500-2000 cm^{-1} and a Specord M80 (Karl Zeiss, Jena) spectrometer in the range 4000-2000 cm^{-1}. Near-infrared spectra were obtained using a SF-20 (LOMO, St. Petersburg) spectrometer in the range 10000-4000 cm^{-1}. The FTIR spectrometer is equipped with a microscope attachment which was used to focus the beam when faceted stones were being measured. In this study the beam was directed perpendicularly to table facet of the stone on the microscope stage.

The emerald specimens were analyzed for Na_2O, FeO, V_2O_3, Cr_2O_3, NiO, CuO, Al_2O_3, SiO_2, and Cl by a Camebax Micro electron microprobe at an operating voltage of 15 kV and beam current of 20 nA. Samples of Biron hydrothermal synthetic emerald were also qualitatively studied using secondary ion mass spectroscopy (SIMS) using a Cameca S-6 ion microprobe.

Results

Chemical composition

Elements substituting major beryl components (Si, Al and Be)

Microprobe and wet chemistry analyses of emeralds studied are presented in *Table I*. One can conclude from *Table I* that the most important impurities in the emeralds are the chromophoric elements Cr, V and Fe. Tairus synthetic emeralds commonly have negligible V and higher Cr contents in comparison to Biron synthetic emerald. Tairus synthetic emeralds also contain traces of Ni and Cu which are commonly acquired during growth by solution from the walls of the steel autoclaves. Detailed zone analyses revealed that in Tairus synthetic emeralds the Cr_2O_3 and FeO contents gradually decreased away from the beryl seed, while in Biron synthetic emeralds there was a more uniform element distribution across the overgrowth.

Almost equal Cr and V contents are one of the most important chemical features of the Biron synthetic emeralds. They are also extremely low in iron and this contrasts with the Tairus emeralds which contain significant quantities of this element (*Table I*). No other elements are present that can substitute for Al in the octahedral site of the beryl structure.

Natural emerald from the Malyshev mine has a low Cr_2O_3 content in contrast to the Biron and Tairus synthetic emeralds. The highest Cr_2O_3 content of intensely coloured

Table I:: *Chemical compositions of synthetic and natural emeralds.*

Biron synthetic emerald*						Tairus synthetic emerald***				Ural	
Wt.%	R29(6)	R30(4)	R32(7)	R34(13)	R35(22)	420	361/1	310	309	U1(1)	U2(1)
SiO_2	66.35	66.63	66.75	65.66	65.46	65.90	65.70	66.00	65.80	63.99	64.86
Al_2O_3	17.91	18.66	18.29	18.16	17.87	15.31	16.36	16.00	16.40	16.63	16.89
Cr_2O_3	0.625	0.110	0.288	0.498	0.653	0.61	0.22	0.39	0.23	bdl	0.165
V_2O_3	0.756	0.132	0.348	0.874	0.917	bdl	bdl	bdl	bdl	bdl	bdl
BeO	nd	nd	13.72**	13.63**	nd	13.80	13.60	13.50	13.30	nd	nd
FeO	bdl	bdl	bdl	bdl	bdl	2.54	2.05	2.32	0.28	0.28	0.28
MgO	bdl	bdl	bdl	bdl	bdl	bdl	0.05	0.02	0.04	1.74	1.29
NiO	bdl	bdl	bdl	0.023	bdl	0.15	0.20	0.10	0.10	bdl	bdl
CuO	bdl	bdl	bdl	bdl	0.034	0.10	0.00	0.00	0.00	bdl	bdl
Na_2O	bdl	bdl	bdl	bdl	bdl	0.06	0.07	0.01	0.00	1.11	0.82
Cl	0.329	0.386	0.410	0.378	0.397	bdl	bdl	bdl	bdl	bdl	bdl
LOI	nd	nd	nd	nd	nd	1.00	1.20	1.10	1.20	nd	nd
Total	86.00	85.94	99.80	98.71	85.37	99.47	99.45	99.44	99.27	83.75	84.32

bdl – below detection limit;
nd – not determined, LOI – loss on ignition;
U1 – pale coloured zone of Ural emerald,
U2 – intensely coloured zone of the same crystal;

** – average composition: number of probe points are shown in parenthesis;*
*** – BeO concentrations for R32 and R34 were determined by wet chemistry;*
**** – wet chemistry analyses of Tairus emerald; Li_2O content is 0.1 wt.%, MnO and K_2O contents are around the detection limit.*
Cl and V_2O_3 were determined by electron microprobe and appeared to be below the detection limit.

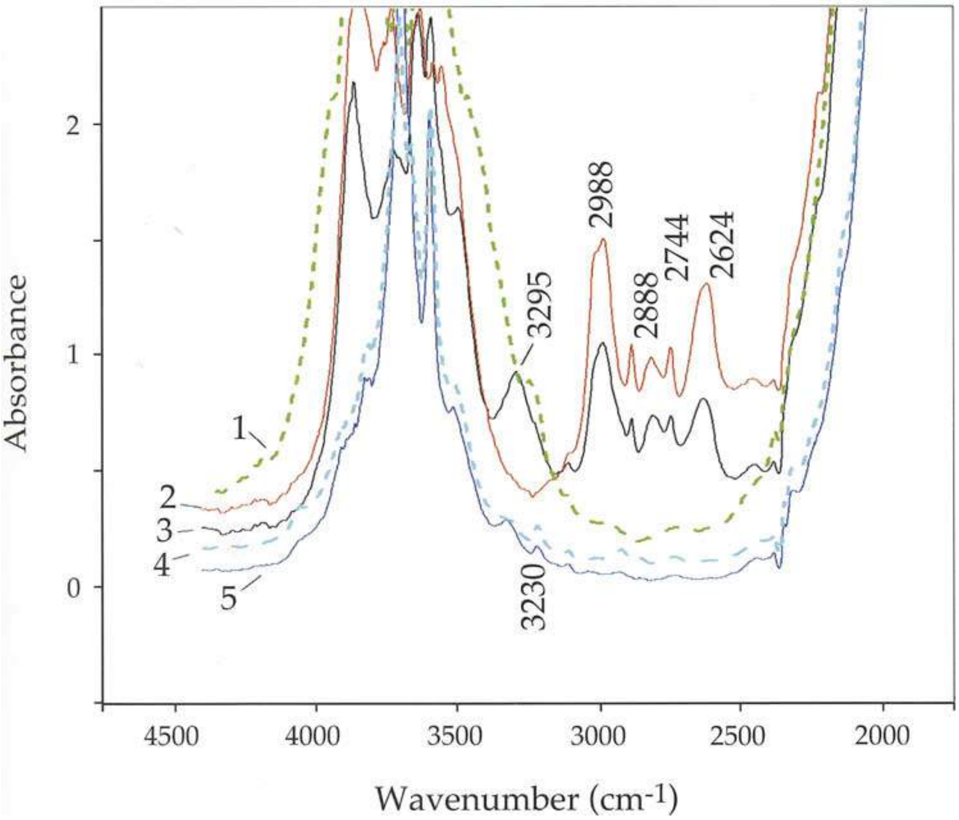

Figure 1: The mid-infrared spectra of natural emerald from the Urals (1) and hydrothermal synthetic emeralds Biron (2), Regency (3), and Tairus (4, 5). Note that the Tairus hydrothermal synthetic emerald spectra were obtained from two stones with different orientations of their table facet relative to the optic axis, namely angles of 30 degrees (4) and 60 degrees (5) to the optic axis.

Ural emeralds of about 0.2 wt. % was measured in the studied sample (*Table I*). A similar maximum Cr_2O_3 content (up to 0.5 wt.%) might be expected from the reports by Vlasov and Kutakova (1960), Schmetzer *et al.* (1991) and Schwartz (1991). In contrast, average Cr_2O_3 contents of Tairus and Biron synthetic emeralds are 0.54 – 1.24 wt. %. The average Cr_2O_3 content of Biron synthetic emerald (0.11–0.65 wt.%) is close to the upper limit of that of Ural stones. The colours and compositional zoning can be characteristic features of natural emeralds, and the Cr_2O_3 contents of Ural emeralds do vary significantly from zone to zone, resulting in contrasting intense and pale colours. On the basis of the reported (Schmetzer *et al.*,1991) and our own data (*Table I*), we conclude that the FeO content of Ural emerald is comparable with the lower limit of Tairus synthetic emerald and is much higher than that of Biron synthetic emerald.

MgO may be present in Tairus emeralds in quantities up to 0.1 wt.%, but its average is 0.04 wt.%. Biron synthetic emeralds usually do not contain detectable MgO, but it is worth noting that Pool synthetic emerald, which is analogous to Biron synthetic emerald, contains relatively high MgO (Bank *et al.*, 1989).

Elements occupying channel sites in the beryl structure

The most important chemical feature of the Biron synthetic emeralds is the relatively high Cl content, which is consistent with previous work (Hänni, 1982; Stockton, 1984; Kane and Liddicoat, 1985; Bank *et al.*, 1989; Yu *et al.*, 2000). It is worth noting that all the studied synthetic emeralds are low in or free of alkalis, while the Ural emeralds have relatively high Na_2O contents.

Infrared spectroscopy

The infrared spectra of the faceted stones are demonstrated in *Figure 1*. High absorbances are generally present in the range of the water absorption bands between 3400 and 3900 cm^{-1} for large faceted stones. Also atmospheric CO_2 has hindered the measurements in the range between 2300 and 2400 cm^{-1} when using the microscope attachment of the FTIR spectrometer. So for faceted emeralds the narrow range from 2400 to 3400 cm^{-1} is more accessible for measurements. To measure

Table II: The main features of IR spectra of hydrothermal synthetic and Ural emeralds and their appearance in emeralds of different origin.

Peak location cm^{-1}	Polarization relative to *c*-axis	Emerald type					
		Biron*	Regency*	Tairus*	Ural*	Assignment**	
2360	$\perp$				s	CO_2	[a]
2624	$\perp$	m	w-uo			HCl	[b]
2744	$\perp$	m	w-uo			HCl	[b]
2816	$\parallel$	vs	s-w			HCl	[b]
2888	$\perp$	m	w-uo			HCl	[b]
2988	$\perp$	s	m-uo			HCl	[b]
3230	$\parallel$			m-w	s-m	H_2O II	[a]
3232	$\perp$		sh			NH_4^+	[b]
3295	$\parallel, \perp$		s-m			NH_4^+	[b]
3520	$\perp$	w	w	w	m	H_2O I	[a]
3560	$\perp$			w	w	H_2O I	[a]
3600	$\parallel$	vw	vw	m	s	H_2O II	[a]
3608	$\parallel$	w	w	w		OH	[d]
3650	$\perp$			w	m	H_2O II	[a]
3700	$\parallel$	s	s	s	vs	H_2O I	[a]
3888	$\perp$	m	m	m	s	H_2O I	[a]
4065	$\parallel$			w	w	H_2O II	[b,e]
5097	$\perp$	w	w	w	w	H_2O I	[a]
5271	$\perp$			m	s-m	H_2O II	[a]
5274	$\parallel$	s	s	s	s	H_2O I	[a]
5460	$\perp$	m	m	m	m	H_2O I	[a]
5520	$\parallel$	w				HCl	[b]
6494	$\parallel$			m-uo		Ni^{2+}	[c]
6820	$\parallel$	m	m	m	m	H_2O I	[a]
6990	$\perp$	w	w	w	w	H_2O I	[a]
7042	$\perp$	w				OH	[b]
7072	$\parallel$			w	w	OH	[d]
7092	$\perp$				w	H_2O II	[a]
7143	$\parallel$	s	s	s	s	H_2O I	[a]
7320	$\perp$	m	m	m	m	H_2O I	[a]
8475	$\perp$			m-uo		Cu^{2+}	[c]

* m - moderate, s - strong, w - weak, vw - very weak, vs – very strong, uo – unobserved, sh – shoulder

** References: [a] Wood and Nassau (1967, 1968); [b] Mashkovtsev and Solntsev (2002) and this work; [c] Solntsev (1981); [d] Mashkovtsev and Lebedev (1992); [e] Koivula *et al.* (1996)

polarized spectra in the range 2000 to 10000 cm^{-1} (*Figures* 2 and 3), emerald plates cut from the crystals were used.

The main spectroscopic data are listed in *Table II*. The well-known bands related to type I water molecules were observed in the spectra of all the samples. Type II water peaks are clearly present in Ural and Tairus emeralds, but in Biron and Regency emeralds, absorption traces related to type II water are weak or not present. Five absorption bands in the range 2600 – 3000 cm^{-1} are always present in Biron emeralds (cf. Leung *et al*., 1986; Schmetzer *et al*., 1997; Zecchini and Maitrallet, 1998). This system of bands may be so weak in Regency emeralds that only the central band at 2816 cm^{-1} may be observed on the background of other broad bands between 2400 and 3050 cm^{-1} (*Figure 2A*). Regency emerald spectra also display a double band with the maximum at 3295 and shoulder near 3232 cm^{-1} and a broad band between 3000 and 2500 cm^{-1} with a transmission window near 2870 cm^{-1}.

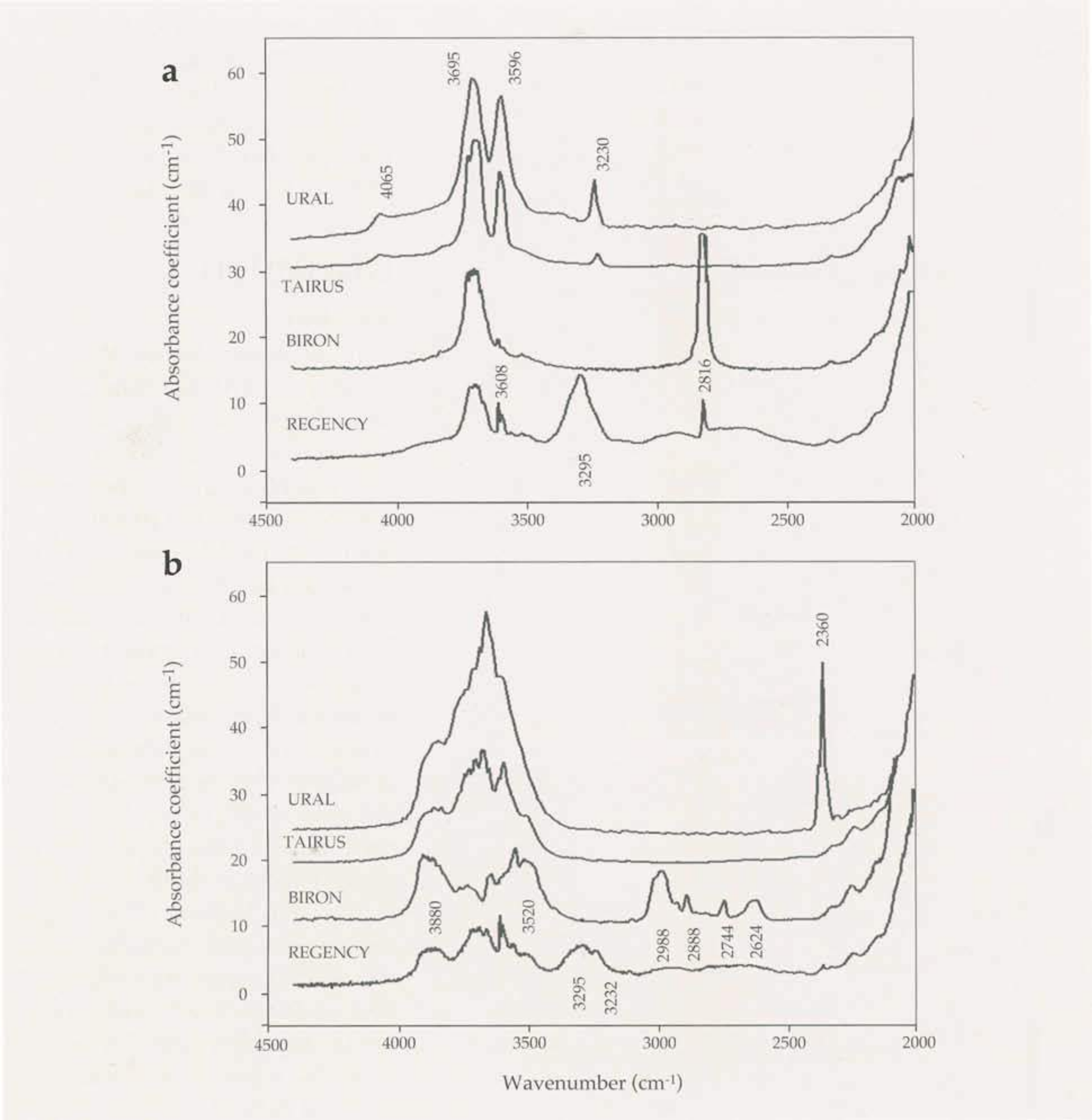

Figure 2: Mid-infrared extraordinary-ray (a) and ordinary-ray (b) spectra of thin plates of Regency (thickness t=0.65 mm), Biron (t=0.95 mm), Tairus (t=1.4 mm) hydrothermal synthetic emeralds and natural emerald from the Urals (t=0.6 mm). The main spectral features shown are discussed in the text and listed in Table II.

In comparing the most intense bands in natural and Tairus emeralds, these are similar except that in the Ural emeralds, there is an intense band at 2360 cm^{-1} related to the CO_2 molecule (Wood and Nassau, 1967, 1968). In synthetic emeralds, this peak is vanishingly small or absent. In Tairus emeralds there are the bands at 4065 and 3230 cm^{-1} which relate to type II water (Wood and Nassau, 1967; Koivula *et al.*, 1996), and there are weak peaks in the region around 2300 cm^{-1} as well as in the region between 2700 and 3105 cm^{-1} which are not related to water (see *Figures 1* and *2*); this system of bands between 2700 and 3105 cm^{-1} was obtained from Tairus faceted stones (*Figure 1*), but only certain of these were observed in thin plates (*Figure 2*). Also, the Tairus emeralds are the only emeralds to contain the broad bands at 6494 cm^{-1} and at 8475 cm^{-1} related to optical transitions in Ni^{2+} and Cu^{2+} ions respectively (Solntsev, 1981; see also Koivula *et al.*, 1996). The band at 3608 cm^{-1} is present in all three synthetic emeralds. Weak peaks visible near 7000 cm^{-1} include the line

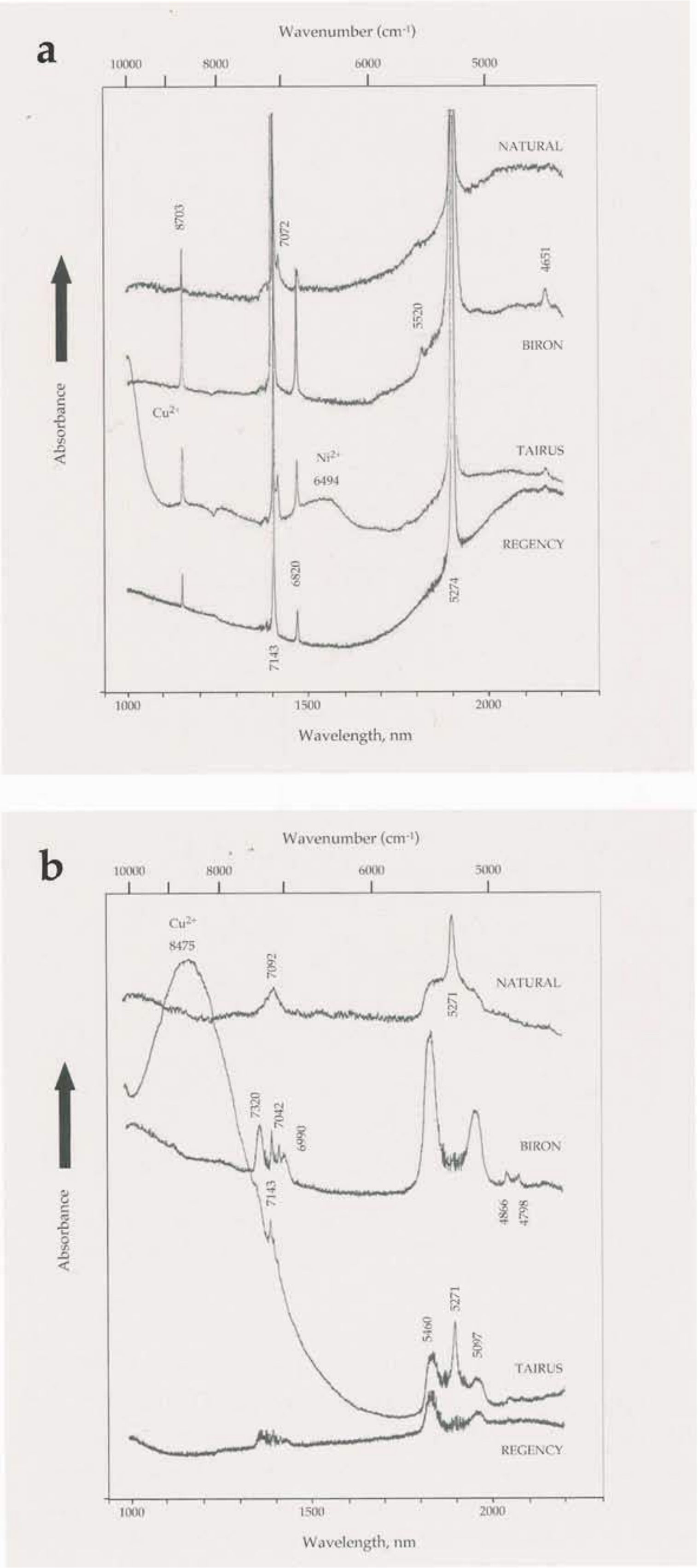

Figure 3: Near-infrared extraordinary ray (a) and ordinary-ray (b) spectra of the same plates as shown in Figure 2 except that the Biron plate is 3.3 mm thick. Note the broad absorption bands due to Ni^{2+} and Cu^{2+} ions in Tairus emerald, the additional peak at 5520 cm^{-1} due to HCl in Biron emerald, and other peaks which are discussed in the text and listed in Table II.

at 7042 cm^{-1} in Biron emerald and one at 7072 cm^{-1} in Tairus and natural emeralds (*Figure 3*). The relative thickness of the Biron plate enabled the weak band at 5520 cm^{-1} to be detected.

Discussion

Impurities

It has already been stated (Stockton, 1984) that composition of synthetic emeralds is of great importance in their identification. In this context, the components, which either are not present in natural mineral-forming solutions, or can not be incorporated in beryl structure under natural conditions are of the greatest interest, and chlorine is one example. Cl is one of the most important constituents of natural mineral-forming solutions. The concentrations of chlorides in the mineral-forming medium of a schist-type emerald deposit average about 5 – 10 wt. % (Moroz and Vapnik, 1999), and in evaporite type deposits, concentrations are typically as high as 38 wt. % (Cheilletz *et al.*, 1994). Very high salinities (up to 38 wt. % of NaCl) have also been detected in fluids at the Gravelotte schist-type deposit in South Africa (Nwe and Morteani, 1993). In contrast, Cl contents of most natural emeralds determined by PIXE (proton-induced X-ray emission) methods typically are very low, about 0.01 – 0.09 wt. % (Yu *et al.*, 2000), although in some Colombian, Zambian and Brazilian emeralds, contents can be as high as 0.12 – 0.18 wt. % (Yu *et al.*, 2000). Thus a content of more than 0.2 wt. % Cl is a very powerful indication that the emerald is hydrothermal synthetic.

Using our own data on composition of the emeralds and data available from the literature, synthetic emeralds may be roughly divided into two groups: low-chlorine and high-chlorine. Typically low-chlorine are flux emeralds, excluding some Gilson and Lennix stones (see Yu *et al.*, 2000), Russian hydrothermally-grown emeralds and most natural emeralds. In this study Cl was not detected in Tairus synthetic or in Ural emeralds, thus they belong to low-chlorine emeralds. High-chlorine emeralds include hydrothermally-grown Linde or Regency, Biron and new Chinese synthetic emeralds. It is known that hydrochloric acid and alkali chloride water solutions were used to grow Linde or Regency synthetic emeralds (Nassau, 1976). It has also been found that alkali chlorides are the major salt constituents of nail-head and spicule-like fluid inclusions in Biron synthetic emeralds (Smirnov – unpublished data). Although there are no obviously appropriate sites within the beryl structure that chlorine ions could occupy, the high Cl-contents in synthetic emeralds, determined by electron microprobe or PIXE analyses, indicate that Cl is a structural impurity rather than a constituent of inclusions. We therefore suggest that channels in the beryl structure are the only appropriate sites for chlorine.

IR spectroscopy

From infrared spectroscopic data we conclude that five bands in the range 2600-3000 cm^{-1} observed in Biron and Regency emeralds are related to HCl molecules arranged in the channels of the beryl structure (Mashkovtsev, 1996; Mashkovtsev and Solntsev, 2002). Schmetzer *et al.* (1997) also associated this group of bands with chlorine content. In support of this conclusion it was noted that (i) in these emeralds chlorine was invariably detected by Hänni (1982), Stockton (1984), Kane and Liddicoat (1985) and by other authors (see *Table I*), and (ii) the vibrational frequencies of various forms of HCl molecules trapped in inert matrices stretch from 2700 to 3000 cm^{-1} (Hallam, 1973). Here we want to refine the early assignment (Mashkovtsev, 1996) to various forms of HCl molecules (single HCl, dimer and trimer) and state that all five of the absorption bands in the 2600 – 3000 cm^{-1} region are related to the HCl dimer (two bound HCl molecules). In a solid Ar matrix at a temperature of 20 K, the spectrum of the HCl dimer has one very weak band at 2855 cm^{-1} and another strong band at 2817.5 cm^{-1}, which depends only slightly on the matrix (Mailard *et al.*, 1979). Therefore we assume that the strong band at 2816 cm^{-1} observed in chlorine-bearing hydrothermal synthetic emeralds is related to the HCl dimer (the band near 2855 cm^{-1} in our case is probably too weak to be observed). The two pairs of the bands (one at 2624 and 2988 cm^{-1} and another at 2744 and 2888 cm^{-1}) are near-symmetrical about the main band at 2816 cm^{-1}, whereas the intensities of the bands at 2624 cm^{-1} and at 2744 cm^{-1} are always weaker than those of their counterparts at 2888 and at 2988 cm^{-1}. We assume that these so-called combination bands have resulted from the hindered rotation (or libration) of the HCl dimer about two axes of the dimer compound. The full justification will be published elsewhere. Here we note only that in a similar way the libration of molecular water gives rise to the combination bands at 3520 and 3888 cm^{-1}, which are near-symmetrical about a strong band at 3700 cm^{-1} and are related to the type I H_2O (Wood and Nassau, 1967). The uneven intensity and slightly asymmetrical disposition of these combination bands about the main band are explained by a dissimilar mechanism of their excitation (Herzberg, 1945).

Hence we suggest that the system of the bands in the 2600-3000 cm^{-1} region is related to an L-shaped dimer of two HCl molecules (*Figure 4*). The extraordinary-ray near-infrared spectra show a narrow absorption band at 5520 cm^{-1} related to an overtone (it is a replica of the main band at nearly double the frequency but with very weak intensity) of dimer HCl vibration at 2816 cm^{-1} (see *Figure 3*).

It is known that for the growth of Linde hydrothermal emeralds, ammonium halides were used (Nassau, 1976). Furthermore, the Tairus experimental beryl, synthesized

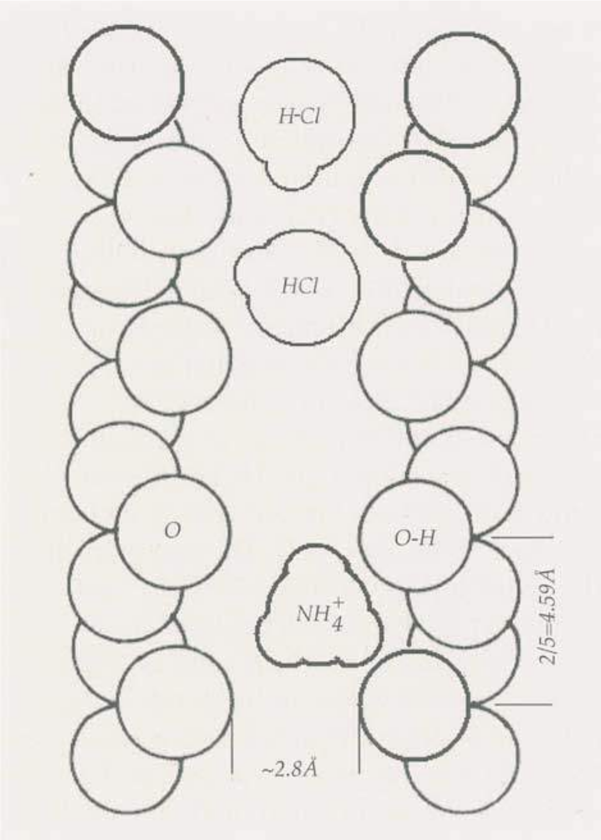

Figure 4: The proposed model for ammonium ion and HCl molecules in the structural c – channel of beryl. Shown are the H-Cl bond of one HCl molecule which is hydrogen-bonded with another HCl molecule, and the O-H bond of structural oxygen which is hydrogen-bonded with an ammonium ion.

hydrothermally in an NH_4Cl salt solution, shows IR spectral features similar to those of a Linde emerald (Mashkovtsev and Solntsev, 2002). Hence we have proposed that the band at 3295 cm^{-1} (with shoulder at 3232 cm^{-1}) and the broad band between 3000 and 2500 cm^{-1} are related to NH_3 molecules and NH_4^+ ions, respectively, in the structural *c*-channels. This conclusion was supported by careful study of the NH_3^+ radical observed after γ-irradiation by the use of electron paramagnetic resonance (Mashkovtsev and Solntsev, 2002). However, more data are needed for unambiguous determination of the cause of all the above-mentioned bands. Besides the stretching bands between 3000 and 3400 cm^{-1}, in the IR spectra there are characteristic bending modes at 1630, 968 and 930 cm^{-1} for NH_3 molecules and at 1680 and 1450 cm^{-1} for NH_4^+ ions (Nakamoto, 1978; Likhacheva *et al.*, 2002) but these bands were not detected in beryl because they are veiled by lattice vibrations. The IR spectrum in the range from 5000 to 4000 cm^{-1} for a thick plate of Tairus emerald was also obtained (Mashkovtsev *et al.*, 2004) and revealed a weak peak at 4651 cm^{-1} (related to an overtone of a water molecule (Wood and Nassau, 1967)) superimposed on a background band with a broad maximum centred near 4770 cm^{-1}; this is probably a result of the linear combination of the ammonium bending mode (typically near 1680 and 1450 cm^{-1}) and the stretching mode at 3295 cm^{-1}. Furthermore we can explain the origin of the broad band between 3000 and 2500 cm^{-1} with a transmission window near 2870 cm^{-1} in the following way (Mashkovtsev *et al.*, 2003; Mashkovtsev *et al.*, 2004). Ammonium can be regarded as a proton donor; it results in a hydrogen-bonded complex with oxygen in the lattice and forms an O-H bond (see *Figure* 4) which gives rise to an absorption continuum in the range 3000 – 2500 cm^{-1}. Fermi resonance produces a transmission window in this continuum at 2870 cm^{-1} because of interaction with a sharp overtone of the bending mode near 1450 cm^{-1} (Wood, 1973).

The narrow peaks at 3608 and the overtone at 7072 cm^{-1} (*Figures* 2 and 3) have been observed previously in Russian hydrothermal synthetic beryls and assigned to OH groups (Mashkovtsev and Lebedev, 1992). Analogously the band at 7042 cm^{-1} observed in Biron emeralds (*Figure* 3) may be an overtone of the main band near 3600 cm^{-1}. In this region the main band is masked by the intense water absorptions. Aines and Rossman (1984) showed how to distinguish the spectrum of the H_2O molecule from that of an OH group in the 7000 and 5200 cm^{-1} region. In contrast to H_2O molecules the OH groups have no bending vibrations with a frequency near 1600 cm^{-1}, which give, together with stretching vibrations near 3600 cm^{-1} for H_2O, the combination band near 5200 cm^{-1}. In our case there are no weak peaks near 5200 cm^{-1} associated with the intense bands related to the type I and type II molecular water. The presence or absence of the bending-related absorption near 1600 cm^{-1} is the primary criterion of distinction between H_2O and OH. According this criterion the band at 7042 cm^{-1} observed in Biron emeralds may be assigned to an OH group, and the difference in the frequencies of this (7042 cm^{-1}) and the Tairus emerald (7072 cm^{-1}) may relate to substitution of OH for oxygen at different positions in the emerald structure.

Visibility of an additional system of the weak bands between 2700 and 3105 cm^{-1} in Tairus emeralds (*Figure 1*) depends on the orientation of cut stones relative to the incident light and, probably, has been camouflaged in other emeralds by intense absorption bands in this range. This system may be related to the overtones of beryl lattice vibrations. The Tairus emerald is the only synthetic emerald which displays the bands at 3230 and 4065 cm^{-1}; these are related to type II water (cf. Stockton, 1987; Koivula *et al.*, 1996).

Obviously the detection of the weak absorption bands in cut stones depends on sensitivities of the instruments used, dimensions of the gems and on the orientation of the polished facet to the incident light. So although Koivula *et al.* (1996) did not reveal any weak band at 7072 cm^{-1}, their mid-infrared spectra did show a peak at 3608 cm^{-1} in Russian synthetic emeralds. Although the Tairus emeralds studied here failed to show a number of bands around 2300 cm^{-1} reported by Stockton (1987) and Koivula *et al.* (1996), there are a sufficient number of strong distinguishing features to enable separation of natural from Russian hydrothermal synthetic emeralds. The broad bands in the near-infrared range, which we attributed to Ni^{2+} and Cu^{2+}, have been reported by Koivula *et al.* (1996). In some modern Tairus emeralds the peaks are small, indicating only traces of Ni and Cu. In the visible range spectra, any bands relating to Ni^{2+} and Cu^{2+} are camouflaged by the intense bands due to Cr^{3+}, Fe^{3+} and Fe^{2+}, especially when the concentrations of Ni^{2+} and Cu^{2+} are small (cf. Schmetzer, 1988). In this case, it is more productive to measure the near-infrared range which lacks interfering bands.

Conclusion

So far as we know, HCl (the system of the bands in the range between 2600 and 3000 cm^{-1}) and ammonium (double band near 3300 cm^{-1} and broad band between 3000 and 2500 cm^{-1} with transmission window near 2870 cm^{-1}) molecules have not been found in natural beryls. It is known that ammonium halides and acid media are used in the growth of synthetic emeralds (Nassau, 1976). Therefore, detection of HCl and ammonium in the IR spectra of emeralds serves to identify them as hydrothermal synthetic emeralds. Incorporation of different impurities in the beryl structure originates from the chemical reagents and autoclaves used for crystal growth by different manufacturers, so, if required, hydrothermal synthetic emeralds of the different well-known manufacturers should be distinguishable. In Biron hydrothermal emeralds for example, strong bands in the range from 2600 to 3000 cm^{-1} due to HCl molecules are visible, and Regency (Linde) emeralds show an additional strong double band near 3300 cm^{-1} due to ammonium (*Figures 1, 2* and *Table II*). The important distinguishing features of Russian hydrothermal synthetic emeralds are the broad bands in the near-infrared range due to Cu^{2+} and Ni^{2+} ions which result from dissolution of the autoclave walls (*Figure 3, Table II*). Now the use of IR spectroscopy is a powerful tool in separation of natural from synthetic emeralds. However, it is still preferable to combine the techniques of trace-element analysis, microscopic study and spectroscopic method for the unequivocal determination of whether an emerald is synthetic or natural.

Acknowledgements

The authors thank the following for the loan of material for this study: A.S. Lebedev (Institute of Mineralogy and Petrography, Novosibirsk), V.G. Thomas and S.D. Pantsurkin (joint venture 'Tairus', Novosibirsk). This work was supported by RFBR grant 03-05-64555.

References

Aines, R.D., and Rossman, G.R., 1984. Water in minerals? A peak in the infrared. *J. Geophys. Res.*, **89**, 4059-71

Bank, H., Henn, U., and Lind, Th., 1989. Synthetische smaragde aus Australien (synthetische 'Pool emeralds'). *Zeitschrift der Deutschen Gemmologischen Gessellschaft*, **38**, 11-16

Bosshart, G., 1991. Emeralds from Colombia (Part 2). *J. Gemm.*, **22**(7), 409-25

Cheilletz, A., Feraud, G., Giuliani, G., and Rodriguez, C.T., 1994. Time-pressure and temperature constraints on the formation of Colombian emeralds: An ^{40}Ar/^{39}Ar laser microprobe and fluid inclusion study. *Econ. Geol.*, **89**, 361-80

Diaz, J., Lorenzo, A., Sole, J.G., Jaque, F., Hoyos, M.A., and Vara, I., 1994. Optical spectroscopy as a tool to discern natural and synthetic emeralds. *Proceedings of the 16th General Meeting of the International Mineralogical Association*, Pisa, Italy, p. 96.

Flanigen, E.M., Breck, D.V., Mumbach, N.R., and Taylor, A.M., 1967. Characteristics of synthetic emeralds. *Am. Mineral.*, **52**, 744-72

Fritsch, E., Stockton, C.M., 1987. Infrared spectroscopy in gem identification. *Gems & Gemology*, **23**(1), 18-26

Fritsch, E., and Rossman, G.R., 1987. An update on color in gems. Part 1: Introduction and colors caused by dispersed metal ions. *Gems & Gemology*, **23**(3), 126-39

Fritsch, E., and Rossman, G.R., 1988. An update on color in gems: Part 2: Colors involving multiple atoms and color centers. *Gems & Gemology*, **24**(1), 3-15

Hallam, H.E., 1973. Molecules trapped in low-temperature molecular matrices. In H.E. Hallam, Ed., *Vibrational Spectroscopy of Trapped Species: Infrared and Raman Studies of Matrix-Isolated Molecules, Radicals and Ions.* Wiley-Interscience, London 68-132

Hänni, H. A., 1982. A contribution to the separability of natural and synthetic emeralds. *J. Gemm.*, **18**(2), 138-44

Herzberg, C., 1945. *Infrared and Raman Spectra of Polyatomic Molecules*, D. Van Nostrand, Inc. New York.

Kane, R. E., and Liddicoat, R.T., 1985. The Biron hydrothermal synthetic emerald. *Gems & Gemology*, **21**(3), 156-70

Koivula, J.I., Kammerling, R.C., DeGhionno, D., Reinitz, I., Fritsch, E., and Johnson, M.L., 1996. Gemological investigation of a new type of Russian hydrothermal synthetic emerald. *Gems & Gemology*, **32** (1), 32-9

Likhacheva, A. Yu., Paukshtis, E.A., Seryotkin, Yu. V., and Shulgenko, S.G. 2002. IR spectroscopic characterization of NH_4-analcime. *Phys. Chem. Minerals*, **29**, 617-23

Leung, C.S., Merigoux, H., Poirot, J.-P., and Zecchini, P., 1986. Use of infrared spectrometry in gemmology. *In: Proceedings of the 13th General Meeting of the International Mineralogical Association*, Varna, 1982, Vol. 2, publ. Sofia 1986, 441-8

Mailard, D., Schriver, A., and Perchard, J.P., 1979. Study of hydracids trapped in monoatomic matrices. I. Near infrared spectra and aggregate structures. *J. Chem. Phys.*, **71**, 505-16

Mashkovtsev, R.I., 1996. The application of spectroscopy to discern natural from synthetic emeralds. *In: Annual Meeting of the Russian Mineralogical Society*, St. Petersburg, 47-48 [in Russian]

Mashkovtsev, R.I., and Lebedev, A.S., 1992. Infrared spectroscopy of water in beryl. *J. Struct. Chem.*, **33**, 930-3

Mashkovtsev, R.I., and Solntsev, V.P., 2002. Channel constituents in synthetic beryl: ammonium. *Phys. Chem. Minerals*, **29**, 65-71

Mashkovtsev, R.I., Paukshtis, E.A., and Thomas, V.G., 2003. The state of molecules and ions in the structural channels of synthetic beryl. *In: X-ray Diffraction and Crystal Chemistry of Minerals. Book of Abstracts of the XV International Conference*, St. Petersburg, 182-3

Mashkovtsev, R.I., Stoyanov, E.G., and Thomas, V.G., 2004. The state of molecules and ions in the structural channels of ammonium-bearing synthetic beryl. *J. Struct. Chem.* **45**, 62-9

Moroz, I., Vapnik, Ye., 1999. Fluid inclusions in emeralds from schist-type deposits. *Can. Gemm.*, **20**, 8-14

Nakamoto, K., 1978. *Infrared and Raman spectra of inorganic and coordination compounds.* Wiley, New York:, 281 pp

Nassau, K., 1976. Synthetic emerald: the confusing history and the current technologies. *J. Cryst. Growth*, **35**, 211-22

Nwe, Y.Y., and Morteani, G., 1993. Fluid evolution in the H_2O-CH_4-CO_2-NaCl system during emerald mineralization at Gravelotte, Murchison Greenstone belt, Northeast Transvaal, South Africa, *Geochim. Cosmochim. Acta*, **57**, 89-103

Schmetzer, K., 1988. Characterization of Russian hydrothermally-grown synthetic emeralds. *J. Gemm.*, **21**(3), 145-64

Schmetzer, K., 1990. Two remarkable Lechleitner synthetic emeralds. *J. Gemm.*, **22**(1), 20-32

Schmetzer, K., and Kiefert, L., 1990. Water in beryl – a contribution to the separability of natural and synthetic emeralds by infrared spectroscopy. *J. Gemm.* **22**(4), 215-23

Schmetzer, K., Bernhardt, H.-J., and Biehler, R., 1991. Emeralds from the Ural Mountains, USSR. *Gems & Gemology*, **27**(2), 86-99

Schmetzer, K., 1996 Growth method and growth-related properties of a new type of Russian hydrothermal synthetic emerald. *Gems & Gemology*, **32**, 40-3

Schmetzer, K., Kiefert, L., Bernhardt, H.-J., and Beili, Z., 1997. Characterization of Chinese hydrothermal synthetic emerald. *Gems & Gemology*, **33**(4), 276-91

Schwarz, D., 1991. Die chemischen Eigenschaften der Smaragde. III Habachtal/Osterreich und Uralggebirge/UdSSR. *Zeitschift der Deutschen Gemmologischen Gessellschaft*, **40**, 103-43

Solntsev, V.P., 1981. Nature of color centers and EPR in beryl and chrysoberyl. *Trudy Instituta Geologii i Geofiziki, Akademiya Nauk SSSR, Sibirskoe Otdelenie*, **499**, 92-140 [in Russian].

Stockton, C.M., 1984. The chemical distinction of natural from synthetic emeralds. *Gems & Gemology*, **20**(3), 141-5

Stockton, C.M., 1987. The separation of natural from synthetic emeralds by infrared spectroscopy. *Gems & Gemology*, **23**(2), 96-9

Vlasov, K.A., and Kutakova, E.I., 1960. *Izumrudnye Kopi* (Emerald Mines). Moscow: AN USSR. 252 pp [in Russian].

Wood, D.L., and Nassau, K., 1967. Infrared spectra of foreign molecules in beryl. *J. Chem. Phys.*, **47**, 2220-8

Wood, D.L., and Nassau, K., 1968. The characterization of beryl and emerald by visible and infrared absorption spectroscopy. *Am. Mineral*, **33**, 777-800

Wood, J.L., 1973. The vibrational spectra of hydrogen-bonded complexes. In: Ed. By J. Yarwood, *Spectroscopy and Structure of Molecular Complexes*. Plenum Press, London and New York, 303-85

Yu, K.N., Tang, S.M., and Tay, T.S., 2000. PIXE studies of emeralds. *X-Ray Spectrometry*, **29**, 267-78

Zecchini, P., and Maitrallet, P., 1998. Que peut apporter la spectrographie infrarouge dans l'Étude des Émeraudes? In: Giard, Ed., *L'émeraude. Connaissances Actuelles et Prospectives*, Association Française de Gemmologie, Paris 81-96

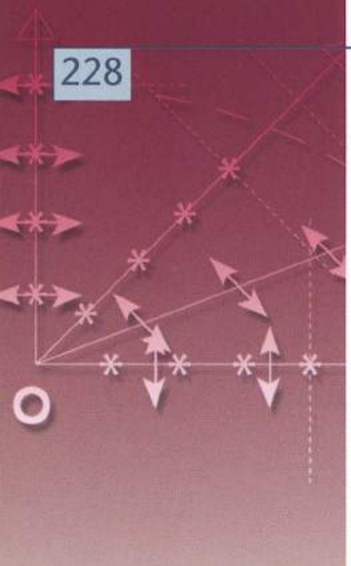

A new definition of optic axis for gemmology

and the four kinds of optic axis

Richard H. Cartier

Toronto, Ontario, Canada
richardcartier@rogers.com

Abstract: *Longstanding misuse of terminology in gemmological literature and course notes has allowed an inaccurate definition of optic axis to confuse understanding of this simple and fundamental concept. The problem is addressed with the proposal of a succinct new definition for* ***optic axis****. A review of anisotropic optics and discussion of the four kinds of optic axis explains how the proposed definition accords with optics theory.*

Keywords: *birefringence, double refraction, optic axis, polarization*

Introduction

The common definition of optic axis in gemmology, 'a direction of single refraction in a doubly refracting crystal[1]', is unsatisfactory because light at normal incidence in this direction would not refract at all, so refraction is irrelevant. Even when it is reworded to eliminate the refraction / refringence[2] confusion, 'an isotropic direction in a birefringent medium' does not leave an opening for minerals with optical activity[3]. This inadequate wording would not allow, for example, that quartz has an optic axis. Careful consideration of optical properties in biaxial media will show that, unlike the simpler uniaxial media, there are no isotropic directions in a biaxial medium. There is clearly a need for a new definition of optic axis that is in accord with modern understanding of optics. A definition that uses the phrase 'single refraction' is simply wrong, and a definition that specifies *isotropic* excludes some uniaxial and all biaxial material.

The proposed new definition for optic axis is:

Optic axis: a propagation direction in a birefringent medium that by some criterion has zero birefringence. It is a direction where birefringence (BI) = 0 in a medium with BI>0.

Isotropic and anisotropic media

A brief iteration about isotropic and anisotropic media may be a logical place to start. The measure of refringence[4] (optical density) is refractive index (RI), and materials that have more than one RI are said to be birefringent. The numerical difference between the lowest and the highest RI along one propagation direction is called the birefringence (BI) of that reading. A test in another direction through that same medium can yield other RI values with a changed birefringence particular to that new direction tested. Each direction through the medium

ISSN: 1355–4565

will have its own birefringence value. When referencing the medium (rather than one specific test direction) all possible test directions are considered. The 'birefringence' (BI) of the medium is presumed to mean 'maximum birefringence'. The BI of the stone will almost always be greater than the BI of one direction tested.

To understand the interaction of light with an anisotropic medium, one must consider the vibration direction of the light. It must be appreciated that randomly vibrating light can be sorted by a medium into one portion of light having specifically definable vibration, and another portion of light vibrating in a direction perpendicular[5] to the vibration of the first portion. Where birefingence is observed, the different RI readings are related to different vibration directions in the medium. For each propagation direction, the birefringence is for mutually perpendicular[5] directions of vibration. Light vibrating in specifically definable directions is called polarized light.

For most birefringent media, the mutually perpendicular vibrations that each medium produces will be two sets of plane-polarized light. One set of linear vibrations will be at 90° to the vibration of the companion set. For most directions of propagation through the medium, each direction of vibration interacts differently with the medium in terms of velocity of transmission, which interactions result in birefringence. The numerical value of birefringence will vary according to the propagation direction tested because vibrations are limited to within the wave front[6] in transverse relationship[7] to the direction of travel.

Optic axes

There will always be at least one direction through a birefringent medium where the numerical value of birefringence is zero. This special propagation direction in a birefringent medium is an optic axis.

As stated above, an optic axis is a propagation direction in a birefringent medium that *by some criterion* has zero birefringence (BI=0). The qualifying *by some criterion* in the definition of optic axis allows insertion of specifics to enable distinction of different kinds of optic axes.

There are four different kinds of optic axis; each is definably monorefringent.

1. An isotropic propagation direction in a birefringent medium[8].
2. An optically active propagation direction with nil birefringence for linearly polarized light.
3. A ray direction in which mutually perpendicular vibrations travel at the same velocity.
4. A propagation direction in which all vibrations travel at the same wave-normal velocity.

Materials with tetragonal, hexagonal, or trigonal structure have[9] either the first or the second type of optic axis. Materials with orthorhombic, monoclinic or triclinic symmetry, have[10] both the third and the fourth kinds of optic axes.

Uniaxial minerals

In uniaxial media, the direction parallel to the *c* axis differs from and is 90° to the directions in the plane of the '*a*' axes.
In biaxial media, all the crystal axes differ.
To visualize the optical properties of a medium it is helpful to consider the shapes of wave fronts of light as they progress.
The relationship between the wave front, the direction of travel, and the direction of vibration can be understood by considering the activity of the light at one point on the wave front.

Imagine that a single-point light source inside the medium produces a momentary flash of light, somewhat like a pinpoint size photographic flash bulb. Using our imagination to stop time a little while after our pulse of light is produced, we can picture the shape of the wave front at any particular moment as it progresses through the medium.

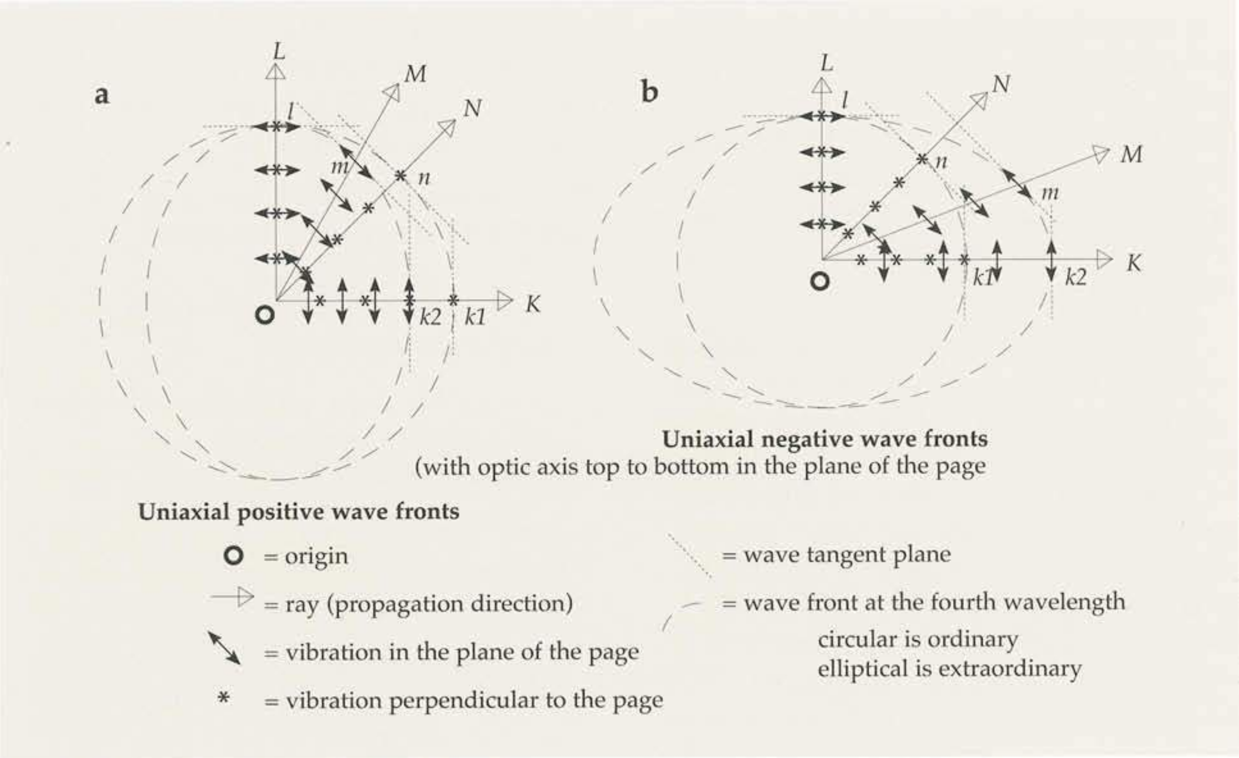

Figure 1: ***Uniaxial wave fronts: (a) positive, and (b) negative. The optic axis is top to bottom in the plane of the page.***

The three-dimensional shape of the progressing wave fronts is called the ray-velocity surface in optics terminology.

Figure 1 shows a central cross-section of wave fronts of light radiating from a point light source and travelling in a uniaxial medium (positive (a) and negative (b)) with the direction of vibration indicated once every wavelength and the shape of the wave front shown by dashed lines at the fourth wavelength. With the optic axis set top-to-bottom in the plane of the diagram, each diagram shows the direction of propagation for rays vibrating in a plane perpendicular to the optic axis, for rays vibrating in a plane parallel to the optic axis and for rays vibrating in a plane at 45° to the optic axis. In simple cases, such as zircon, beryl, calcite or tourmaline, the two wave fronts are in contact with each other at two diametrically opposite points that locate the optic axis. All normally incident light in this propagation direction will travel (without refracting)[11] with no optical variation for differing vibration directions. In terms of refringence, every ray will travel at the same velocity regardless of direction of vibration. Every vibration will continue at the velocity imposed by the refringence with no change in the sense of vibration; that is the vibration direction will not be altered by the medium. This direction is isotropic.

Quartz

To show the wave fronts and vibration directions for the more complex case of quartz, a perspective view of a wedge section is more helpful than a cross-section. For *Figure 2*, which shows the vibration directions for dextrorotatary and laevorotatary quartz[12], imagine that the single point light source is at floor level in the corner of a room that is completely filled, wall-to-wall and floor to ceiling, with quartz crystal structure. The optic axis is oriented parallel to the edge where the floor and a wall meet on our left as we look down into the corner. Stopping time a moment after a pulse of light is produced, we can see the shape of the wave fronts against the floor and the two walls. Either of these sections together with the missing seven comparable sections would show

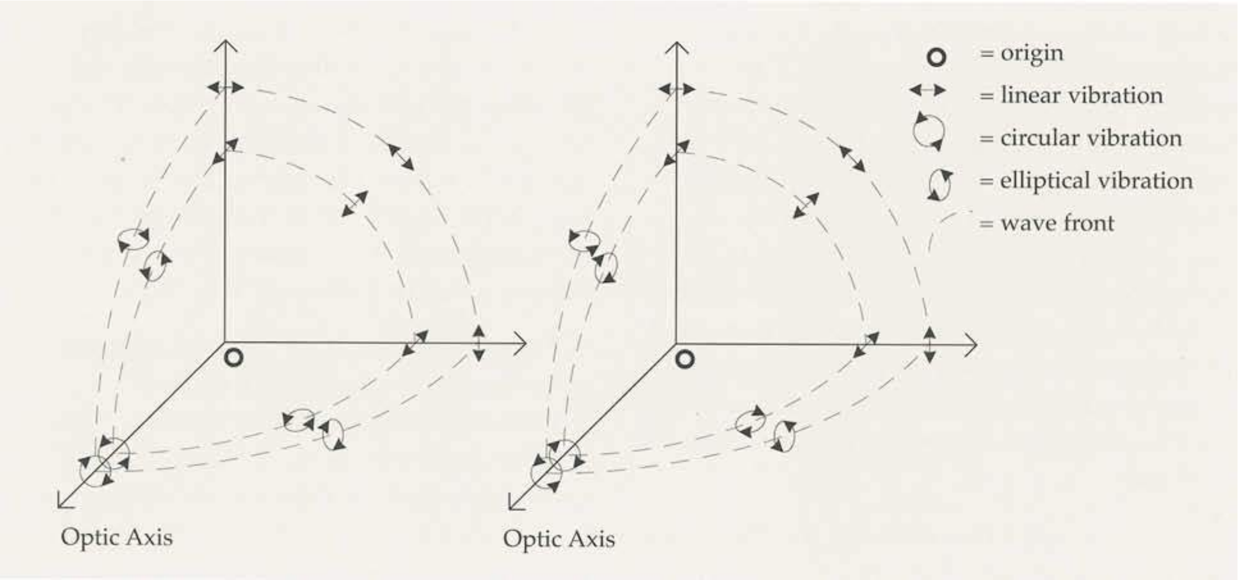

Figure 2: ***Vibration directions in quartz.***

a fully rounded three-dimensional shape indicating proportional velocity from the centre for all vibration directions.

The vibration direction of the light is shown in six points on each of the two wave fronts. The vibration direction for light travelling perpendicular to the optic axis is linear[13], the vibration direction for light travelling along the optic axis is circular[14], and the vibration direction for other directions of travel is elliptical[15].

In this helical medium, two circularly polarized rays with opposing sense of rotation yield circular birefringence in one propagation direction, but this circularly birefringent direction is monorefringent with respect to the wave-normal velocity[16] of linearly polarized light. For this, the second kind of optic axis, velocity is the same regardless of the direction of linear vibration, whilst the direction of linear vibration changes over the course of transmission. This rotation of the direction of linear vibration is called optical activity, which is produced by the circular birefringence.

Biaxial minerals

These first two kinds of optic axes, which are seen in uniaxial media, are too highly symmetrical to be found in media with orthohombic, monoclinic, or triclinic structure. When these lower-symmetry structures are tested it is found that birefringence does vary from maximum to zero, however.

For these cases narrow and more specific language is needed to define a special direction that can be termed an optic axis. There are two different directions that can be defined as monorefringent in biaxial media; one relates to light rays and the other to light waves. These two directions are the third and fourth kinds of optic axis.

In every birefringent medium, there will be at least one direction of propagation through the medium where mutually perpendicular vibrations can progress along the same path at the same velocity. In uniaxial media this defined direction coincides with the one optic axis, but in the lower symmetry media two directions within the optic plane[17] satisfy this definition. These materials are said to be biaxial. This direction is monorefringent with respect to ray velocity and is the optic axis for light rays. In optics texts it is called the secondary optic axis. This direction is easier to recognize in a wave-front diagram but, as will be shown, has optical properties that make it deserve the status of secondary.

For every birefringent medium, there will be at least one direction into the medium where vibrations in all normally incident light continuously share the same wave-tangent plane as the light progresses through the medium. In uniaxial media this defined direction coincides with the one optic axis, but in the lower symmetry media two directions within the optic plane satisfy this definition and the biaxal label is reinforced. This direction is monorefringent with respect to wave-normal velocity and is the optic axis for light waves. In optics texts this direction is called the primary optic axis, or just the optic axis.

It may be helpful to consider the directions defined in terms of equal ray velocity as the internal optic axes. *Figure 3* shows[18] a centre section in the optic plane through the wave fronts of light travelling in a biaxial medium. Two rays with mutually perpendicular vibrations are travelling along one internal optic axis sloped to the right; the other internal optic axis has that same slope to the left through the other point where the two wave fronts cross. This internal optic axis is a direction shared by the rays for two mutually perpendicular vibration directions. The ray vibrating in the optic plane and the ray vibrating perpendicular to the optic plane travel at exactly the same velocity in this direction through the biaxial medium. Even though they are travelling at the same velocity, each vibration has a different wave-normal. It must be remembered that the wave-normal is perpendicular to the vibration and not necessarily in the ray direction. The wave front containing the vibration perpendicular to the optic plane is circular, so that wave-normal continues in a straight line from the origin. The wave front containing the vibration in the optic plane is an ellipse, so that vibration direction sets the wave-normal in a different direction.

The special directions defined in terms of the continuously coinciding plane of vibrations have been called 'primary optic axes' or just 'optic axes'. It may be helpful to consider them as the **external optic axes.** *Figure 4* shows a centre section through the wave fronts in the optic plane with one optic axis direction detailed. The other external optic axis is sloped in from the other side at that same angle.

This optic axis direction is oblique, within the optic plane, and normal to the wave-tangent plane shared by both wave fronts. Collimated light incident at the normal in the direction of the external optic axis[19] will experience conical refraction upon passing through an incident surface at AB. Vibrations in the principal vibration direction for β travel straight on. Vibrations in all other directions are refracted as the vibrations travel in shared parallel planes through the medium. In the *Figure 4* side view, vibrations 90° to the page are β. In the end view, vibrations in the tangent shared by all the circular wave front sections are β as they

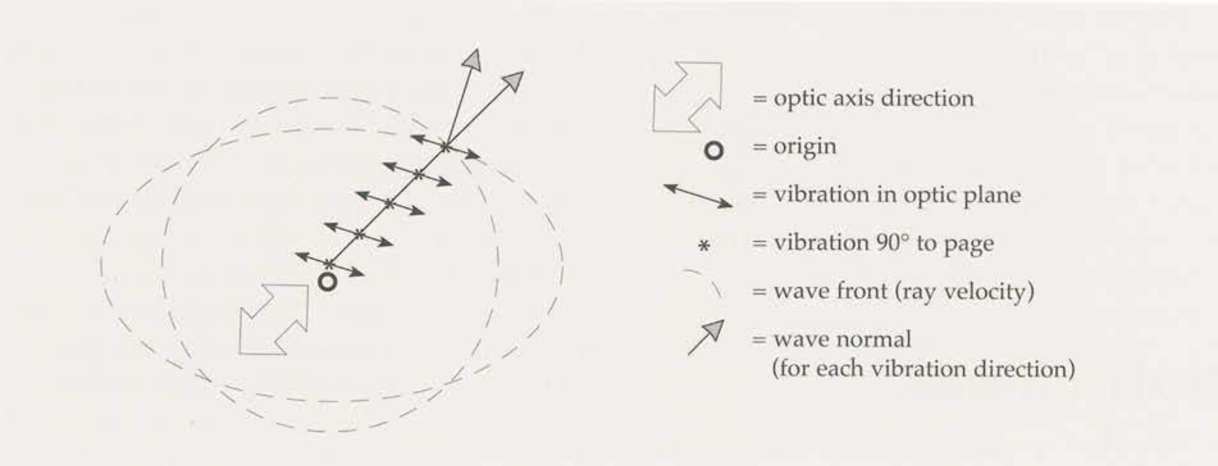

*Figure 3: **Internal (secondary) optic axis.***

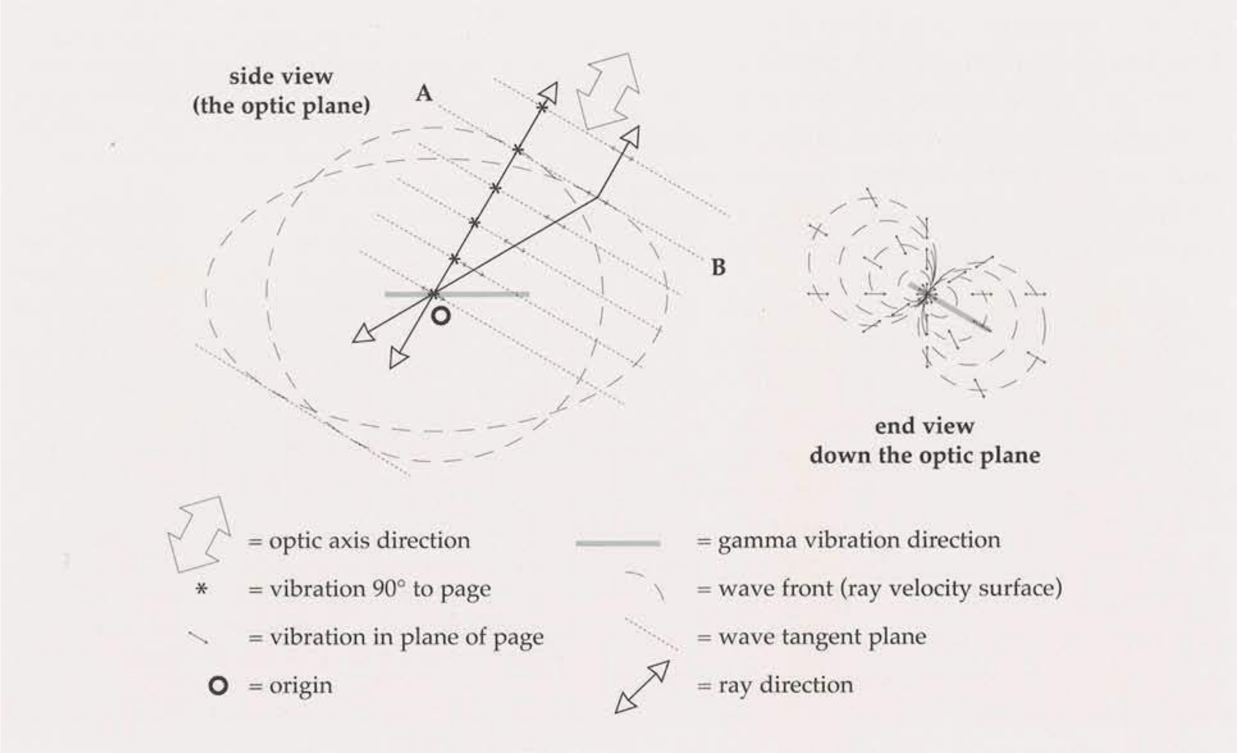

Figure 4: ***External (primary) optic axis wave-front diagram.***

continue past the origin of the ray-velocity surfaces depicted in the side view.

Discussion

Practical testing related to optic axes involves examining material from an exterior perspective. Looking in from the outside, external optic axes are being observed. External optic axes are defined as monorefringent with respect to wave-normal velocity, and wave-normal directions are easiest to consider in understanding refraction. External optic axes are the optic axes for waves of light, and waves actually exist. Internal optic axes are the optic axes for rays of light, and rays do not exist except in our imagination. It is therefore understandable that external optic axes are routinely considered as *the* optic axes while the internal optic axes are considered secondary.

Curiously, the internal optic axis is monorefringent because it provides one velocity for mutually perpendicular vibrations, whilst it is doubly refracting because of the different wave-normal directions (although the angle between the diverging refracted rays would be smaller than the angle between the internal wave-normals). The idea of a doubly refracting optic axis sounds self-contradictory, but that clearly is the case here.

The case of a doubly refracting monorefringent direction in biaxial media also reinforces the importance of differentiating double refraction from birefringence[2]. This peculiar state of affairs underlines the suitability of considering the internal optic axes as secondary. Discussions of biaxial optic axes, therefore, usually sensibly refer to only the two external optic axes.

For readers having difficulty with the subtle difference between the two kinds of biaxal optic axes, a careful comparison of the optic axis direction shown in *Figure 4* (side view), with the secondary optic axis shown in *Figure 3*, should help clarify the concepts. For most people a ray is relatively easy to visualize, so the direction of the secondary optic axis shown in *Figure 3* makes sense. Wave fronts are more difficult to visualize, so the optic axis depicted in *Figure 4*, as perpendicular to shared wave tangent planes, requires careful consideration to understand that this direction differs (by a small angle) from the secondary optic axis direction.

Finally, correct use of terminology can help avoid misunderstanding. The contraction 'DR' should be expunged from future texts and articles in favour of 'BI'. 'Doubly refracting' or a variation of this phrase is usually a misuse of terminology that clouds the issue by confusing a property of a medium with action taken by light. The word 'refract' (and all variations of it) should only and always refer to light, not a medium. If a medium is birefringent, some of the light it transmits experiences double refraction. If double refraction of light is observed, the medium is birefringent. It is incorrect to refer to a medium as 'doubly refracting' because the medium does not bend, it is only the light that bends.

References

1. Webster, R., edited by Read, P.G., 1994. *Gems*. 5th edn. Butterworth-Heinemann Ltd., Oxford, p. 668
2. Cartier, R.H., 2002. Birefringence vs. double refraction divergence. *Journal of Gemmology*, 28(4), 223-6
3. Optical activity, which is the rotation of linearly polarized light during transmission, occurs along the optic axis of a uniaxial crystal structure that spirals around in one direction (such as quartz), in different crystal systems where units of internal structure can be described in terms of mirror isomerism (such as the optic axes of Rochelle salt) or enantiomorphism (such as the four triad axes in sodium chlorate), and can also occur in amorphous media that include left- or right-handed molecules (such as fluids containing some organic molecules such as sucrose). See: E.E. Wahlstrom, *Optical Crystallography*, 5th edn, chapter 13
4. Wahlstrom, E.E., 1979. *Optical crystallography*. 5th edn. John Wiley & Sons, New York. p. 50, first paragraph
5. (and/or of reverse sense, if rotation is involved)
6. The two-dimensional space containing the vibration is usually represented by a flat plane. If the wave front is not flat, the plane of vibration is represented by a flat plane tangent to the wave front at the point under consideration. This is called the wave-tangent plane.
7. The phrase 'transverse relationship' holds for the isotropic case, where the vibration may be any random direction within a plane perpendicular to the direction of propagation. It also holds for all anisotropic cases including polarized light (with linear, circular, or elliptical polarization) and a flat vibration plane that is tilted from being perpendicular to the ray direction (to conform with the wave-tangent plane).
8. This first kind of optic axis is monorefringent (exhibits zero birefringence) for all criteria that are not self-limiting. That is, for any kind of polarized light, for ray velocity, and for wave-normal velocity this optic axis is a propagation direction that will exhibit zero birefringence.
9. One of (so uniaxial because when looking for one kind of optic axis only one will be found).
10. Two of each (so biaxial because when looking for one kind of optic axis two of that kind will be found).
11. Much literature has referred to this as a direction of 'single refraction' but such wording is clearly inaccurate when no refraction takes place.
12. After G.R. Fowles, *Introduction to modern optics*, 2nd edn, reprinted 1989. Dover Publications, New York. Figure 6.19, p.190 (with correction)
13. Companion vibrations have mutually perpendicular vibrations.
14. Companion vibrations have reverse sense of rotation.
15. Companion vibrations have reverse sense of rotation and the ellipses' major axes are mutually perpendicular.
16. Wave-normal velocity is velocity in that direction perpendicular to the wave tangent plane. In isotropic media, in uniaxial optic axes, and in anisotropic propagation directions that coincide with a principal vibration direction, this corresponds with the ray direction.
17. The optic plane is that plane that contains both the highest RI (γ) and the lowest RI (α) vibration directions.
18. *Figure 3* also shows the wave-normal for each of the rays travelling along the internal optic axis. The ray direction of the refracted external rays will depend, of course, upon the slope of the exit surface. The exit surface cannot be tangent to both wave fronts at the same time, so the external rays cannot be along the internal wave-normal. If, for example, the exit surface is tangent to the elliptical wave front at the internal optic axis, then the ray vibrating in the circular wave front will refract toward the ray at the wave-normal for the elliptical wave front. If the exit surface is tangent to the circular wave front at the internal optic axis, then the ray vibrating in the elliptical wave front will refract toward the wave-normal for the circular wave front while the other ray travels straight on. Other slopes of the exit surface will cause both rays to refract, and they will always be travelling with an angle between them significantly less than the angle between the internal wave-normals.
19. Every ray direction is reversible, so the double-headed depiction of rays allows that this diagram could be interpreted as showing light travelling from the origin 'O' to exit through the surface 'AB' and then travel as collimated light.

Abstracts

Diamonds

Gem News International.

B.M. LAURS (ED). *Gems & Gemology*, **39**(4), 2003, 322-46.

The gemmological properties of three famous blue diamonds (the Hope, Blue Heart and Heart of Eternity) are described, together with those of natural yellow diamond with Ni-related optical centres. R.A.H.

Diamond formation and source carbonation: mineral associations in diamonds from Namibia.

I. LEOST, T. STACHEL, G.P. BREY, J.W. HARRIS AND I.D. RYABCHIKOV. *Contributions to Mineralogy & Petrology*, **145**(1), 2003, 15-24.

Mineral inclusions in diamonds from Namibia document a range of mantle sources, including eclogitic, websteritic and peridotitic parageneses. Based on unusual textural features a group of inclusions showing websteritic, peridotitic and transitional chemical features is assigned to an 'undetermined suite' (12% of the studied diamonds). The mutual characteristic of this group is the occurrence of lamellar intergrowths of clinopyroxene and orthopyroxene. In addition, the 'undetermined suite' is associated with a number of uncommon phases: in one diamond $MgCO_3$ is enclosed by clinopyrozene. Other minerals that form touching inclusions with the pyroxene lamellae are: 1) a SiO_2 phase observed in three diamonds, together with $CaCO_3$ in one of them, 2) phlogopite and a Cr-rich 'titanite' (probably lindsleyite). The inclusions document a metamorphic path of decreasing P and T after entrapment in diamond. First, homogeneous low-Ca clinopyroxenes were entrapped at high T, then they exsolved orthopyroxene and probably also SiO_2 (coesite) on cooling along a P, T trajectory that did not allow garnet to be exsolved. Phlogopite, carbonates and LIMA phases are the result of overprint of a peridotitic source rock by a carbon-rich agent. The resulting unusual, olivine-free mineral association and the host diamonds are interpreted as products of extensive carbonation of the peridotite. G.L.B.

Diamond geezer.

J. MCCALL. *Geoscientist*, **14**(3), 2004, 10-11.

Short review of the history of diamond recovery in India. M.O'D.

Diamond crystals.

T. MOORE. *Mineralogical record*, **35**(1), 2004, 9-63.

Notes on the crystallization of diamond are followed by descriptions and illustrations of diamond crystals from various parts of the world. Many are linked to individual mines. M.O'D.

On unusual deep-violet microcrystals of diamonds from placers of Ukraine.

M.N. TARAN, V.M. KVASNYTSYA AND K. LANGER. *European Journal of Mineralogy*, **16**(2), 2004, 241-5.

Ukrainian deep-violet diamond crystals have a distinctive broad absorption band centred at ~560 nm (17850 cm^{-1} or 2.21 eV). The intensity of this band is almost two orders of magnitude greater than that in a light rose diamond from Yakutia. Although previously this band was attributed to the N-V centre because the absorption spectrum of the negative N-V centre in irradiated and unannealed type 1b diamonds is known to have an absorption band with a maximum at a similar wavelength, this assignment is not confirmed. At ~ 77 K, the 17850 cm^{-1} band displays no fine structure that unambiguously shows that it cannot be the band at ~ 2.2 eV, commonly attributed to the N-V centre. This band is probably caused by 'plastic deformation', typical of pink diamonds from the Argyle field. R.A.H.

Carbonatitic melts in cuboid diamonds from Udachnaya kimberlite pipe (Yakutia): evidence from vibrational spectroscopy.

D.A. ZEDGENIZOV, H. KAGE, V.S. SHATSKY AND N.V. SOBOLEV. *Mineralogical Magazine*, **68**(1), 2004, 61-73.

Micro-inclusions (1-10 μm) in 55 diamonds of cubic habit from the Udachnaya kimberlite have been shown by IR and Raman spectroscopy to contain a multiphase assemblage which includes carbonates, olivine, apatite, graphite, water and silicate glasses. These micro-inclusions preserve the high internal pressure and give confidence that the original materials were trapped during growth of the host diamond. These internal pressures, extrapolated to mantle temperatures, lie within the stability field of diamond; the relatively low temperatures are typical for the formation of cuboid diamonds. In contrast to previous data for African diamonds, the micro-inclusions in the Udachnaya cuboids are extremely carbonatitic in compostion, $(H_2O)/(H_2O + CO_2) \sim 5\text{-}20\%$, with an observed assemblage of micro-inclusions similar to some types of carbonatites. The low water and silica content testify that the material in the micro-inclusions of the Udachnaya diamonds was near-solidus carbonatitic melt. R.A.H.

Gems and Minerals

Recent discoveries at the Jeffrey mine, Asbestos, Quebec.

M. AMABILI, A. MIGLIOLI AND F. SPERTINI. *Mineralogical record*, **35**, 2004, 123-35.

A short history of the Jeffrey mine, Asbestos, Quebec, Canada, describes a number of gem-quality minerals, including orange grossular, clear colourless grossular with emerald-green cores (a speciality of this location) and pink grossular. Emerald-green, deep violet and multi-coloured vesuvianite are also described. Collecting at the mine, always restricted to professionals, has

ISSN: 1355-4565

now ceased due to safety problems as full-scale mining has ceased. M.O'D.

Achate aus Nordwestsachsen: 14 Fundstellen.

W. Beck, U. Thonfeld and H. Prawitz. *Lapis*, **29**(2), 2004, 29-34.

Fourteen locations are described for agate in the NW of Saxony, Germany. Many specimens are of ornamental quality. M.O'D.

Crazy Lace-ein bemerkenswerter Achat aus Mexiko.

W. Beck, *Lapis*, **29**(6), 2004, 26-7.

An ornamental agate with elaborate white markings and known as 'Crazy lace' is described from the Santa Rita claim in the Sierra Santa Lucia, northwest Chihuahua, Mexico. Some examples are pseudomorphous after calcite. M.O'D.

Achate aus Nordwestsachsen: 14 Fundstellen.

W. Beck, U. Thonfeld and H. Prawitz. *Lapis*, **29**(2), 2004, 29-34.

Fourteen locations are described for agate in the NW of Saxony, Germany. Many specimens are of ornamental quality. M.O'D.

Topaz from Killiecrankie, Flinders Island, and other Bass Strait islands.

R.S. Bottrill, R.N. Woolley and A.B. Forsyth. *Australian Gemmologist*, **22**(1), 2004, 2-9, 1 illus., 1 map.

Flinders Island is one of the Furneaux group of islands in Bass Strait between Tasmania and the Australian mainland. The main occurrence of colourless to pale-coloured gem topaz on Flinders Island is in the fossicking area around Killiecrankie Bay at the north-eastern end of the island. Gem topaz crystals, locally known as *Killiecrankie diamonds*, have been recovered in some abundance from around the Bay since at least 1803. Some of the topaz occurs as well formed, pale-coloured glassy crystals, but most are moderately to highly rounded and frosted in the alluvial deposits. The primary deposits are in cavities in granitic pegmatite veins up to a metre or more wide. Details are given of the chemistry, crystallography and the typical inclusions of the topaz crystals. P.G.R.

The origin of precious opal – a new model.

B. Deveson. *Australian Gemmologist*, **22**(2), 2004, 50-8, 1 map, 1 illus.

This new model for the formation of precious and potch opal is based on the association between opal and natural artesian springs called mound springs. The Lightning Ridge opal field lies on a line of such springs, and active and extinct mound springs are found in the general proximity of several sedimentary opal fields in New South Wales, South Australia and Queensland. Where the mound spring waters have the appropriate chemistry (i.e. alkaline with a high silica content), a mechanism is suggested in which the physico-chemical properties of the water are changed so that suitable silica spheres and then linear chains of these spheres are formed. A final component of the new model is the presence of suitable voids lined with clay that can act as a semi-permeable membrane to concentrate and purify the silica spheres by ultra filtration and dialysis. P.G.R.

Recent study of fluid inclusions in corundum of Sri Lanka.

M.D.P.L. Francis, H. Matsueda, J. Torimoto, P.G.R. Dharmaratne and G. Giuliani. *Gemmologie. Z. Dt. Gemmol. Ges.*, **52**(4), 2003, 163-76. 10 photographs, 1 map, 4 diagrams, bibl.

It was possible to confirm the theory that fluid inclusions in Sri Lankan corundum contained more or less pure CO_2 and that the most common daughter minerals included were graphite and diaspore. The necking observed was similar to that found in Malawi material. The fluid inclusions were classified into four categories according to shape, size and microscopically visible contents of the voids. A model was formulated to describe the fluid inclusions in relation to the formation of corundum in Sri Lanka. E.S.

Le contexte minéralogique des gisements d'opale de la région de São Geraldo do Araguaia, Etat de Pará (Brésil).

J-P. Gauthier, D.B. Rosa, S. Rantsordas and J-C. Samama. *Revue de gemmologie AFG*, **149**, 2004, 11-14.

Opal of ornamental quality is described from the area of São Geraldo do Araguaia, Pará, Brazil. Specimens have SG between 2.0-2.65, RI 1. 43-1.46, H 5.5-6.5. M.O'D.

L'opale d'Ethiopie: gemmologie ordinaire et caractéristiques exceptionelles.

J-P. Gauthier, F. Mandaba Mazzero and E. Fritsch. *Revue de gemmologie AFG*, 2004, **149**, 15-23.

Details of gem opal from Ethiopia are given; SG 1.39-2.06, RI 1.40-1.46. Values are affected by porosity. The opal shows a play-of-colour against a brownish background. Traces of strontium, lead and niobium have been found in some specimens. Internal features are described; parallel lines probably associated with grain boundaries may turn out to be helpful in distinguishing these opals. The opal-bearing sites are located approximately 250 km from Addis Ababa in the province of Shewa. Opal is found as rhyolitic nodules which are often near-spherical and may reach 20 cm. M.O'D.

New interpretation of the origin of tiger's-eye.

P.J. Heaney and D.M. Fisher. *Geology*, **31**(4), 2003, 323-6.

Tiger's-eye is an attractive and popular gemstone. For more than a century, textbooks and museum displays have identified the material as an archetype of pseudomorphism, i.e. the replacement of one mineral by another with the retention of the earlier mineral's shape. This new study has revealed that the textures responsible for the shimmer of tiger's-eye do not represent pseudomorphic substitution of quartz after pre-existing crocidolite asbestos. Rather, it is argued that tiger's-eye classically exemplifies synchronous mineral growth through a crack-seal vein-filling process. P.B.L.

Sapphire-blue kyanite from Nepal.

U. Henn. *Australian Gemmologist*, **22**(1), 2004, 35-6, 5 illus.

Kyanite is known to be an important rock-forming mineral, but gem-quality specimens are relatively rare and mostly used as a collector's stone. Attractive intense blue kyanite of high transparency was recently brought into the gemstone market from a new occurrence in Nepal. The faceted stones investigated are of up to 12.2 ct in weight and possess the typical physical characteristics of blue gem kyanite. P.G.R.

Spinel from Kayah State (Myanmar).

U.T. Hlaing. *Australian Gemmologist*, **22**(2), 2004, 64-6, 1 map, 1 illus.

A sample of gem-quality mainly pink to red spinels from Kayah State in the east of Myanmar was given to the author for testing and evaluation. Kayah State is one of the smallest states in Myanmar and is bounded on the east by Thailand, to the south and west by Karen State and to the north by the Shan State. The approximate location of this new alluvial deposit is indicated in the paper and on the accompanying map, and details are given of the area's geology. P.G.R.

Amino acids in the nacre layers of shell from *Magnavicula penguin* and blister pearls from Sanya, China.

Huang Fengming, Chen. Zhonghui, Zhou Ying and Yang Mingxing. *Australian Gemmologist*, **22**(1), 2004, 29-31, 1 table.

The compositions and contents of amino acids in the nacre layers of shells of the oyster *Magnavicula penguin* from Sanya, China, and in blister pearls produced in the same oyster, were determined using a Model 835-50 Hitachi automatic meter. Comparison measurements were also taken from cultured freshwater pearls from Ezhou, Hubei, and cultured seawater pearls from Indonesia and Beihai, Guangxi, China. Tabulated results showed that the shells and blister pearls of the *Magnavicula penguin* from Sanya both contained similar amino acids. Other measurements showed that the total concentration of amino acids in the nacre layer close to the hinge line is higher than that of amino acids in the margins of the shell. Blister pearls produced by the *Magnavicula penguin* contain the highest concentration of amino acids in all the tested samples. P.G.R.

Culturing abalone half-pearls.

P. Hutchins. *Australian Gemmologist*, **22**(1), 2004, 10-20, 19 illus.

New Zealand is presently the one of at least two successful abalone pearl culture operations utilising the New Zealand paua, *Haliotis iris*. Roger Beatie, Managing Director of the Eyris Blue Pearl Company, is responsible for the creation of the Eyris cultured half pearl after becoming interested in farming paua. He currently has three pearl farms (in the Whangamoe inlet on New Zealand's Chatham Islands, in Akaroa Harbour on the Banks Peninsular, and at Tory Channel in the Marlborough Sounds). These farms are geographically isolated from each other to minimise the risk of loss of stock due to algal bloom and other natural disasters. The paper provides information on the history of the abalone and then describes the technologies and methods used by the Eyris Company to culture and harvest half pearls. Criteria used to grade the pearls are also illustrated and briefly described. P.G.R.

Achate aus der Sierra Pintada, Argentina.

P. Jeckel and M. Henkel. *Lapis*, **28**(10), 2003, 33-7.

Agate of strikingly deep red and white patterning is described from locations in the Sierra Pintada, Argentina. A brief description of the occurrences is given. M.O'D.

Der Stein des Regenbogens: 'Rainbow Calsilica'.

L. Kiefert, J. Hänni, P. Vandenabeele, L. Moens and V.M.F. Hammer. *Gemmologie. Z. Dt. Gemmol. Ges.*, **52**(4), 2003 151-62. 7 photographs, 4 diagrams, bibl. (English abstract)

The spectacularly colourful gem material from Mexico was offered on the market as 'rainbow calcilica', 'calcilica' and 'fossilized clay'. It was marketed as a natural material with pictures of the mine and certified by a laboratory in Arizona. Examination by Raman spectra showed the material to be artificial, partly coloured by artificial pigments and stabilised by a waxy resin. E.S.

Pink gem quality orthoclase from the Mogok Stone Tract, Myanmar.

U.H. Kyi and U.K. Thu. *Australian Gemmologist*, **22**(1), 2004, 29-34, 4 illus.

Although transparent pink orthoclase is rare, particularly in Myanmar, a pink gemstone discovered in the rough in the Mogok Stone Tract was studied and found to be a facetable orthoclase feldspar. This paper provides details of the feldspar's physical/optical properties, XRD features and trace element analysis. P.G.R.

Moonstone from the Karkonosze pegmatites (the Sudety Mountains, Poland).

W. Łapot and E. Szełeg. *Mineralogia polonica*, **34**(1), 2003, 27-36.

Gem-quality moonstone is described from pegmatites in the Karkonosze area of the Sudety Mountains, Poland. The nature of the K-feldpar structure determines the shade of blue seen: thus micromezoperthite gives a pale blue, microperthite blue and cryptoperthite violet-blue. The quality of the moonstones is said to be the equal of good Sri Lanka material. M.O'D.

Gem News International.

B.M. Laurs (Ed.). *Gems & Gemology*, **39**(4), 2003, 322-46.

A 23 x 14.5 mm crystal and five cabochons of afghanite (the latter speckled with inclusions of lazurite) are reported as is a variety of rough and polished quartz crystals ('platinum quartz') containing blades of brown or tan brookite coated with precisely oriented needles of rutile. A 3.84 ct faceted yellow stolzite and a 147 ct golden orange scapolite are also described, along with new synthetic opal varieties and carved plastic imitation 'scrimshaw' walrus tusks. R.A.H.

Pezzottaite from Ambatovita, Madagascar: a new gem material.

B.M. Laurs, W.B. Simmons, G.R. Rossman, E.P. Quinn, S.F. McClure, A. Peretti, T. Armbruster, F.C. Hawthorne, A.U. Falster, D. Günther, M.A. Cooper and B. Grobéty. *Gems & Gemology*, **39**(4), 2003, 284-301.

Pezzottaite, ideally $Cs(Be_2Li)Al_2Si_6O_{18}$, is a new Cs, Li-rich member of the beryl group. It was discovered in a granitic pegmatite near Ambatovita in central Madagascar. The limited number of transparent faceted stones and cat's-eye cabochons that have been cut usually show a deep purplish-pink colour. Pezzottaite can be distinguished from beryl by its higher RI (typically ϵ 1.607-1.610, ω 1.615-1.619) and *D* of 3.09-3.11 g/cm³. The IR and Raman spectra and XRD pattern are also distinctive, while the visible spectrum is similar to that of morganite. The colour is probably caused by radiation-induced colour centres involving Mn^{3+}. R.A.H.

Iridescence of a shell of *Pteria Sterna* (Gould 1851): an optical and structural investigation.

Y. Liu, K.N. Hurwit and L. Tian. *Gemmologie. Z. Dt. Gemmol. Ges.*, **52**(4), 2003, 145-50, 7 photographs, bibl.

The shells of the pearl-producing *Pteria sterna* show strong iridescence, usually green and purple, but also violet blue and golden yellow. The aragonitic nacre layers are characterized by growth lines or grooves which form diffraction reflection gratings. The density of these grooves changes with the position within the shell. Change of the groove density corresponds directly to a change in the strength of the iridescence. E.S.

Inclusions in Vietnamese Quy Chau ruby and their origin.

P.V.LONG, H.Q.VINH AND N.X.NGHIA. *Australian Gemmologist*, **22**(2), 2004, 67-71, 10 illus.

Samples of rubies from Quy Chau, Vietnam, were collected for this study by the authors during several field trips. The characteristics of the inclusions were examined by optical microscopy, and their compositions were analysed by Raman scattering and SEM. The abundant inclusions listed in the paper are quite diverse in chemical composition, suggesting the possibility of two origins – by metamorphism or by metasomatism. P.G.R.

Heliotrop in Sachsen... und Fluoritachat.

M. LÜTTICH. *Lapis*, **28**(12), 2003, 44-5.

Ornamental-quality opaque green chalcedony with red flecks and agate with fluorite banding are described from areas of Saxony, Germany. M.O'D.

The Trimouns quarry, Luzenac, Ariège, France.

F. MARTY. *The Mineralogical record*, **35**, 2004, 225-47.

Among mineral species occurring as crystals of possible ornamental quality at the Trimouns quarry, Luzenac, Ariège, France, is bastnasite-(Ce). M.O'D.

Gemmological Notes.

C.C.MILISENDA. *Gemmologie. Z. Dt. Gemmol. Ges.*, **52**(4), 2003, 123-6. 4 photographs.

Some translucent, apple green rough material weighing between 1 and 3 g was found to be opal, said to come from a locality near the border of Croatia and Macedonia. SG 2.08-2.10. Some other green opal was submitted with similar appearance, but with much lower SG (1.33-1.37); this material melted when touched with a hot needle and was found to be artificial. Some emerald imitations on the market proved to be dyed quartzes.

Some cabochons weighing approximately 5 g each were made of an intergrowth of ruby with fuchsite and kyanite. The material comes from India, but is not dissimilar to material from Zimbabwe and Mashishimala in South Africa. The suggested name is corundum fuchsite; the combination of red (ruby), green (fuchsite) and blue (kyanite) is very attractive.

Some transparent yellow-brown to orange-brown rough weighing up to 5 g and a faceted specimen weighing 3.19 ct were examined and found to be bastnasite. The material comes from a new source in the Peshawar district of Pakistan. It is hexagonal with a low hardness of 4-4½ and is a rare earth carbonate. It is named after a locality in Sweden. E.S.

What's new in minerals.

T. MOORE. *The Mineralogical record*, **35**, 2004, 249-63.

Among crystals and gemstones exhibited at the Tucson Show of 2004 were: a dark greenish-blue euclase crystal from Colombia measuring near 18 cm, pink scapolite crystals from Badakhshan, Afghanistan, a colourless natrolite crystal about 3.9 cm, Mont St Hilaire, Quebec, Canada, and blue scheelite crystals from Baia Sprie (formerly Felsőbánya), Maramures, Romania. M.O'D.

Lab Notes.

T.M. MOSES, I. REINITZ, S.F. MCCLURE AND M.L. JOHNSON (Eds). *Gems & Gemology*, **39**(4), 2003, 314-21.

Items noted include artificially coated diamonds, a bluish-green dichroic emerald, a high-RI violet-blue glass (*n* 1.700) simulating tanzanite, blue sapphires treated to give an unusual colour zoning and filled cavities in a cut spinel. R.A.H.

Moganite and water content as a function of age in agate: an XRD and thermogravimetric study.

T. MOXON AND S. RÍOS. *European Journal of Mineralogy*, **16**(2), 2004, 269-78.

The crystallite size, and the content of moganite, molecular surface water and internal water in agates from volcanic host rocks ranging from 38 to 1100 Ma have been measured. Water is shown to be involved in the transformation of moganite into chalcedony; the maximum amount of moganite found in agate was 14%, but after ~ 410 Ma it is only present in trace amounts. Changes in the degree of crystallinity of agates from 10 host rocks < 412 Ma have been determined; for eight regions, agate genesis appears to have been roughly penecontemporaneous with formation of the host rock; in the other two regions hydrothermal activity from a second volcanic event may have occurred. R.A.H.

L'émeraude de la Vallée de Binn.

T. MUMENTHALER AND A. FREY. *Schweizer Strahler*, **4**, 2003, 4-11 and 24-30.

Emerald of near-gem quality is described from the Binn valley, Valais, Switzerland where aquamarine has also been found. Speculations on origin are presented. Illustrations in this French issue differ from those in the German version on pp 24-30. M.O'D.

Agates and geodes from the Khur area, Central Iran.

M. NAZARI. *Australian Gemmologist*, **22**(1), 2004, 21-8, 38 illus. (27 on separate insert).

The Khur agates of Central Iran have long been celebrated for their fine blue banding and this paper is the first scientific study of the agates and their associated minerals. These minerals have been identified either visually, microscopically, and/or by XRD, SEM and EDS. The numerous colour illustrations are individually supported by descriptive texts. P.G.R.

Zagi Mountain, Northwest Frontier Province, Pakistan.

H. OBODDA AND P. LEAVENS. *The Mineralogical record*, **35**, 2004, 205-20.

Bastnasite-(Ce) of gem quality is described from Zagi Mountain, which is located about 5.5 km SE of Warsak Dam on the Kabul River in the Peshawar District, North West Frontier Province, Pakistan. Crystals and an orange-red transparent faceted stone are illustrated; transparent rutile and orange zircon are also found in the area. The rutile contains Hg as a trace element, a composition not previously reported. M.O'D.

Der Pegmatit von Anjiahamiary bei Fort Dauphin, Madagaskar.

F. PEZZOTTA AND M. JOBIN. *Lapis*, **29**(2), 2004, 24-8.

A pegmatite located at Anjiahamiary, NE of Fort-Dauphin, Madagascar, has produced gem-quality tourmaline group species (liddicoatite and rossmanite) in pink, green and blue colours. M.O'D.

Rätsel im breenendheissen Sand: das libysche Wustenglas.

C. PINTER AND H. STEHLIK. *Lapis*, **28**(10), 2003, 11-6.

Natural transparent lemon-coloured glass is found as lumps in the Libyan desert. Specimens are described and their origin speculated upon. M.O'D.

Ungewöhnliche Turmaline vom Erongo, Namibia.

P. RUSTEMEYER. *Lapis*, **28**(11), 2003, 29-41.

Tourmaline of ornamental quality is described from the Erongo massif in Namibia, north-west of Windhoek. Crystal forms and habits are investigated and colour zoning effects illustrated. M.O'D.

Mineralien der Turmalingruppe. Anwendungsmöglichkeiten in Technik, Haushalt und Medizin.

K. SCHMETZER. *Lapis*, **28**(10), 2003, 38-50.

Minerals of the tourmaline group find many uses other than ornamental ones. Some technical, household and medicinal applications are described. M.O'D.

Red beryl from Utah: a review and update.

J.E. SHIGLEY, T.J. THOMPSON AND J.D. KEITH. *Gems & Gemology*, **39**(4), 2003, 302-13.

The Ruby Violet (or Red Beryl) mine in the Wah Wah Mts of Beaver County, Utah, is the only known commercial occurrence of gem-quality red beryl in the world. It is found along fractures (often clay-filled) in a topaz rhyolite, and crystallized as a vapour-phase mineral from the reaction of rhyolite-derived gases, vapours originating from heated groundwaters and pre-existing minerals and volcanic glass in the rhyolite. The production over the past 25 years is estimated to have been >60 000 ct, of which about 10% were facetable. R.A.H.

Crocoite.

S.P.SORREL. *Australian Gemmologist*, **22**(2), 2004, 59-63, 1 map, 7 illus.

Tasmania has long been famous among mineralogists and geologists for its specimens of crocoite, a brilliant orange to red lead chromate. Its fame may now spread as the result of crocoite being chosen as Tasmania's Mineral Emblem. Apart form Russia, Tasmania is one of the few places in the world where such beautiful specimens are found. This paper describes the occurrence and gemmological properties of the rare mineral. A group of crystal specimens and two faceted specimens are illustrated. P.G.R.

Geochemie und Petrologie von Smaragdvorkommen – Erfahrungen aus dem Smaragdbergbau in Sambia und Simbabwe – Teil 2: Sandawana, Simbabwe.

K.C. TAUPITZ. *Gemmologie. Z. Dt. Gemmol. Ges.*, **52**(4), 2003, 127-44, 4 maps, 1 diagram, 2 tables, bibl.

Detailed article about the local geological conditions around Sandawana. The two occurrences of Sandawana in Zimbabwe and Kafutu in Zambia are compared. E.S.

Grün, gelb, rot und blau. Über die Färbung von Titanitkristallen in alpinen Klüften.

S. WEISS AND B. HOFMANN. *Lapis*, **28**(10), 2003, 30-2.

Titanite (sphene) crystals originating in Alpine-cleft deposits show a variety of colours whose origin is discussed. M.O'D.

Sphenkristalle aus der Laghetti-Amphibolitzone, Narètgebiet, Schweiz.

S. WEISS AND F. RIZZI. *Lapis*, **28**(10), 2003, 17-29.

Crystals of sphene and accompanying minerals are described from the amphibolite zone at Laghetti, Ticino, Switzerland. Other Swiss locations for sphene are described. M.O'D.

The early history of the Mineralogical Record.

J.S. WHITE. *Mineralogical Record*, **35**(1), 2004, 73-85.

The origins and development of the *Record* are described by its founder, John S. White. M.O'D.

Quality enhancement of Vietnamese ruby by heat treatments.

P. WINOTAI, P. LIMSUWAN, I.M. TANG AND S. LIMSUWAN. *Australian Gemmologist*, **22**(2), 2004, 72-77, 8 illus.

A suitable heat treatment specifically designed for a particular ruby must be used to enhance both its quality and value. Results of experiments at various temperatures in an oxygen atmosphere suggest that Vietnamese rubies should be treated only at 1500-1600°C to convert them into more valuable rubies of enhanced colour and clarity. Higher temperatures will only yield slightly bluish-red rubies. All samples exhibited better clarity after the treatment, which enhanced the colour of the stones but could not eliminate inclusions. P.G.R.

What's new in minerals.

VARIOUS AUTHORS. *Mineralogical record*, **35**, 2004, 143-79.

Among gem and ornamental-quality specimens described from various mineral shows in Europe and North America are elbaite from Paprock, Kunar, Afghanistan (in the specimen shown the outer green zone has been selectively removed), near-transparent amazonite, clear pink scapolite and clear light green diopside, also from Afghanistan. Pakistan has produced some greenish-grey fluorite octahedra from a locality in the Hunza area. Fine orange-red 'imperial' topaz has been found in the Kolwezi area in the Republic of Congo close to the border with Zambia, and sherry-brown topaz is reported from Pakistan. M.O'D.

Instruments and Techniques

The sclerometer and the determination of the hardness of minerals.

U. BURCHARD. *Mineralogical record*, **35**, 2004, 109-20.

While Mohs' scale is still used for determining the approximate scratch hardness of minerals the sclerometer was developed in the 19th century to give a more precise value of hardness. Different models are described and illustrated. M.O'D.

Synthetics and Simulants

L'opale de synthèse.

J-P. GAUTHIER. *Revue de gemmologie AFG*, **149**, 2004, 24-6.

The difference between synthetic and natural gem-quality opal is reviewed. Hexagonal markings within colour patches continue to be the distinguishing features of the synthetic product. M.O'D.

[Growth of diamond from solution in the $CaCo_3$ melt.]
A.F. Khokhryakov, Yu.M. Borzdov. Yu.N. Pal'yanov and A.G. Sokol. *Proceedings of the Russian Mineralogical Society*, **132**(2), 2003, 87-95 (Russian with English abstract).

Diamond nucleation and growth kinetics on the [100] and [111] faces of seed diamond crystals in the $CaCO_3$-C system were studied in a non-pressing device of 'cross-cut sphere' type at 7 GPa and 1700–1750°C in experiments of 10 min to 18 h duration. The growth of [100] develops in the diffusion-limiting regime, and growth on [111] is determined mainly by the kinetics of superficial processes. Evolution of the surface accessories on the [111] faces was traced from triangular frame defects up to large trigonal pyramids. Comparison with similar Si and Ge patterns shows that the trigonal pyramids are complex twins. The only stable cubic forms of diamond growth in the $CaCO_3$-C system are tetragontrioctahedron faces; among them only {322} faces achieve the habit scale of development. R.A.H.

[About mechanism of the fibrous structure appearing in cubic diamond crystals.]
V. M. Sonin, D. G. Bagryantsev, A.I. Chepurov and J.-M. Dereppe. *Proceedings of the Russian Mineralogical Society*, **132**(2), 2003, 95-8 (Russian with English abstract).

The growth of diamond crystals at high *P* in the Fe-Ni-C system was studied in terms of a *T* decrease of ~1-2°/sec. A phenomenon has been detected of octahedral crystals re-facing via the transformation of numerous tiny cubic sub-individuals on their faces. Data show that this is possibly the formation mechanism of natural cubic diamond crystals with a fibrous structure. This is based on the growth of cubic sub-individuals parallel to one another in the {111} direction with the formation of subparallel fibres. Because of this phenomenon, sectors of cubic growth become enlarged while the octahedral growth sectors are declining; the main cause of this change in the growth mechanism is the sharp increase of supersaturation in the crystallization media provided by the falling *T*. R.A.H.

Gem-quality synthetic diamonds grown by a chemical vapor deposition (CVD) method.
W. Wang, T. Moses, R.C. Linares, J.E. Shigley, M. Hall and J.E. Butler. *Gems & Gemology*, **39**(4), 2003, 268-83.

Brown to grey and near-colourless single-crystal type IIa synthetic diamonds grown commercially using a chemical vapour deposition technique have gemmological properties that are distinct from those of both natural diamonds and HPHT-grown synthetic gem diamonds. The tabular crystals range from up to 1 ct or more and a few millimetres thick, and consist of an overgrowth on a natural or synthetic diamond substrate. Faceted CVD synthetic diamonds generally cannot be distinguished from natural diamond (unless portions of the substrate are still present). In a gemmological laboratory, however, they can be identified by the combination of a strong orangey-red fluorescence seen with the DiamondView deep-UV imaging system, a characteristic anomalous birefringence (strain) pattern and distinctive features in their IR absorption spectra. R.A.H.

Abstractors

G.L. Barron	G.L.B.	P.B. Leavens	P.B.L.	P.G. Read	P.G.R.
R.A. Howie	R.A.H.	M. O'Donoghue	M.O'D.	E. Stern	E.S.

Book Review

Rock-forming minerals. Vol. 4B. (2nd edn). Framework silicates: silica minerals, feldspathoids and the zeolites.
W.A. Deer, R.A. Howie, W.S. Wise and J. Zussman, 2004. The Geological Society, London. pp xiv, 982. Hardcover ISBN 1 86239 144 0. £62 (to Fellows of the Geological Society).

Minerals of especial interest to readers of *The Journal* include quartz and opal, petalite, leucite, species of the sodalite group and the scapolite group; mineral collectors will welcome the revision of the zeolite group. Readers unfamiliar with the series will find unexpected treasures. The authors state their criteria for a mineral's inclusion in the preface to the first edition (1962): [the text will include] only those minerals which, by their presence or absence, serve to determine or modify the name of a rock. In their preface to the second edition the editors make the point that a far greater sophistication in determinative methods has enabled them to improve the quality of information formerly available. This is particularly true of chemical compositions.

For the most part each mineral or group is considered in five distinct parts. These are structures, chemistry, optical and physical properties, distinguishing features (details of determinative tests are given here), and paragenesis, giving the rock types in which the mineral is found and outlining some characteristic mineral assemblies. A concise table of properties precedes each entry and a list of references ends it.

Many will find it pleasing that "light microscopy remains the basic petrological tool underpinning all other methods" but clearly the use of electron microprobe analysis and, to take one example quoted in the preface to the new edition, of environment-controlled specimen stages, will lead to a far deeper understanding of mineral formation and determination. For any serious study of minerals, 'DHS' is vital. M.O'D.

Proceedings of the Gemmological Association and Gem Testing Laboratory of Great Britain and Notices

New appointments at Gem-A

President

We are delighted to announce that at the Annual General Meeting held on Tuesday 14 September E Alan Jobbins was elected President of the Association for the term 2004-2006.

E Alan Jobbins BSc CEng FIMM FGA was Curator of Minerals and Gemstones at the Geological Museum in London from 1950 to 1983. During these years he acted as consultant to a wide range of enquirers from which a series of research papers developed. These included, among many others, a major study of East African garnets, the first papers characterizing the structure and identification of synthetic opals, the discovery of a new mineral magnesio-axinite and the field study of the Barwell meteorite fall. His many overseas assignments (for the United Nations and the British Government) included setting up a gemmological laboratory in Rangoon, Burma (now Myanmar) and the subsequent training of a cadre of students who successfully passed the Gemmology Diploma examinations; a major study of the Pailin ruby and sapphire deposits in Cambodia with recommendations for improved working methods; an assessment of diamond and opal deposits in Piaui State, Brazil; a survey of the Sri Lankan gemstone industry to improve cutting techniques and many other projects. In 1988 he gave a series of lectures and initiated gemmological training with new laboratory facilities at the China University of Geosciences in Wuhan. In the UK his record includes 32 years as a gemmological lecturer at the Sir John Cass College (now the London Metropolitan University), some 20 years as an examiner for the Association's gemmology examinations and eight years as Editor of *The Journal of Gemmology*. He is a popular lecturer and has presented papers in some 30 countries around the world. In 1986-89 he was privileged to be a member of the team which conducted the first gemmological examination of the English Crown Jewels. These researches were published as part of a major two volume catalogue. He is an Executive Member of the International Gemmological Conference and is currently President of the Society of Jewellery Historians.

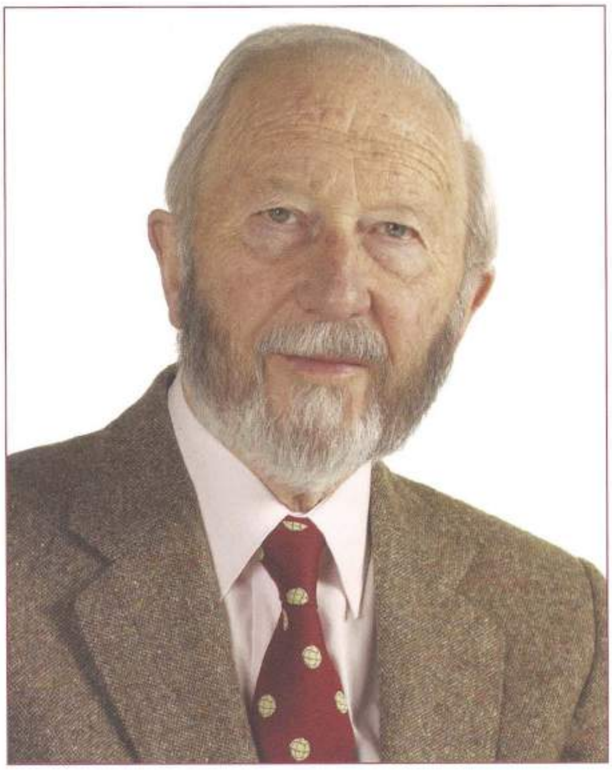

E Alan Jobbins, President

ISSN: 1355-4565

Chief Executive Officer

Dr Jack Ogden, a Fellow of Gem-A and a founder member of the SJH, has been appointed Chief Executive Officer of Gem-A on the retirement of Terry Davidson on 1 November 2004. A report of the appointment was published in the September 2004 issue of *Gem & Jewellery News*.

Honorary Life Member

Ian Thomson, who retired from the Council at the Annual General Meeting after serving for 14 years, has been awarded an Honorary Life Membership in recognition of his substantial contribution and commitment to the Association.

Members' Meetings

London

On 27 July at 27 Greville Street, London EC1, an Extraordinary General Meeting was held, a report of which appears below. The EGM was followed by a talk by Terry Davidson on the jewellers of Bond Street.

Midlands Branch

On 24 September at the Earth Sciences Building, University of Birmingham, Edgbaston, Professor A T Collins gave a lecture entitled 'Colour in natural and artificial diamonds'.

North East Branch

On 26 July at Evans of Leeds Ltd, Millshaw, Alan Hodgkinson gave a talk and practical workshop entitled 'Putting the Gee back into gemmology'.

On 19 October at Evans of Leeds Ltd, Millshaw, Martin Vainer gave a talk with the title 'Fancy diamonds?!'

North West Branch

On 15 September at Church House, Hanover Street, Liverpool 1, Alan Hodgkinson gave a talk and workshop entitled 'A few of my favourite things'.

On 20 October at Church House Marcus McCallum gave a talk entitled 'Pearls: the trade industry today'.

Scottish Branch

On 26 September a gold panning field trip to Tyndrum was arranged.

On 6 October at the British Geological Survey, Murchison House, West Mains Road, Edinburgh, Guy Clutterbuck gave a talk entitled 'The coloured stone business from a global perspective'.

On 19 October at the Hunterian Museum, University of Glasgow, Neil Clark, the Curator of Palaeontology at the Hunterian Museum, gave a talk on the inclusions in amber.

South East Branch

On 22 August at Gem-A headquarters at 27 Greville Street, London EC1, David Lancaster gave a presentation entitled 'Can provenance be valued?'

South West Branch

On 12 September at the Bath Royal Literary and Scientific Institution, 16-18 Queen Square, Bath, Maggie Campbell Pedersen gave a presentation and practical session entitled 'Organics in the afternoon'.

Annual Report

The following is the Report of the Council of the Gemmological Association and Gem Testing Laboratory of Great Britain for the year ending 31 March 2004.

Officers, Councils and Committees

Gem-A The Gemmological Association and Gem Testing Laboratory of Great Britain is a company limited by guarantee and is governed by the Council of Management. The Council of Management was strengthened by the election of L M Hudson FGA, an American financier and private investor with international banking and investment portfolio experience.

J Kessler retired as chairman of the Trade Liaison Committee. W Roberts and J Evans-Lombe were elected chairman and vice-chairman respectively of the Committee. C Winter and P Dwyer-Hickey continued as Chairman and Vice-Chairman respectively of the Members' Council. *(Continued on p.246)*

Gem-A Awards

Gem-A Examinations were held worldwide in June 2004. In the Examinations in Gemmology 258 candidates sat for the Diploma Examination of whom 92 qualified, including two with Distinction and 13 with Merit. In the Foundation Gemmology Examination, 178 candidates sat of whom 121 qualified. In the Gem Diamond Examination 95 candidates sat of whom 60 qualified, including ten with Distinction and seven with Merit.

The Anderson Bank Prize for the best non-trade candidate of the year in the Diploma in Gemmology Examination, the Anderson Medal for the candidate who submitted the best set of answers in the Foundation Certificate examination which, in the opinion of the Examiners, are of sufficiently high standard, and the Hirsh Foundation Award for the best candidate of the year in the Foundation Certificate examination, have been awarded to Jiang Huijing, Zhuhai City, Guangdong, P.R.China.

The Christie's Prize for Gemmology for the best candidate of the year in the Diploma Examination who derives his or her main income from activities essentially connected with the jewellery trade has been awarded to Anu D. Manchanda, Smethwick, West Midlands.

The Deeks Diamond Prize for the best candidate of the year in the GemDiamond Examination has been awarded to Emma L. McMillan, Dalkeith, Midlothian.

The Tully and Bruton Medals were not awarded.

The names of the successful candidates are listed below:

EXAMINATIONS IN GEMMOLOGY

Gemmology Diploma

Qualified with Distinction

Jiang Huijing, Zhuhai City, Guang Dong, P.R. China
Scott, John R.J., Vancouver, British Columbia, Canada

Qualified with Merit

Choi, Eun Jung, Jeolanam-Do, Korea
Landmark, Vicky, Harpenden, Hertfordshire
Lee Yu Mi, Gyeonggi-Do, Korea
Liao Baoli, Guilin, Guangxi, P.R. China
Manchanda, Anu Dippal, Smethwick, West Midlands
Ramerison, Tokinomena A., Antananarivo, Madagascar
Ren Ming, Wuhan, Hubei, P.R. China
Sordini, Federico, Cagli, Italy
St John Lewis, Delyth, South Norwood, London
Tsutsui, Kazumi, London
Wells, Miranda, Hartlebury, Worcestershire
Wong Ching Man, Discovery Bay, Hong Kong
Zhang Kui, Wuhan. Hubei, P.R. China

Qualified

Agrawal, Puru, New Delhi, India
Aki, Miou, Osaka City, Osaka, Japan
Anderson, Tricia, Helen's Bay, Bangor, N. Ireland
Aung, Htet Su, Yangon, Myanmar
Aura, Kimmo, Espoo, Finland
Blanksma, Eelco, Arnhem, The Netherlands
Brard, Jagvinder Singh, Pinner, Middlesex
Broglie, Nicole, Zurich, Switzerland
Chandhok, Jasmeet Singh, New Delhi, India
Curtis-Taylor, Tracey, London
Dong Xinzhi, Wuhan, Hubei, P.R. China
Drijver, Joyce M-L., Utrecht, The Netherlands
Fu Ming, Guilin, Guangxi, P.R. China
Gaskin, Clare Kathryn, Putney, London
Gerber, Doris C., Zurich, Switzerland
Goel, Amita, New Delhi, India
Gray, Matthew N., Lismore, New South Wales, Australia
Hasegawa, Akemi, Akashi City, Hyogo Pref., Japan
Hearnden, Rachel C., Sheffield, South Yorkshire
Hemlin, Colette, Anjou, Quebec, Canada
Hirst, Catherine, Harborne, West Midlands
Hsin Shih Meng, Wuhan, Hubei, P.R. China
Htin Lynn Aung, Yangon, Myanmar
Huang Qiulan, Wuhan, Hubei, P.R. China
Ideno, Yumi, Nishinomiya City, Hyogo Pref., Japan
Inoue, Koichi, Suita City, Osaka, Japan
Kao Oi Shan, Patsy, Chai Wan, Hong Kong
Khaing Win Win, Yangon, Myanmar
Kueon, Seon-Il, Bupyong-ku, Inchon, R. of Korea
Kwok Sau Mei, Halisa, Tai Po, Hong Kong
Lai Mei Oi, Emily, Tuen Mun, Hong Kong
Lee Young Shin, Kyunggido, Korea
Lee Jeong Im, Seoul, Korea
Lee Kyu Ho, Jeonlanam-Do, Korea
Li Mo Ching, Hong Kong
Li Yue, Shanghai, P.R. China
Liu Bao, Wuhan, Hubei, P.R. China
Liu Fang, Wuhan, Hubei, P.R. China

Gem-A Awards

Lovelock, Justina E., London
Lyons, Annabel H., London
Manolia, Evgenia, Zografou, Greece
Marsh, Claire, Stourbridge, West Midlands
Moe Tin Tin, Yangon, Myanmar
Moore, Katherine, Symington, Ayrshire
Pai, S. Vishnunarayan, Kerala, India
Pang Shing Kwan, New Territories, Hong Kong
Pang Taotao, Guilin, Guangxi, P.R. China
Piacenza, Maria Rene, Sutton, Surrey
Pumpang, Sureeporn, Nakoonpathom, Thailand
Ruan Yaohua, Guilin, Guangxi, P.R. China
Sien Pe (a) Yang Cheng Pei, Yangon, Myanmar
Singh, Amrinder Pal, Nagar, Delhi, India
Song Dong, Shanghai, P.R. China
Stanyer, Natasha, Lewes, East Sussex
Turku, Jenni J., Helsinki, Finland
Valvio, Raija L.M., Vaajakoski, Finland
van Gorkom, Annemarie, Utrecht, The Netherlands
van Schaik, Persis L., Groot-Ammers, The Netherlands
Visschers-Villerius, Cornelia, Heerde, The Netherlands
Wai Yee Tak, Elise, New Territories, Hong Kong
Welton-Cook, Elsa, West Kensington, London
Wessels, Jurie H.W., London
Williams, Benjamin J., Blockley, Gloucestershire
Wold, William, Joure, The Netherlands
Wong, Rosemary M.N., New Territories, Hong Kong
Wong Chung Yan, Kowloon, Hong Kong
Wu Shengfan, Wuhan, Hubei, P.R. China
Xu Ping, Shanghai, P.R. China
Yang Jiaru, Wuhan, Hubei, P.R. China
Yang Ruochen, Wuhan, Hubei, P.R. China
Zhang Tao, Wuhan, Hubei, P.R. China

Gemmology Foundation Certificate

Qualified

Alcock, Kate, Byford, Hereford and Worcester
Asavaroengchai, Suwanna, Bangkok, Thailand
Barker, Matthew, Taipei, Taiwan, R.O. China
Baskerville, Fenella, London
Bayoumi, Nevin, London
Chan Ching Han, New Territories, Hong Kong
Chan Fung Ping, Kowloon, Hong Kong
Chau Lok Yuen, Amy, Kowloon, Hong Kong
Chiu Shu-Fen, Taipei, Taiwan, R.O. China
Chiu Ka Ming, Kowloon, Hong Kong
Choi Eun Jung, Jeolanam-Do, Korea
Chu Yan Yan, Joey, New Territories, Hong Kong
Chu Hon Chung, New Territories, Hong Kong
Coene, Helena I.I., Wezembeek Oppem, Belgium
Comerford, Elaine-Sarah, Dunhill, Co. Waterford, Ireland
Costello, Michael P., Pen-y-lan, South Glamorgan
Costin, Charlotte, Horsham, West Sussex
Cullen, James, Dublin, Ireland
Dawson, Jane, Ashbourne, Derbyshire
Devitt, Isobel, Dublin, Ireland
Eakins, June E., Heswall, Merseyside
Eddery, Colette M., Dublin, Ireland
Eeckhout, Tiphaine, Thomery, France
Espinoza, Juls, Roseville, California, U.S.A.
Fellows, Andrew S., Aldridge, West Midlands
Fong Yan, William, Kowloon, Hong Kong
Gibbons, Timothy B., Battersea, London
Gigg, Daryl B., Stevenage, Hertfordshire
Gillman, Scott, Sudbury, Massachusetts, U.S.A.
Godfrey, Kay, Halstead, Essex
Gogna, Sanjeev, Distt Una, Himachal Pradesh, India
Goodwille, Zoe F., Battersea, London
Hardwick, Christine J.E., Crail, Fife
Heltzel, Christopher, Kilkenny, Ireland
Huang Shieh-Yen, Taipei, Taiwan, R.O. China
Huang, Yvonne, Taipei, Taiwan, R.O. China
Huck, Perry, Stanford-in-the-Vale, Oxfordshire
Hui Wan Man, Kwun Tong, Hong Kong
Hunter, Sara, Athboy, Co. Meath, Ireland
Huth, Melvin G., Orangevale, California, U.S.A.
Kitching, Katherine, London
Ko Hoi Fu, Kowloon, Hong Kong
Kwok Men Yee, New Territories, Hong Kong
Kyaw Cho Cho, Yangon, Myanmar
Kyaw Swar Htun, Yangon, Myanmar
Kyaw Tun Aung, Yangon, Myanmar
Lai Sau Han, Winnie, Kowloon, Hong Kong
Lai Suk Kwan, Eleanor, Kowloon, Hong Kong
Lawton, Sarah, Huncote, Leicestershire
Lee Mi Yu, Gyeonggi-Do, Korea
Lee Kyu Ho, Jeonlanam-Do, Korea
Lee Tin Wan, New Territories, Hong Kong
Leung Chi Fai, Hong Kong
Leung Ka Lok, Kowloon, Hong Kong
Leung Ka Yi, Kowloon, Hong Kong
Li On Kei, New Territories, Hong Kong
Lim Yee Lam, Hong Kong
Lima Pontes, Beatriz, Rio de Janeiro, Brazil
Lin Wai Kei, Tseung Kwan, Hong Kong
Lindstrom, Christina, Spanga, Sweden
Liu Haimei, Guilin, Guangxi, P. R. China
Liu Xianyu, Guilin, Guangxi, P.R. China
Lo Wing See, Kowloon, Hong Kong
Looney, Eimear, Dublin, Ireland
Lu, Shan, Kofu City, Yamanashi Pref., Japan
Malone, Helena, Portlaoise, Co. Laois, Ireland
Marsh, Shona K., Birmingham, West Midlands

Gem-A Awards

Maury-Laribiere, Volodia, Saint Trieix, France
Mera, Kanako, Toyonaka City, Osaka, Japan
Miller, Jodie L., Hinckley, Leicestershire
Mo Mo Win, Yangon, Myanmar
Munich, Lita E., Sacramento, California, U.S.A.
Murphy, Lawrence C., Sacramento, California, U.S.A.
Naw Htar Phyu, Yangon, Myanmar
Newton, Naomi C., Birmingham, West Midlands
O'Dwyer, Michael, Wicklow Town, Co. Wicklow, Ireland
Ogata, Etsuko, Suita City, Osaka, Japan
Palmares, Richard P., Sale, Cheshire
Pan Han, Guilin, Guangxi, P.R. China
Pany, Emmanuel, Clotilde Reonion, France
Peers, Sofia L.R., Leamington Spa, Warwickshire
Pelletier, Lise, Montreal, Quebec, Canada
Pham Quoc, Sacramento, California, U.S.A.
Phisuthikul, Piyamaporn, Bangkok, Thailand
Poole, Jessica, Portadown, Co. Armagh, Northern Ireland
Powar, Krishna, Hockley, Birmingham, West Midlands
Pun Kwok Kong, Kowloon, Hong Kong
Rakotoson, Eric, Montreal, Quebec, Canada
Rana, Ashka, Sureshkumar, Vastapur, Gujarat, India
Ravaoarimalala, Fanjaniaina V., Antananarivo, Madagascar
Ray, Stuart, Gillingham, Dorset
Rouni-Belhadj, Khedidja, London
Ruan Qingfeng, Guilin, Guangxi, P.R. China
Russell, Marie, Bromsgrove, Hereford and Worcester
Sanders, Jacqueline, Towcester, Northamptonshire
Sardjono, Grace W., New Territories, Hong Kong
Saull, Elanor Nico, Stourbridge, West Midlands
Serafim, Evangelia, Glyfada, Greece
Shwe Li, Yangon, Myanmar
Sinclair, Michelle, Nottingham
Smithie, Sheila B., Boston, Massachusetts, U.S.A.
Sordini, Federico, Cagli, Italy
Surangsuriyakul, Nualwan, Samut Prakarn, Thailand
Takahata, Yoshichika, Takamatsu City, Kagawa Pref., Japan
Tam Tin Sang, Daniel, Kowloon, Hong Kong
Tang Yin Tung, Chai Wan, Hong Kong
Taylor, Daniel, Moseley, West Midlands
Teng, Terry, West Hampstead, London
Tripathi, Pooja, Jaipur, Rajasthan, India
Tsang Kwai Ying, Yau Yat Tsuen, Hong Kong
Tsoi Mei Yu, New Territories, Hong Hong
Underwood, Anthony D., Sumner, Texas, U.S.A.
Voulgaris, Apollo, Athens, Greece
Ward, John E.C., London
Wong Lok Yin, Rocky, Kowloon, Hong Kong
Wong Oi Chun, New Territories, Hong Kong
Wongkar, Franky, London
Yamout, Sabah I., Leeds, West Yorkshire
Yang Ping, Guilin, Guangxi, P.R. China
Zhong Lihong, Zhongshan, Guangzhou, P.R. China
Zong Yu, Zhongshan, Guangzhou, P.R. China

Gem Diamond Diploma

Qualified with Distinction
Chen Jianzhi, Wuhan, Hubei, P.R. China
Edwards, Trevor, London
Hanlon, Adrienne K., Ingol, Lancashire
Hira, Vijender Singh, New Delhi, India
Lam Kwi Peng, Singapore
Lim Yee Lam, Hong Kong
Ren Chunhua, Wuhan, Hubei, P.R. China
Surawy, Laura K., Haywards Heath, West Sussex
Tavelov, Dan, Moseley, West Midlands
Thornhill, Helen V., Sheffield, South Yorkshire

Qualified with Merit
Claydon, Louise, Carshalton, Surrey
Fisher, Abigail, London
Lau Siu Ying, Emily, Hong Kong
Pearson, Isabel J., Tilehurst, Berkshire
Shaw, Sinead, London
Tan Mingwei, Wuhan, Hubei, P.R. China
Van Rooij-Roeloffzen, Marjolein, Almere Buiten, The Netherlands

Qualified
Chan Chee Pang, Hong Kong
Chan Lim Chi, Hong Kong
Chan Wing Tung, New Territories, Hong Kong
Chan Ying Hon, New Territories, Hong Kong
Chan Yun Ping, Anna, Southall, Middlesex
Chang Wing Chi, Vivian, Kowloon, Hong Kong
Cheng Wai Yee, New Territories, Hong Kong
Cheung Ching Ping, Candy, Kowloon, Hong Kong
Chie, Christine, Hong Kong
Ching Chin Pang, Kowloon, Hong Kong
Ching Chin Ping, Tung Chung, Hong Kong
Farrell, Ann Marie, Greenford, Middlesex
Hui Wai Wai, Hong Kong
Huo Zhi Yong, Beijing, P.R. China
Hynes, Lola, Dublin, Ireland
Jelinska, Emma, London
Jones, Lorraine, Farnworth, Greater Manchester
Kiamos, George K., Athens, Greece

Gem-A Awards

Kwok Sau Mei, Halisa, Hong Kong
Lawattanatrakul, Thidarat, London
Leung Suk Kay, Hong Kong
Li Bo, Beijing, P.R. China
Lin Yang, Beijing, P.R. China
Manolia, Evgenia, Zografou, Greece
Pennington, Maria, Sprowston, Norfolk
Rebmann, Olivier, Carlsbad, California, U.S.A.
Richmond, Sonia, Herne Hill, London
Romero, Michelle A., St Andrews, Fife
Simo Ooi Kok, London
So Yiu Ki, Eric, Hong Kong
Southam, Karen L., Oldbury, West Midlands
Sowa, Ali Med, Tilbury, Essex
Szymanska, Zofia, London
Thein Myint Myint, Whetstone, London
Thesia, Ashish P., Northolt, Middlesex
Van Rensburg, Stefan, Ealing, London
Wells, John, Bickerstaffe, Lancashire
Whalley, Joanna, Walthamstow, London
Xie Hui, Beijing, P.R. China
Ye Hui Hui, Preston, Lancashire
Yeung Wing Chuen, Benny, New Territories, Hong Kong
Zhang Rui, Beijing, P.R. China
Zhang Yilin, Wuhan, Hubei, P.R. China

(Continued from p.242)

In January 2004 the death was reported with great regret of Alexander E. Farn FGA, a Vice President of the Gemmological Association since 1992.

Gem-A

The financial year 2003/2004 proved to be even more challenging than the previous year. Business in the jewellery trade faced increasing competition from other 'Must have' products and saw the closure and restructuring of many retail and manufacturing companies. Even so, Gem-A managed a modest increase over budgeted income.

Monthly departmental meetings have continued which ensure a continuous flow of up-dated information and the cross fertilization of ideas.

The 2003/2004 appeals to members and the UK trade resulted in 446 donations totalling £12,180. Donations of specimens, including rough and cut stones, synthetics and simulants, has enabled the Association to expand educational courses and examinations.

Education

The Education Office Team have worked tremendously hard over the past year, with final development and promotion work on the new Foundation Certificate Course notes and exam, preparation and launch of the new bi-annual Five-month course, and the varied and new short courses and travelling tutorials. The last year has again seen the London gemmology and gem diamond courses fully subscribed, with students coming from far and wide.

A range of courses and tutorials was held at the Greville Street Gem Tutorial Centre, including a very successful new rough diamond short course. Custom built trade tutorials have continued. D.J. Garrod gave his popular short talks and tutorials at various venues including Norway, Hong Kong, Tucson and several locations around Great Britain.

A greater number of students attended the gemmology and gem diamond examinations compared with the previous year. The Anderson Bank Prize was awarded to Jessica Banks of London. The Christie's Prize for Gemmology was awarded to Xie Jing of Shanghai, China. The Anderson Medal and Preliminary Trade Prize were both awarded to Antoinette Jackson of London. The Deeks Diamond Prize was awarded to Lu Lili of Wuhan, China. Neither the Tully nor the Bruton Medal was awarded.

The Presentation of Awards was again held at Goldsmiths' Hall where the President, Professor A. Collins, presided and welcomed the successful students and their families and friends, who had travelled from as far afield as Hong Kong, Japan, Canada, Sri Lanka and the USA, as well as those from the UK and Europe. Anthony Hirsh presented the awards.

The new Hirsh Foundation Award of £1000 per year had a well-attended press launch at the Las Vegas show. The existing

Gifts

The Association is most grateful to the following for their gifts for research and teaching purposes:

Maggie Campbell Pedersen FGA, London, for an imitation tortoiseshell decorative box.

Mrs K. Findlay, Randburg, South Africa, in memory of her husband, the late Kenneth Findlay FGA; a portable diamond balance in a travel box with a set of weights, a Beck prism spectroscope with wavelength scale, a Beck UV spectroscope and a Beck wavelength reversion spectroscope.

John R. Führbach FGA, Amarillo, Texas, U.S.A., for a collection of specimens including the following: rough specimens of selenite, opalized chert (UV fluorescent), an obsidian slab (New Mexico),quartz and agate (Texas), peridot in lava (Moorea, Tahiti), sugilite slabs (Africa), amethyst (Brazil and Zambia), corundum (Georgia, U.S.A.), turquoise slabs (New Mexico) and a packet of miscellaneous quartz, calcite, agate, chert and garnet; a selection of crystals including rubies (India and North Carolina, U.S.A.), beryl (Colorado, U.S.A.), sapphire (Georgia, U.S.A.), tourmaline (Brazil), emerald (Brazil), calcite slabs (New Mexico), Chatham synethic emerald (very early production), and a large packet of tourmaline; organics including whale 'ivory', shells from Texas.

Mark Saul, Arusha, Tanzania, for a selection of rough specimens from Tanzania including five pieces of vesuvianite, two samples of kornerupine displaying strong pleochroism, and a packet of actinolite from the Tanga district.

Adrian S. Smith FGA, Perth, Scotland, for a Perfect Diagram CD showing different types of facet arrangements.

Abe K. Suleman, Arusha, Tanzania, for a sample of metamorphic emerald source rock from the Manyara emerald deposit, Tanzania.

Ian Thomson FGA, London, for a framed cultured pearl collage.

M. Walsh, Beckenham, Kent, for a presentation set of CZ master cuts.

Anderson Medal is now a discretionary award, on a similar basis to that of the Tully and Bruton Medals.

On the recommendation of the Board of Examiners, S Greatwood and N Rose were appointed examiners for Foundation Certificate in Gemmology and Gem Diamond theory respectively. R Lake was appointed to shadow E Stern on the diamond examination. The Education Review Meeting was held in November and provided useful discussion and exchange of views between tutors, lecturers, examiners and staff of the Education Office.

Lorne Stather's development work on courses, examinations and promotion has increased in scope and included bringing the Diploma in Gemmology notes into continuity with the new Foundation course during the normal process of updating; the development of a new promotional, annual Education Prospectus, now into its second edition; a Gem-A Education leaflet produced for widespread circulation; and a new CD-ROM of Tutor Help and Advice, provided for all ATC and Correspondence Course tutors.

Several new Allied Teaching Centres are at various stages of development world-wide, under the eye of Ian Mercer, with Brenda Hunt's coordination.

Ian Mercer initiated the re-accreditation of Gem-A courses with the QCA during the year; this will include renewal of the levels for our qualifications; to be followed by a European-led credit transfer system.

Gem-A hosted the Federation of European Education in Gemmology (FEEG) General Assembly and Seminar, from 22 to 25 January. Ian Mercer oversaw the FEEG Seminar, held at the Royal College of Surgeons of England, which proved to be a success, with the great organizational assistance of Mary Burland.

Membership

There was a slight decrease in Fellow, Diamond and Associate membership during the year, with Laboratory membership remaining static.

The Gem-A Branch network was expanded in 2003 with the launch of the North East Branch which held its inaugural meeting in Leeds on 10 October. The Midlands Branch held eight meetings as well as their Summer Supper Party and a 51st Anniversary Dinner, and a one-day Conference in February with keynote speaker Stephen Dale. The North West Branch held seven meetings. The Scottish Branch held eight meetings at venues in both Edinburgh and Glasgow, and their Annual Conference in Perth at the beginning of May with John Koivula of the GIA's Gem Trade Laboratory as the keynote speaker. The South East Branch held seven meetings during the year at venues in Central London and Guildford, Surrey. The South West Branch held a meeting in Bath in September. Council is most grateful to the Branch Officers and Committee Members who work so hard to present interesting and varied programmes of activities each year.

Laboratory

Stephen Kennedy, head of the Gem Testing Laboratory, resigned in August 2003 to enable him to spend more time with his family. He has continued on a consultancy basis working two days a week producing reports for coloured stones and pearls. Diamond grading continues to develop with an increasing demand for the new Gem Testing Laboratory of Great Britain report. There was an increase in the number of larger fine quality diamonds and also an increase in type IIa diamonds recorded.

T M J Davidson represented the laboratory at the gem industry and laboratory conference in Tucson in February 2004.

Gem-A USA

Our national office in the United States grew steadily, increasing in visibility with workshops, lectures and exhibits at trade shows including JCK Las Vegas, JA New York and AGTA Tucson Gem Fair. Gem-A USA became a member of AGTA and the Gem Fair contributed much to Gem-A's American exposure; Colin Winter and Jerry Root donated their time and knowledge in hands-on Workshops. A book-signing event for Colin's new Student's Guide to Spectroscopy was a big hit during the show. The splendid annual dinner gathering for members and friends of Gem-A USA brought in many international and American supporters to hear our Gem-A USA Honorary Consultant, Gabi Tolkowsky who, as always, dazzled his audience with passion for the trade while expressing the importance of gemmological education.

The Stuller Annual Workshop was a 'hands-on' gem identification event at Lafayette Louisiana. This Gem-A USA production was recognized as being the most liked presentation by attendees. During the year Gem-A maintained their arrangements with two Allied Teaching Centres, with four further centres preparing to start ATC operations. Additional ATC and Correspondence Course tutors were assigned.

The nationwide Jewelers of America organization offers an annual $100,000 scholarship program to qualifying members. Gem-A USA was qualified as a participant for those JA members seeking gemmological education.

Publications

The Journal of Gemmology underwent its second major change of format since its first publication in 1947 with an increase in size to A4 in January 2004. This enables more scope for larger illustrations and more varied presentation of the continuing technical advances in gemmology.

In the period April 2003 to March 2004, 19 papers were published with topics ranging from Sri Lanka multi-star quartzes to Scottish marble, and from pearl cultivation in China to the compositions of Thai rubies and sapphires. Abstracts totalled 149 and there were 22 book reviews. The Assistant Editors, Associate Editors and abstractors are warmly thanked for their continued support with academic and technical expertise – more and more appreciated these days as technologies continue to advance. The Mineralogical

Donations

The Council is grateful to the following for responding to the appeal for donations. Donation levels were Circle of Benefactors (£5000 and above), Diamond (£1000 to £4999), Ruby (£500 to £999), Emerald (£250 to £499), Sapphire (£100 to £249) and Pearl (£25 to £99).

The following joins those donors listed in previous issues of *The Journal*.

Pearl Donations
Ikuo Sato FGA, Sendai-Shi, Miyagi-Ken, Japan

Hong Kong Jewellery and Watch Fair 2004

The Council is also most grateful to the following for their generous sponsorship of the Gem-A stand and seminars at the Hong Kong Jewellery and Watch Fair:

Charles & Colvard (HK) Ltd, Central, Hong Kong
www.charlesandcolvard.com

Aaron Shum Jewelry Ltd, Kowloon, Hong Kong
www.aaronshum.com

Opalight Artcrafts & Gems Co. Ltd, Kowloon, Hong Kong
www.opalight.com

Society is also thanked for their permission to reprint mineralogical abstracts that are relevant to gemmology. R. Coleman (of Harley UK) is thanked for his part in developing the new A4 format in January and making the publication much more attractive.

Gem and Jewellery News is published jointly with the Society of Jewellery Historians and in 2004 it too benefited from the change to A4 size and publication in full colour. Another change was the acceptance of advertisements, which helps to offset the increased printing costs, and the whole project has benefited from the expertise of Shelley Nott on the new design and John Goodall on production. As ever, Mary Burland has coordinated and managed this development and continued to pull together a wide range of stimulating articles from both our regular contributors and people new to gemmology.

Conference

The Annual Gem-A Conference was held for the second time at the Kempton Park Racecourse during the late autumn Rock 'n' Gem Show giving delegates the opportunity to browse and buy at the Show during the lunch break. The keynote lecture 'An update on research activities at GIA' was presented by William E. Boyajian, President of the GIA. Professor Henry A. Hänni gave a presentation on gem identification carried out at the SSEF Swiss Gemmological Institute, Dr Jack Ogden explained how jewellery mounts could be scrutinized to authenticate jewellery, Clive Wright gave an update on the Kimberley Process and Paula Crevoshay spoke about Crevoshay designs and using gemmology as a designer tool. Two of the Gem-A USA Advisory Board Members, Gail Levine and Theresa Shannon as well as Director A Dale, attended the conference to show support for the Association in the UK.

A private viewing of the Crown Jewels at the Tower of London with Crown Jeweller David Thomas, a visit to the DTC, and a private viewing and guided tour of the Wernher Collection at the Ranger's House, Greenwich, were arranged for the conference delegates. The Council is most grateful to the Conference sponsors Marcus McCallum and T.H. March Insurance Brokers, and supporters Fellows & Sons, Dreweatt Neate, and Malca-Amit (UK) Ltd.

Visits

The annual visit organized by D J Garrod to the world-famous Idar-Oberstein gem centre in Germany was again very successful. Visits to new venues in Idar and Oberstein were organized, while our 'traditional' visits in and around the twin towns were as popular as ever.

Photographic Competition

The 2003 competition on the theme 'All shapes and sizes' drew a record number of images of particularly high quality, and several were selected to grace the 2004 calendar. The winner was Zeng Chungguang of Singapore, with runners-up Anthony de Goutière of Victoria, BC, Canada, and Luc Genot of Brussels, Belgium. Council is most grateful to Harley (UK) for their sponsorship of the three prizes and for their contributions to conference expenses.

Trade fairs and shows

Gem-A exhibited at International Jewellery London 2003 at Earls Court in September with D Garrod giving a series of lectures. T Davidson, I Mercer, D Garrod and L Stather represented Gem-A at the Hong Kong Jewellery Show in September, where a good attendance was enjoyed at our show booth and seminar. A Clark, D Garrod and L Stather attended Rock 'n' Gem Shows at Kempton Park promoting Gem-A.

Finance

For 2003/2004 Gem-A exceeded its budgeted turnover. Although a small increase on budgeted turnover was achieved, unbudgeted expenditures in cost of sales, consultancy and unforeseen costs in repairs and maintenance along with an increased investment in education expenditure planned to produce dividends in 2004-2005 reduced our operating profit. We have continued to show improvement in our accountancy procedures and have reduced our debtors in Gem-A and Gemmological Instruments Ltd.

Staff and Supporters

Three members of staff left and have been replaced. There have been three additions to the staff: Hayley Smith joined the education team as an examination and course administrator, Michell Henry was employed in office services as a cleaner and Stephen Bennett was appointed IT person responsible for routine PC software, network maintenance, Gem-A website upkeep and development, reporting to YJ Thien, along with Gem-A promotion, education development support including graphics and CD Rom production, reporting to Lorne Stather.

Through the continued dedication and hard work of our staff we continue to strengthen the foundation and build for the future of Gem-A.

Gemmological Instruments Ltd.

Gemmological Instruments Ltd is a wholly-owned company of Gem-A. The company supplies gem-testing equipment of good quality at competitive prices, ranging from stone tweezers to top-of-the-range microscopes, books on gems, gemmology and gem-set jewellery, and a range of thematic sets of gems for students. The turnover and profit generated by GI Ltd were very similar to the figures for the previous year and reflect the need for constant development and improvement in a competitive market. Introduced in the second half of 2003/2004, and for which we have sole world distribution, was the Diamond Trading Company's Diamonds CD ROM on Treatments, Synthetics and Simulants. The world market for gemmological equipment remains highly competitive. We continue to search the world for the best equipment to market at good and realistic retail prices.

Extraordinary General Meeting

At an Extraordinary General Meeting held at 27 Greville Street, London EC1 on 27 July 2004, the following Special Resolutions were approved:

THAT the Gemmological Association and Gem Testing Laboratory of Great Britain should seek registered charity status.

THAT the Gemmological Association and Gem Testing Laboratory of Great Britain adopts the Memorandum and Articles of Association dated 2 June 2004 as posted on their website at www.gem-a.info, subject to any changes required by the Charity Commission, for application for registration as a charity.

Membership

Between 1 July and 31 October 2004 the Council approved the election to membership of the following:

Fellowship (FGA)

Adzovic, Senada, Sarajevo, Bosnia Herzegovina, 1997
Aura, Kimmo T. , Espoo, Finland, 2004
Aziz, Khalid, Karachi, Pakistan, 1987
Chandhok, Jasmeet Singh, New Delhi, India, 2004
Hearnden, Rachel Claire, Sheffield, S Yorkshire, 2004
Jennings, Rick, Roanoke, VA, USA, 1979
Kao Oi Shan, Patsy, Hong Kong, 2004
Li Mo Ching, Hong Kong, 2004
Michaelides, Mapia, Athens, Greece, 1999
Peters, Judith Anne, Falmouth, Cornwall, 1976
Sillem, Hayaatun, London, 2004
Valvio, Raija, Vaajakoski, Finland, 2004
Visschers-Villerius, Conny, Heerde, The Netherlands, 2004
Wong, Chung Yan, Kowloon, Hong Kong, 2004
Wong Man Nea, Rosemary, Hong Kong, 2004

Diamond Membership (DGA)

Beattie, Rosamund, Manor Park, London, 1999
Lam Wai Han, Hong Kong, 2004
Li Chi Wai, Kowloon, Hong Kong, 2004
So Yiu Ki, Eric, Hong Kong, 2004

Associate Membership

Akar, Farah, Finchley, London
Archibong, Elizabeth, London
Anderson, Michael R., Chillerton, Isle of Wight
Bamarra, Jaspac, London
Barrie, Brenda, Woking, Surrey
Berden, Angela C.M., Balham, London
Brennan, Aidan, Dundalk, Co Louth, Ireland
Cader, Lazhar, London
Cardosa Rodriques, Isadora, Surbiton, Surrey
Chang Yuan-Cheng, London
Chawla, Jaspreetkaur, London
Cheong Mun Fong, London
Dowell, Vanessa C.D., Cambridge
Duncan, Barry John, Littlehampton, West Sussex
Groenenboom, Peter, Arnhem, The Netherlands
Hafeez, Mohammed, Dewsbury, West Yorkshire
Hague, Des, Sheffield, South Yorkshire
Hazra, Dibyendu, West Bengal, India
Hemeryck, Marine, Brighton, Sussex
Huck, Perry, Stanford-in-the-Vale, Oxfordshire
Johnson, Bede, Lewes, East Sussex
Kashaka, Jean-Claude M., Surbiton, Surrey
Katembwe, Joseph C., Southsea, Hampshire
Kiilu, Kyalo, Mayfield, East Sussex
Leadbeater, Craig C., Dulwich, London
Luckett, Martin J., Stafford, Staffordshire
Lu Lu, Morden, London
McLeod, Samantha, Wellington Point, Queensland, Australia
Masson, Neil, Bucksburn, Grampian
Mitchell, Shirley D., Windsor, Berkshire
Mortimer, Laura H., South Ockendon, Essex
Morton, Jacqueline A.C., Cambridge
Munalula, Crispin, Harrow, Middlesex
Ota, Shinya, Acton Town, London
Pinckernelle, Kathia, Glasgow, Strathclyde
Points, Jaqueline Elizabeth, Dorset
Sane, Hemant, Mumbai, India
Saull, Elanor N., Stourbridge, West Midlands
Sesay, David Emmanuel, London
Shah, Nilay, Hatfield, Hertfordshire
Shoaie-Nia Pouladi, Shabnam, Goring-by-Sea, West Sussex
Thomson, Alison, Tiptree, Colchester, Essex
Tonkin Jukes, Claire, Newham, London
Tun, Thura, Greenford, Middlesex
Veitch, Tara MacNeil, London
Wadhwa, Pritam, Harrow
Wagner, Olivier, Hammersmith, London
Woolfe, Diana P., Poole, Dorset

Laboratory Membership

M. Abram Ltd, 75 Bond Street, London, W15 1RU
Christopher Klean, Suite 28, 88/90 Hatton Garden, London EC1N 8PI

Transfers

Transfer from Diamond Membership to Fellowship and Diamond membership (FGA DGA)

Manchanda, Anu D., Smethwick, West Midlands
St John Lewis, Delyth, South Norwood, London
Wells, Miranda E.J., London

Transfer from Associate Membership to Fellowship (FGA)

Aki, Miou, Osaka City, Osaka, Japan
Anderson, Tricia K.W., Helen's Bay, Bangor, N. Ireland
Brard, Jagvinder S., Pinner, Middlesex
Curtis-Taylor, Tracey, London
Ideno, Yumi, Nishinomiya City, Hyogo Pref., Japan
Landmark, Vivienne J., Harpenden, Hertfordshire
Lee, Young Shin, Kyunggido, Korea
Moore, Katherine H., Symington, Ayrshire
Sane, Hemant. Mumbai, India
Tsutsui, Kazumi, London

Transfer from Fellowship to Fellowship and Diamond Membership (FGA DGA)

Hynes, Lola, Dublin, Ireland
Jones, Lorraine D., Farnworth, Lancashire
Lam Kwi-Peng, Singapore
Richmond, Sonia, Herne Hill, London
Thein, Myint Myint, Whetstone, London
Van Rooij-Roeloffzen, Marjolein, Almere Buiten, The Netherlands
Wai Yee Cheng, Tsuen Wan, New Territories, Hong Kong
Whalley, Joanna, Walthamstow, London

Transfer from Associate Membership to Diamond Membership (DGA)

Hui Hui Ye, Preston, Lancashire
Rebmann, Olivier, Carlsbad, California, U.S.A.
Sowa, Ali Med, Tilbury, Essex
Szymanska, Zofia, London

Subscriptions 2004

The following are the membership subscription rates for 2005. Existing Fellows, Diamond Members and Associate Members will be entitled to a £5.00 discount for subscriptions paid before 31 January 2005.

	Fellows, Diamond Members and Associate Members	Laboratory Members
UK	£72.50	£250.00 + VAT
Europe	£80.00	£250.00
Rest of the World	£85.00	£250.00

Pearls Coral Amber Bead Necklaces Carvings Cameos Mineral Specimens

Opal Precious Topaz Ruby Star Ruby Sapphire Star Sapphire Tourmaline

Gemstones Aquamarine Alexandrite Amethyst Emerald Jade Lapis-Lazuli

The World of Gemstones

Ruppenthal (U.K.) Limited

Gemstones of every kind, cultured pearls, coral, amber,
bead necklaces, hardstone carvings, objets d'art and
18ct gold gemstone jewellery.

We offer a first-class lapidary service.

By appointment only
1a Wickham Court Road, West Wickham, Kent BR4 9LN
Tel: 020-8777 4443, Fax: 020-8777 2321, Mobile: 07831 843287
e-mail: roger@ruppenthal.co.uk, Website: www.ruppenthal.co.uk

Modern 18ct Gem-set Jewellery

The 11th annual Gem-A visit to

IDAR-OBERSTEIN

**Sunday 13 March
to Saturday 19 March 2005**

Major highlights of the tour include:

- The Steinkaulenberg mine (the source of local agate and amethyst)
- Historic and modern gem-cutting workshops
- Gem carving and cameo cutting demonstrations
- Mineral and gem museums

There will also be arranged visits to gem dealers and a wine tasting evening at Gethmann's Hotel.

Price £695

For further details visit the Gem-A website at
www.gem-a.info
or contact Doug Garrod on +44 (0)20 7404 3334.

**Experience a
New Understanding**

two new books
by Richard Cartier FGA

**Seeing
The Light**
**Understanding Optics
Without the Mathematics**

**Professional
Jewellery
Appraising**
Second Edition

visit **RCartier.com**
or order from your
Gem Association


2

Museums,
Educational Establishments,
Collectors & Students

I have what is probably the largest range of genuinely rare stones in the UK, from Analcime to Wulfenite. Also rare and modern synthetics, and inexpensive crystals and stones for students. Computerised lists available with even more detail. Please send 12 1st class stamps refundable on first order (overseas free).

Two special offers for students:
New Teach/Buy service and free stones on an order.

A.J. French, FGA
7 Orchard Lane, Evercreech
Somerset BA4 6PA
Telephone: 01749 830673
Email: french@frencht.freeserve.co.uk
www.ajfrenchfga.co.uk

Pearls
Gemstones

Lapidary Equipment

GENOT L
Since 1953

CH. De Wavre, 850
B-1040 Bxl – Belgium

Tel : 32-2-647.38.16
Fax : 32-2-648.20.26
E-mail : gama@skynet.be

www.gemline.org
www.geofana.net

ROCK 'n' gem SHOWS

Exhibitors displaying & selling a huge range of minerals, fossils, crystals & jewellery

NEWMARKET RACECOURSE
Newmarket, Suffolk
20 - 21 NOVEMBER

BRIGHTON RACECOURSE
Freshfield Road, Brighton
27 - 28 NOVEMBER

From sparkling crystals and spectacular minerals to ancient fossils; from gemstones in a whole spectrum of colours to jewellery containing them; from insects in amber to beautiful carvings.

It is impossible to list or describe them all so why not come and see for yourself. As the majority of exhibitors are collectors themselves they are more than happy to talk about their speciality, and are both knowledgeable and interested. This makes a friendly atmosphere and a visit to the show even more enjoyable.

There are up to 40 dealers exhibiting, with some of the UK's best-known dealers attending.

The Showgrounds are easy to find being well signposted in the area.

All shows open 10am - 5pm (Trade & Public)

Admission:
All other shows: Adults £2.50, Seniors £2.00
Children (8-16 yrs) £1.25

For further information please contact:
HD Fairs Ltd 01628 621697
Email: info@rockngem.co.uk www.rockngem.co.uk

Forthcoming Events

10 November	**Exhibition tour:** 'Hungary's Heritage: Princely treasures from the Esterházy Collection' at Somerset House
16 November	**Scottish Branch**: Gemstones of Mozambique. *Roger Key*
17 November	**North West Branch**: Branch AGM and social evening
26 November	**Midlands Branch**: Bring and Buy Sale and Quiz
4 December	**Midlands Branch**: 52nd Anniversary Dinner
7 December	**Gem Discovery Club Specialist evening**: Unusual gems with *Marcus McCallum*
2005	
18 January	**Scottish Branch**: Suffragette Jewellery. *Liz Goring*
28 January	**Midlands Branch**: Diamond from crust to core. *Dr Jeff Harris*
22 February	**Scottish Branch**: Diamonds – a research perspective. *Dr Jeff Harris*
25 February	**Midlands Branch**: European jewellery from Elizabeth I to Elizabeth Taylor. *John Benjamin*

BRANCH CONFERENCES 2005

Midlands Branch

Sunday 13 March – Barnt Green, Worcestershire

Scottish Branch

Friday 29 April to Monday 2 May – The Lovat Hotel, Perth

South East Branch

June – Colombo, Sri Lanka

contact details

When using e-mail, please give Gem-A as the subject:

London:	Mary Burland on 020 7404 3334; e-mail mary.burland@gem-a.info
Midlands Branch:	Gwyn Green on 0121 445 5359; e-mail gwyn.green@usa.net
North East Branch:	Neil Rose on 0113 2070702; e-mail gema.northeast@gemro.com
North West Branch:	Deanna Brady 0151 648 4266
Scottish Branch:	Catriona McInnes on 0131 667 2199; e-mail scotgem@blueyonder.co.uk
South East Branch:	Colin Winter on 01372 360290; e-mail info@ga-seb.org
South West Branch:	Richard Slater on 01635 553572; e-mail rslater@dnfa.com

Gem-A Website

For up-to-the-minute information on Gem-A events visit our website on www.gem-a.info

Guide to the preparation of typescripts for publication in *The Journal of Gemmology*

The Editor is glad to consider original articles shedding new light on subjects of gemmological interest for publication in *The Journal*. Articles are not normally accepted which have already been published elsewhere in English, and an article is accepted only on the understanding that (1) full information as to any previous publication (whether in English or another language) has been given, (2) it is not under consideration for publication elsewhere and (3) it will not be published elsewhere without the consent of the Editor.

Typescripts Two copies of all papers should be submitted on A4 paper (or USA equivalent) to the Editor. Typescripts should be double spaced with margins of at least 25 mm. They should be set out in the manner of recent issues of *The Journal* and in conformity with the information set out below. Papers may be of any length, but long papers of more than 10 000 words (unless capable of division into parts or of exceptional importance) are unlikely to be acceptable, whereas a short paper of 400-500 words may achieve early publication.

The abstract, references, notes, captions and tables should be typed double spaced on separate sheets.

Title page The title should be as brief as is consistent with clear indication of the content of the paper. It should be followed by the names (with initials) of the authors and by their addresses.

Abstract A short abstract of 50-100 words is required.

Key Words Up to six key words indicating the subject matter of the article should be supplied.

Headings In all headings only the first letter and proper names are capitalized.

A **This is a first level heading**

B *This is a second level heading*

First and second level headings are in bold and are ranged left on a separate line.

Third level headings are in italics and are indented within the first line of text.

Illustrations High resolution digital files, for both colour and black-and-white images, at 300 dpi TIFF or JPEG, and at an optimum size, can be submitted on CD or by email. Vector files (EPS) should, if possible, include fonts. Match proofs are essential when submitting digital files as they represent the colour balance approved by the author(s).

Transparencies, photographs and high quality printouts can also be submitted. It is recommended that authors retain copies of all illustrations because of the risk of loss or damage either during the printing process or in transit.

Diagrams must be of a professional quality and prepared in dense black ink on a good quality surface. Original illustrations will not be returned unless specifically requested.

All illustrations (maps, diagrams and pictures) are numbered consecutively with Arabic numerals and labelled Figure 1, Figure 2, etc. All illustrations are referred to as 'Figures'.

Tables Must be typed double spaced, using few horizontal rules and no vertical rules. They are numbered consecutively with Roman numerals (Table IV, etc.). Titles should be concise, but as independently informative as possible. The approximate position of the Table in the text should be marked in the margin of the typescript.

Notes and References Authors may choose one of two systems:

(1) The Harvard system in which authors' names (no initials) and dates (and specific pages, only in the case of quotations) are given in the main body of the text, (e.g. Collins, 2001, 341). References are listed alphabetically at the end of the paper under the heading References.

(2) The system in which superscript numbers are inserted in the text (e.g. ... to which Collins refers.[3]) and referred to in numerical order at the end of the paper under the heading Notes. Informational notes must be restricted to the minimum; usually the material can be incorporated in the text. If absolutely necessary both systems may be used.

References in both systems should be set out as follows, with *double spacing* for all lines.

Papers Collins, A.T., 2001. The colour of diamond and how it may be changed. *J.Gemm.*, **27**(6), 341-59

Books Balfour, I., 2000. *Famous diamonds.* 4th edn. Christie's, London. p. 200

Abbreviations for titles of periodicals are those sanctioned by the *World List of scientific periodicals* 4th edn. The place of publication should always be given when books are referred to.

The Journal of
Gemmology

Volume 29 No. 4
October 2004

Contents

Cover Picture: *A brooch consisting of turquoise, sapphires and gold set on a lion's paw shell, created by Cartier (Paris) ca. 1958; courtesy of Primavera Gallery, New York, photo Noel Allum. (See Pearls from the lion's paw scallop p.193)*

The Gemmological Association and Gem Testing Laboratory of Great Britain
Registered Office: Palladium House, 1-4 Argyll Street, London W1F 7LD

Designed & Produced by Harley UK

ISSN: 1355–4565